



Developing Microcontact and Nanocontact Printed Protein Techniques to Investigate Cell and Axon Migration

Integrated Program in Neuroscience McGill University, Montréal

February 2011

A thesis submitted to McGill University in partial fulfillment of the requirements of the degree of Master of Science

TABLE OF CONTENTS

Abstract:	6
Résumé:	7
Acknowledgments:	8
Chapter 1: Introduction:	11
Gradients	
Neuroscience: axonal guidance	11
In Vitro Gradients	15
Techniques for generating solution concentration gradients	15
Techniques for patterning surface bound gradients	23
Microcontact printing:	25
Modern techniques for nanopatterning of proteins:	26
Rationale	
Chapter 2: Microcontact Printing	29
Fabrication of a Master through Microfabrication	29
Microcontact Printing Technique Optimization	30
PDMS mixing:	30
PDMS extraction:	31
Stamp Size:	32
Inking Solution:	32
Incubation:	33
Washing:	34
Drying:	35
Substrate:	35
Printing:	
Co-localization of Marker Fluorescent Antibodies for Visualization:	38
Optimized Microcontact Printing Technique	39
Mask and nanowafer Design:	39
PDMS:	40
Stamp manufacturing:	40
Microcontact printing:	
Conclusions	41
Chapter 3: Cellular Response to Patterns	43
Experimental Methods	43
PEG Backfill:	
Cell cultures:	
Commissural neuron cultures:	
Immunocytochemisty:	
Imaging:	
Cell Culture Technique Optimization:	45
Cell Media:	46
Background of the Printed Protein:	
Results of cell response to patterned protein	
HEK 293 cell are repelled by Sparc stripes:	52
Cell line attraction to netrin-1 stripes:	53

Primary cells respond to netrin-1 patterns:	56
Conclusions	
Chapter 4: Application of Microcontact Printing to Neuroscience- Neuronal Island C	Co-
cultures	59
Experimental Methods	60
Stamp Preparation:	60
Microcontact printing:	62
PEG backfill:	63
Astrocyte seeding and culture:	
Hippocampal neuron seeding and culture:	63
Immunocytochemistry:	63
Imaging:	
Neuronal Co-culture Development:	64
Choosing the proper inking solution:	64
Seeding optimal cell densities:	66
Staining for neuronal markers:	68
Time in vitro required for neurons to polarize and form synapses:	69
Conclusions:	
Chapter 5: Development of Nanocontact Printing Process to study cellular responses	s to
nanogradients	
Materials and Methods:	
Nanowafer fabrication:	
Scanning Electron Microscopy (SEM):	
Atomic Force Microscopy (AFM):	
Nanoarray and Digital Nanodot Gradient (DNG) Design:	
Develop a stamp replication method:	
Intermediate stamp:	
Secondary replica:	
Optimized stamp replication technique:	
Creating a cost efficient liftoff printing method for nanoscale levels of resolution:	
Cell Response to Protein and Peptide Nanopatterns	
Cell line response on nanopatterns	
Neuronal response on nanopatterns	
Conclusions	
Chapter 6: Discussion	
Microcontact Printing	
Specific Cell Response	
Neuronal Island Co-cultures	
Nanocontact Printing Process	
Digital Nanodot Gradients and Cell Migration	
Future Directions	
Conclusion	
References	106

TABLE OF FIGURES

Figure 1: Early devices created to study solution gradients	. 18
Figure 2: Flow-based Microfluidic Gradients	. 21
Figure 3: Diffusion-based Microfluidic Gradients	. 23
Figure 4: Adapted stripe assay technique to create gradients	. 24
Figure 5: Residues transferred through non-extracted microcontact printing stamps	. 31
Figure 6: Effect of incubation time on protein transfer	
Figure 7: Effect of drying times on protein transfer with a quick	. 35
Figure 8: Effect of Plasma treatment of the substrate onto protein transfer	
Figure 9: Quantification of protein transferred onto the substrate from the PDMS stamp	p
during the microcontact printing process	. 37
Figure 10: SNOM images of 5 µm spot of fluorescent secondary antibody patterned	
through microcontact printing	. 38
Figure 11: Fluorescent images of the co-localized antibody with the protein of choice	. 39
Figure 12: Microscale printed patterns of fluorescent antibodies	. 42
Figure 13: Effect of background on cell response to surface-bound features	. 45
Figure 14: Cell response to patterned protein in different media concentrations	. 47
Figure 15: HEK 293 cells grown on fibronectin stripes	. 48
Figure 16: Response of HEK 293 cells to Fibronectin stripes with altered background	. 49
Figure 17: Stripes of Geltrex initiate the formation of focal adhesions	. 51
Figure 18: HEK 293 cell response to patterned SPARC protein	. 53
Figure 19: Cell attraction to patterned protein netrin-1 stripes by U87 cells	. 54
Figure 20: DCC expression in C2C12 cells	
Figure 21: C2C12 cell attraction to patterned netrin-1 stripes over time	. 55
Figure 22: Differing response of Commissural neurons to netrin-1 stripes based on the	
varying background	
Figure 23: Commissural neuron response to netrin-1 micropatterns	. 57
Figure 24: Islands composed of different patterned adhesion proteins to compare their	
ability to recruit astrocytes	. 65
Figure 25: Immunofluorescent image of hippocampal neurons grown on an astrocyte	
monolayer covering printed islands of netrin-1	
Figure 26: Importance of accurate quantification of neurons seeded on the islands	. 68
Figure 27: Fluorescent image of hippocampal neurons grown on astrocytes covered	
netrin-PDL island	. 69
Figure 28: Fluorescent image of hippocampal neurons grown on astrocytes covered ne	
island	
Figure 29: Clewin designs of the gradients mentioned in Table 1	
Figure 30: Diagram of how the intended mass production of disposable replicas will ta	.ke
place	
Figure 31: Image of a parylene intermediate replica and a second NOA63 replica	
Figure 32: Degradation of the PDMS intermediate replica though replication	
Figure 33: Schematic of the double replication procedure of a Si wafer with nanometer	
scale patterns made by e-beam lithography	. 79
Figure 34: Images of the original master and of the replicas	
Figure 35: Schematic of the lift-off printing process	. 81

Figure 36: Successful nanoarray prints of various biomolecules	82
Figure 37: AFM micrographs of nanopatterned arrays of 200 nm in diameter nanosp	ots
with a pitch of 1 μm composed of antibody and netrin-1	83
Figure 38: Gradient composed of 100 nm diameter spots of fluorescent antibody	84
Figure 39: 200nm nanogradients of a variety of biomolecules	86
Figure 40. C2C12 cell on a fibronectin nanoarray	87
Figure 41: C2C12 cells grown on netrin-1 nanogradients	88
Figure 42: Number of C2C12 myoblasts cells in each of 3 high, medium and low de	nsity
areas of the DNG over time	89
Figure 43: Affect of backfill on commissural neuron response to nanogradient of ne	trin-1
	90
Figure 44: Commissural neurons grown on netrin-1 nanogradients	91

Abstract:

Cells navigate by integrating signals derived from the discrete binding of signaling proteins with individual receptors that typically interact with single proteins. There is thus great interest in creating deterministic in vitro protein patterns to address how their density and distribution control intracellular signaling and cell navigation. A thorough in vitro investigation of these issues has been limited by a lack of simple and affordable methods. The objective of this project is to develop a new protein patterning technique at nanoscale levels of resolution in a rapid, inexpensive and reproducible manner. We first optimized a rapid microcontact printing process followed by a backfilling process to alter the background. This new process allowed us to obtain a cell response to surface-bound protein patterns and to apply this technique to create neuronal micro island co-cultures. Once optimized, this process was adapted to pattern proteins at the sub-micron range through a stamp replication process followed by a lift-off printing process. The nanopatterning technique was employed to pattern nanogradients of 200 nm spots on which myoblasts and neurons were shown to respond through migration to increases in protein density. Understanding of the migratory response in neuronal guidance gradients is vital to fully understand organism development and may provide critical insight into the quest to regenerate a damaged central nervous system following injury.

Résumé:

Les cellules naviguent à travers leur environnement en intégrant des signaux provenant de l'adhésion de protéines de signalisation à leurs récepteurs. Il y a donc un grand intérêt pour la création de modèles déterministes in vitro composés de ces protéines pour comprendre comment leur densité et distribution contrôlent la signalisation intracellulaire et la navigation. L'étude approfondie de ces mécanismes a été limitée par un manque de méthodes simples et abordables. L'objectif de ce projet est de développer une nouvelle technique d'impression de patrons de protéines à l'échelle du nanomètre, de façon rapide, peu coûteuse et reproductible. Nous avons d'abord optimisé un processus d'impression par microcontact rapide suivie d'un processus de remblayage pour neutraliser l'arrière-plan. Ce nouveau processus nous a permis d'obtenir une réponse des cellules face aux patrons de protéines imprimées à la surface et d'appliquer cette technique pour créer des micro-îlots de neurones en co-cultures. Une fois optimisé, ce processus a été adapté à l'impression de patrons submicroniques La technique a été utilisée pour créer des nanogradients composés de points de 200 nm sur lesquels des myoblastes et des neurones ont montré une réponse migratoire en fonction de la densité protéique, fonction elle-même de la densité des points. L'étude de la réponse migratoire neuronale sur des gradients directionnels est essentielle pour bien comprendre le développement de l'organisme et peut fournir des informations essentielles à la recherche sur la régénération du système nerveux central endommagé.

Acknowledgments:

The success of the work presented here would never have been possible without the support, collaborations and insights of others to whom I owe my sincerest gratitude. First and foremost, I thank my advisors, Profs. David Juncker and Tim Kennedy. I am grateful for their faith in me and patience as I slowly familiarized myself with a new world of unknown science. That being said I also wish to thank them for supporting me throughout my master career by giving the necessary insights that led to the success obtained in this project. I also wish to acknowledge their support in obtaining the Jeanne Timmins Costello Studentship in 2010 and also funding me for the remainder of my studies through the CIHR Regenerative and Nanomedicine grant.

Thank you to my committee members, Prof. Bruce Lennox and Prof. Craig Mandatto, that despite the complications in finding a time slot that suited the entire committee, came through and contributed greatly by offering not only input, but also materials as well as expertise from their own students.

I also wish to thank my many past and present colleagues from DJGROUP as well as the TEK lab without whose warm presence, insights and contributions, this work would have never been as enjoyable and yielded such positive results in such a short period of time. In particular in DJGROUP I wish to thank Dr. Mateu Pla Roca, Dr. Benjamin Corgier and Dr. Cécile Perrault for their guidance in getting my graduate career kicked off on the right foot and to maintain it that way. I also wish to thank Dr. Sébastien Bergeron for first accepting me into his cubicle and being the best cubicle mate by maintaining a friendly atmosphere as well as offering wise words from his experience in

my times of need. I also wish to thank Mohammad Quasaimeh for being the most reliable person that I had the pleasure to work with and for being an outstanding resource in the late nights we spent working in the office. I also wish to thank Rym Leulmi who brightened each day with her unmatched enthusiasm for telling me what I did not want to hear, but yet needed to hear as well as her numerous hours spent in the microfab teaching the techniques of photolithography as well as electrolithography. Roozbeh Safavieh was essential in the development of the gradient in the design of the original gradients and assistance in the redesign of the 200 nm gradients.

In the Kennedy lab I wish to thank first and foremost James Correia who served as my dissecting hand throughout my masters and was also essential in the design of some of the neuroscience experiments mentioned below. Dr. Benjamin Rappaz was tremendous in supporting me with analysis software as well as imaging knowledge and must be applauded for spending so many hours conducting confocal microscopy with me. I also wish to thank Nathalie Marcal for her help in conducting western blots.

I also wish to thank Natalia Tansky, Justin Philip, Levon Attoyan, Selina Yim and Yannick Devaud for accepting to work under my supervision and not only produce significant results but also teach me about mentoring others and most importantly provide me with entertaining stories to tell for years to come such as dipping pipettes in liquids without tips.

Thank you to Monserratt Lopez for her perseverance in conducting Atomic Force Microscopy and SNOM on the protein micro and nano features which eventually led to successful imaging. François Beaubien provided hippocampal neurons for the island co-culture, Gregoire Morisse and Jenea Bin provided astrocytes for the same experiments.

Tohid Fatanat Didar designed and supplied a number of peptide chains including the RGD peptide chain presented here. Dr. Emma Jones provided SPARC, its specific antibody and HEK 293 cells.

I also wish to thank Prof. Harold Craighead and my mentor Dr. John Mannion, at the NBTC center at Cornell University, for the eye opening experience to take part in their research as a summer REU in 2007, which eventually led to my curiosity in this world of multidisciplinary research and nanobiotechnology. Additionally I wish to thank my past lab mates from the Sweet lab at the Rochester Institute of Technology, in particular Nikki Meadows and Jacqueline McLatchy for their friendship and scientific advice in their respective scientific specialties.

Finally this work could not have been completed without the constant and everlasting support of my parents and brother to who I cannot thank enough for everything they have done and continue to do for me.

Chapter 1: Introduction:

Gradients

Gradients are fundamental to biology. They underlie the development of organisms (Kohidai and Csaba 1998) and regulate angiogenesis, the formation of new blood vessels (Gerhardt, Golding et al. 2003). More recently, gradients of chemotactic cytokines have been found to play a significant role in the maturation of cancer and metastasis (Muller, Homey et al. 2001; Eccles 2005; Zlotnik 2006) and for immune responses (Luster 2002). Gradients are also exploited by microorganisms to find a source of food, among other things (Adler and Tso 1974). The most interesting application for a gradient within the human body, from a neuroscience perspective, is the directed navigation of neuronal axons towards their targets through gradients (McLaughlin and O'Leary 2005).

Neuroscience: axonal guidance

During neuronal development, one of the major events to occur is axonal migration, a process that takes place following the formation of a neural tube (neurulation) during the later stages of an organism's development (Gilbert, Opitz et al. 1996). In this vital developmental stage, neurons extend their axons to the proper synaptic targets; failure to create the correct connections results in severe neurological deficiencies (Engle 2010). In order for the axon to attain its exact destination, the neuron's path is outlined by a number of guidance proteins which cause the growth cone, the sensory portion located at the tip of the axon, to respond and redirect its trajectory accordingly (Tessier-Lavigne and

Goodman 1996; Mortimer, Fothergill et al. 2008). The growth cone senses the environment through dynamic filamentous actin protrusions called filopodia where the actin chains polymerize or depolymerise depending upon the guidance cues encountered by the filopodia (Kater and Rehder 1995). These guidance proteins can be attractive cues, repulsive cues, or the cue can depend upon interactions with other proteins (Carmeliet and Tessier-Lavigne 2005). In the 1940s, Roger Sperry hypothesized that individual neurons express different sets of molecular markers. He proposed that the interactions among these sets of markers on the presynaptic neuron and the postsynaptic neuron provide a system of molecular addresses for the formation of specific synapses in the body. Sperry called this concept the chemoaffinity hypothesis (Sperry 1963). Guidance cues, attractive and repulsive, function at either short-range or long-range. For short range cues, contact attraction/repulsion, neighbouring cells make contact, binding the receptor on one cell with the ligand on the surface of the second. In long-range cues, chemotropism, cells expressing a receptor respond to gradients of diffusible guidance cues secreted by distant cells.

The neural development of the spinal cord and the optic system have been intensely studied. These studies have shown that chemotrophic gradients play important roles in the guidance of axons. The ephrin family of guidance cues has been found to play a major part in the topographic mapping of the optic system through the graded distribution of ligands and receptors (Drescher, Bonhoeffer et al. 1997). However, in the migration of commissural neurons of the spinal cord, a number of gradients of various protein types have been identified: sonic hedgehog (Charron, Stein et al. 2003), BMPs (Tanabe and Jessell 1996) and netrin-1 (Kennedy, Serafini et al. 1994). One neuron population whose

response to all these cues is currently widely studied are the commissural neurons. These neurons mature in the dorsal portion of the spinal cord where the neurons extend axons down the spinal cord to the ventral floor plate where they cross the commissure before extending along the length of the spinal cord towards the brain, where they make their synapses (Kandel, Schwartz et al. 2000; Dickson 2002). For these axons to extend properly, they are affected by a number of guidance proteins at different points throughout the process to ensure correct pathfinding. Some of the main guidance proteins identified to be involved in this process are sonic hedgehog (Trousse, Martí et al. 2001), wnt (Lyuksyutova, Lu et al. 2003), and members of the semaphorin (Zou, Stoeckli et al. 2000), slit (Brose, Bland et al. 1999), ephrin (Imondi, Wideman et al. 2000), and netrin (Kennedy, Serafini et al. 1994) families. Netrin-1 is a guidance protein that is of interest to our lab.

In mammals, the netrin family of guidance proteins is composed of three secreted proteins (netrin-1, 3 and 4) and two glycosyl-phosphatidylinositol (GPI) linked proteins (netrin-G1 and G2) (Moore, Tessier-Lavigne et al. 2007). The first family member isolated and the most studied to date is netrin-1. Since its isolation, netrin-1 has been shown to be widely distributed throughout the body (Serafini, Kennedy et al. 1994). Recombinant netrin-1 protein has been purified in relatively large quantities using heparin affinity chromatography. The availability of functional epitope tagged netrin-1 has facilitated the discovery that netrin plays a vital role in axonal guidance and in the proper targeting of these axons to their targets in the brain (Yee, Simon et al. 1999), retina (de la Torre, Hopker et al. 1997) and spinal cord (Kennedy, Wang et al. 2006). More specifically, netrin-1 plays an attractive role in some instances through interaction

with its DCC receptor, such as in the case of commissural neurons (KeinoMasu, Masu et al. 1996) or with its receptor neogenin (Srinivasan, Strickland et al. 2003), such as in the case of C2C12 myoblasts (Kang, Yi et al. 2004; Bae, Yang et al. 2009). It has also been found to play a repulsive role through the interaction with a complex of the receptors DCC and Unc5 (Dickson 2002). In the spinal cord, netrin-1 is responsible for commissural axon crossing at the midline. Consistent with this function, netrin-1 is expressed in a gradient with high concentration at the floor plate where it is thought to be secreted and the lowest concentration at the roof plate (Kennedy, Wang et al. 2006).

As shown above, the mechanisms by which neural cells attain their synaptic targets through the process of axonal migration have become increasingly clearer with the discovery of gradients composed of long-range chemotrophic factors. However, with the standard *in vitro* tools and the molecular biology techniques available, the understanding of the present system is limited. These techniques are unsuitable to clearly comprehend how neurons respond to variations in gradient geometries. A clear knowledge of the neuronal response to gradients is critical in the field of development, where gradient geometry changes as the organism develops. It is also critical in the field of regeneration, where gradients are most likely going to play a role in future spinal cord regeneration applications. To obtain a better understanding of how gradients influence biological systems, research has been conducted to develop technologies that create gradients that can be tailored in vitro to facilitate the study of axonal migration.

In Vitro Gradients

Gradients arise as a result of a source-sink configuration and may occur either as (i) free diffusion gradients (Lander, Nie et al. 2002) generated for example when a subset of cells secrete a protein that diffuses in the extracellular space until it is eventually degraded by enzymes or internalized by other cells, (ii) as surface-bound gradients in the form of membrane bound proteins (Gurdon and Bourillot 2001), or from proteins that were secreted from cells and bound by the extracellular matrix (ECM) (Yu, Burkhardt et al. 2009) or (iii) as a combination of both (Goodman 1996). Due to the variety in types of gradients, their wide applications within living systems and the critical roles they play, tremendous work has been conducted to reproduce gradients *in vitro* that would replicate each type of gradient. These gradients would be used to create a system that can be used to study the gradient effects on cells and also to discover the mechanism whereby cells respond to these gradients (Genzer and Bhat 2008; Kim, Kim et al. 2010). Given the two main categories of gradients, solution and surface bound, and their differing modes of establishment, differing methods have been developed to address each.

Techniques for generating solution concentration gradients

An abundance of methods have been developed over the last 50 years that have been fully quantified through simulation. Over the years, devices have grown from relatively simple techniques (Figure 1) to increasingly complex systems that yield better controlled and more stable gradients (Figure 2) (Keenan and Folch 2008).

Some of the early gradient generators use a porous gel, usually composed of agarose (Nelson, Quie et al. 1975), collagen (Parkhurst and Saltzman 1992) or fibrin (Moghe, Nelson et al. 1995) through which two wells are usually created. In one well, the

cell solution is inserted and in the second (which is a distance away from the first), the chemotrophic factor is inserted. The chemotrophic factor will then diffuse through the gel and create a gradient to which cells respond and migrate through the gel. Hydrogels are still common for chemotaxis studies due to the simplicity of this method. It is easy to replicate the 3D in vivo environment and one can easily expose cells to a variety of chemotrophic factors simultaneously by adding more source wells. A second population of cell secreting chemotrophic factors can also be used as the source in the co-culture assay (Lumsden and Davies 1983). Some setbacks render this technique innapropriate for certain applications. The most striking weakness is that the reproducibility of the gradient using this technique is low due to the lack of temporal-spatial control (Toetsch, Olwell et al. 2009). Additionally, the 3D structure of a hydrogel does not yield a very successful analysis of single cell responses to chemotrophic gradients. More recently, a printing assay has been developed in which a collagen gel substrate can be printed upon with a nanoplotter. The spots of proteins then diffuse over time in the gel and create gradients that remain relatively stable over a period of ~2 days (Rosoff, Urbach et al. 2004; Rosoff, McAllister et al. 2005). Through the arrangements of the printed spots, the geometry of the gradient can be engineered, but again, the thickness of the gel prevents high resolution imaging of the migration process. This technique has recently been used to investigate the response of growth cones to nerve growth factor (NGF) (Mortimer, Fothergill et al. 2008; Mortimer, Pujic et al. 2010).

To facilitate the visualization of single cell response to these gradients, the pipette (growth cone turning) assay was developed in 1979 (Gundersen and Barrett 1979). This assay makes use of a glass pipette connected to a pneumatic pump stabilized on a

microscope stage. The pipette is then used to puff a trophic factor onto a single cell. The factor will diffuse through the environment and create a gradient for that single cell to respond to as it is imaged. Like the hydrogel techniques, the method allows very little control of the shape of the gradient and thereby allows very limited reproducibility or flexibility. Additionally, this method necessitates extensive preparation and requires expensive equipment. Despite the limitations of this technique, it has been one of the goto techniques for neuroscientists due to the wealth of information that can be acquired by capturing the response of a single cell. Among other chemotrophic factor responses tested on neuronal growth cones were NGF (Gundersen and Barrett 1980), netrin-1 (Ming, Song et al. 1997), semaphorin 3F (Atwal, Singh et al. 2003), agrin (Xu, Fu et al. 2005) and cAMP (Lohof, Quillan et al. 1992). In order to generate steeper gradients using the pipette, the Soon chamber was created in which the guiding factor is injected using the same setup as the pipette assay on a coverslip set at a 40° angle which will trickle down to create a much steeper gradient (Soon, Mouneimne et al. 2005).

The Boyden chamber (transwell assay) also makes use of passive diffusion through a chamber composed of two wells separated by a porous membrane which permits the passage of chemotrophic factors from one well to the other in one direction and the migration of cells in response to these factors in the other (Boyden 1962). One disadvantage of this technique is the lack of ability to track the cell migration over time. Instead, the only results that can be obtained is a quantification of cells that have successfully migrated from one well to the other by the end of the experiment. To address this deficiency, the Zigmund chamber was developed. It reproduced the gradient present across a single pore within the Boyden chamber and extends it along a linear axis. The

gradient is obtained by having one well containing high concentrations of a chemotrophic factor diffuse through a small slit into a second well containing a much lower concentration of this trophic factor. The two wells and the small channel are etched within a glass slide allowing time-lapse imaging of the migration progression (Zigmond 1977). In addition, through the designed device, the gradients obtained are very reproducible and are stable for a limited time period due to the non-renewed limited concentration of chemotrophic factor and the vulnerability of this device to evaporation, the gradient is only stable for a single hour. The one hour time limit renders this device useless for slow growing cells such as neurons but it can be used for rapidly migrating cells. To limit the evaporation that occurs in the Zigmond chamber, the device was revamped into a device composed of two concentric rings separated by the same bridge present in the Zigmond chamber which again yields a gradient through the limited diffusion of chemotrophic factors from one circular well to the other (Zicha, Dunn et al. 1991). Even though the evaporation is drastically reduced in this device known as the Dunn chamber and the stability of the gradient is greatly increased, most of the other

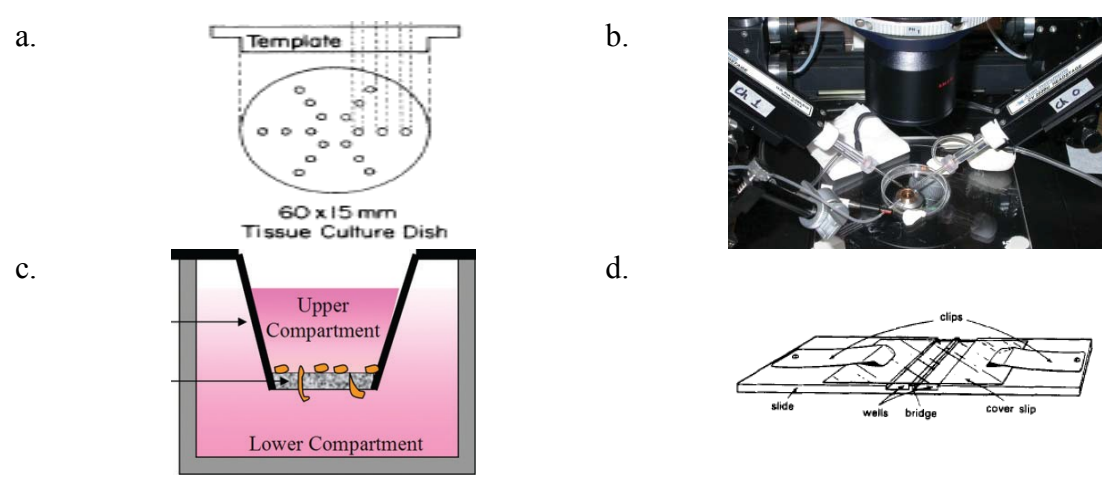


Figure 1: Early devices created to study solution gradients (a) gel assay reproduced from Nelson et al., 1975, copyrighted 1975. The American Association of Immunologists, Inc. (b) pipette assay adapted from Keenan et al., 2008 with permission from the Royal Society of Chemistry, (c) Boyden chamber, adapted from Boyden, 1962, (d) Zigmond chamber, reproduced from Zigmond, 1977.

downfalls of the Zigmond chamber associated with the lack of design control remain. Regardless of the limitations, the Dunn Chamber has been widely used (Webb, Pollard et al. 1996; Bhatwadekar, Glenn et al. 2008; Meira, Masson et al. 2009) and more recently has even been used to study the turning response of neurons to chemotrophic factors such as Sonic Hedgehog (Yam, Langlois et al. 2009), 14-3-3 Proteins (Kent, Shimada et al. 2010) or Glial cell-derived neurotrophic factor (GDNF) (Dudanova, Gatto et al. 2010).

More recently attention has been directed towards employing microfluidics to generate solution based gradients due to the advances in microfabrication that have rendered the technology more attainable to the general scientific community (Whitesides 2006). The advantage of reducing fluid volumes is that not only does it reduce the cost of experiment but it allows for the employment of particularities of the fluid flow that only arise at these minute volumes. One major particularity is that viscosity and surface tension overshadow the effect of inertial fluidic forces (Karniadakis, Be kök et al. 2005). Given this lack of inertial force, microfluids follow laminar flow and mix only through diffusion without the presence of turbulent mixing (Tian and Finehout 2009). Using these properties of fluids, a number of temporal-spatially controlled and stable gradients have been created by following two main approaches: controlling the flow or the diffusion of the fluid within the device (Figure 2)(Kim, Kim et al. 2010).

Flow based gradients make use of the laminar flow and limited mixing through diffusion characteristic of microfluidics. The T- and Y-junctions have been at the base of the simplest gradient designs because of the above mentioned properties, the two solutions will flow next to one another in the merged channel and diffuse one into the other (Hatch, Kamholz et al. 2001; Holden, Kumar et al. 2003). Unfortunately, because

diffusion is a continuous process, the diffusion profile is only stepwise immediately after the junction. As the distance increases, the diffusion profile becomes increasingly sigmoidal (Ismagilov, Stroock et al. 2000). This type of gradient can easily be generated without much thought of design; however with this simple design only very crude gradients can arise. In order to create more complex gradients, complicated flow schemes have been designed. One such design is the "premixer gradient generator" microchannel network where two solutions are mixed by a series of bifurcations and recombinations of solutions with various mixing ratios (Jeon, Dertinger et al. 2000). Using the original design, only linear gradients were possible, however by altering the geometry, more complex gradients such as parabolic or periodic shapes were obtained (Dertinger, Chiu et al. 2001). Additionally, multiplexing was rendered possible by designing juxtaposed gradient generators. Another approach leading to a further flexible gradient is the "universal gradient generator", where a central cavity with two separated inlets is separated by a number of longitudinal dividers aimed at restricting the interdiffusion mixing between the two flows. Using this device it was shown that complex gradients could reliably be obtained (Irimia, Geba et al. 2006). Further designs have pushed the limit of gradient generation by increasing the number of splitting channels (Amarie, Glazier et al. 2007), altering the gradient-driving flow (Liu, Sai et al. 2008), opening or closing electrostatic valves (Lin, Saadi et al. 2004) or even reversing the direction of the flow (Irimia, Liu et al. 2006). The limitation with all of the microfluidic devices mentioned above is that they all require a clean room facility and an extensive understanding of microfluidic principals to design the fluid generators which will ultimately yield a desired gradient (Campbell and Groisman 2007).

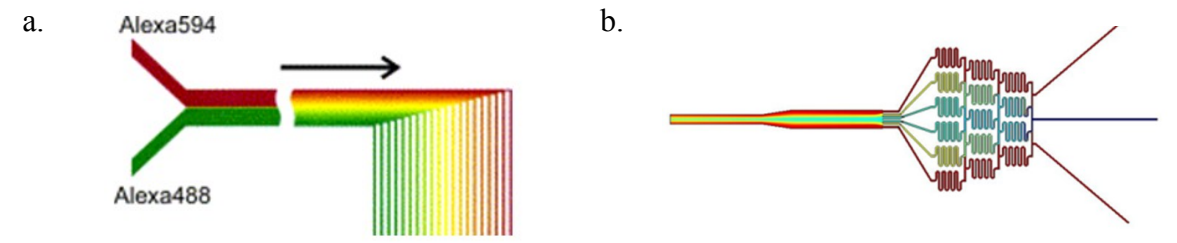


Figure 2: Flow-based Microfluidic Gradients (a) Y-channel, adapted from Holden et al., 2003 with permission from Elsevier; (b) "Christmas tree" gradient generator (Qasaimeh, M.; Juncker, D., unpublished results).

Diffusion-based gradients as the name indicates rely exclusively on the property of diffusion with the lack of flow to generate gradients (Figure 3). Unlike the macroscale devices presented above, the microfluidic systems employ microchannels throughout the contraption to flow the fluids in which high fluidic resistance is present to isolate the secretion chamber from the aspirating one (Fredrickson and Fan 2004). One of the simpler devices fabricated is the "Ladder Chamber" which has two source wells and one sink with a microchannel connecting each source with the sink and running parallel to one another. In order for gradients to arise, perpendicular channels connect the two parallel channels. Using this device, chemotactic response of neutrophils to a linear gradient of IL-8 was observed (Saadi, Rhee et al. 2007). Since the flows are constantly renewed, the gradient can be maintained for unlimited time periods, however the tiem required to obtain a completely linear gradient was quite slow (56 minutes), fluidic convection was quite high therefore limiting the use of this device to study cells and in addition this device was limited to producing linear gradients. Another design tackled the challenge of high fluidic convection by producing a device with a large open chamber placed in the middle of the narrow ladder of perpendicular channels where the gradient will diffuse. Using this technique the migration of shear-sensitive HUVEC cells was observed in response to a VEGF gradient (Shamloo, Ma et al. 2008). Even though the shear stress effect on cells was reduced, the stabilizing time of the gradient remains quite high (45 minutes) and the gradient design remains limited. Newer devices have become increasingly complex, but have been successful at drastically increasing the diversity of the gradients generated, and they have also reduced the stabilization time (Atencia, Morrow et al. 2009). The limitations here again are that all these gradients require a clean-room setting to create the devices.

In addition to microchannels, membranes with a range of porous properties were generated for diffusion based gradients. One of the most primitive constructs is a device composed of a source and a sink connected by a long microfluidic channel. The entry of the source into the fluidic channel is blocked by a polyester membrane which reduces flow (Abhyankar, Lokuta et al. 2006). With this device it was found that the gradient stabilization period is about 6 hours, a time by which rapidly growing cells present in the chamber might have already completed their migration. Another approach that uses three channels with a nitrocellulose membrane has reduced the stabilization time to 20 minutes and yields a static linear gradient in the central channel (Diao, Young et al. 2006). A third technique uses a self-fabricated membrane with a pore size of 100nm. This device is composed of two source channels and two sinks connected by a microchannel that lead into an observation channel. Flow is prevented from entering the triangular chamber by limiting access with the porous membrane (Kim, Lokuta et al. 2009). Other labs have also used gels to separate the two chambers such as collagen based matrix where attractive molecules are diffusing through the hydrogel in the same three channel design used by Diao et al. (Cheng, Heilman et al. 2007; Haessler, Kalinin et al. 2009). Overall, diffusion based gradient generators yield gradients that are significantly gentler than the

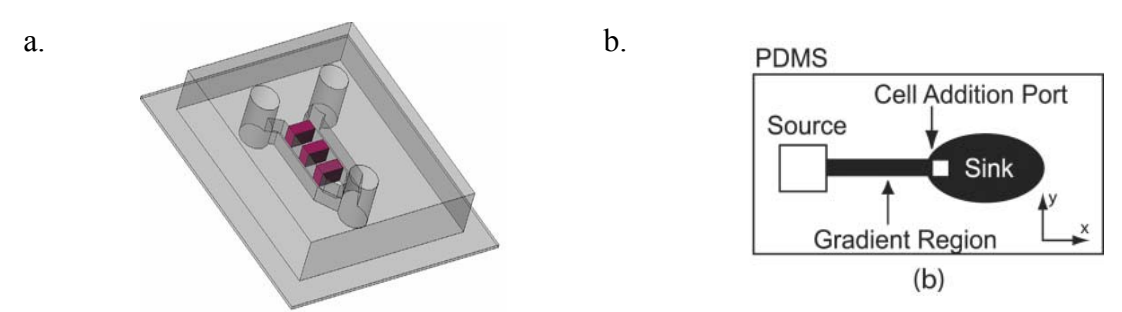


Figure 3: Diffusion-based Microfluidic Gradients (a) ladder device, adapted from Saadi et al., 2007 with permission from Springer; (b) basic membrane device, adapted from Abhyankar et al., 2006 with permission from the Royal Society of Chemistry.

fluidic driven gradients that create large shear stress and render those gradients inappropriate for experimentation with fragile cells. The shortcomings of these gradients are a long stabilization period as well as gradient shapes limited to linear gradients.

Techniques for patterning surface bound gradients

Even though surface bound gradients have not been as successfully reproduced through a plethora of techniques as gradients in solution, a number of successful techniques have been developed. Most of the techniques have been developed by patterning these gradients on polymers. Most of these techniques are not suitable for cell studies because the harsh techniques are not suitable for protein patterning. Either the polymers on which these gradients are patterned are toxic to cells or the materials used complicate the imaging of cell migration (Genzer and Bhat 2008). The first approach that established protein gradients for cell studies was through a technique now known as the stripe assay (Walter, Kernveits et al. 1987). In this technique, a silicon matrix with low pressure channels 90 µm wide are placed equally spaced under a capillary pore filter. Through aspiration, a solution of cell membranes was flowed through the microchannels and bound to the membrane exclusively in the mesh under the channel opening. Once the first type of membrane was bound to the substrate and had clogged the pores, the silicon channels were removed and a second type of membrane was flowed through the

membrane that filled the areas between the first stripes. This technique was adapted to create gradients by using a mechanically controlled coverslip that would slide along the stripes as the protein is filtered through the matrix to create a concentration gradient (Rosentreter, Davenport et al. 1998).

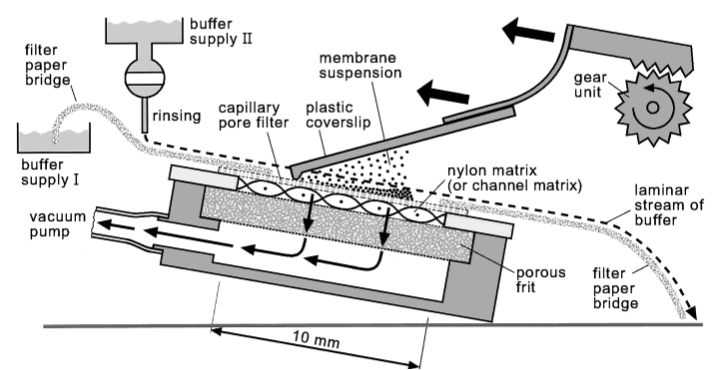


Figure 4: Adapted stripe assay technique to create gradients by aspirating a cell membrane solution through a porous membrane and mechanically moving a coverslip along the length of the stripes as the aspiration occurs to vary the concentration of protein aspirated along the stripes and create a concentration gradient along the length of the stripes. Adapted from Rosentreter et al., 1998 with permission from John Wiley and Sons.

More recent techniques have used microfluidics to flow proteins in solution and let the proteins bind on the surface (Caelen, Bernard et al. 2000; Smith, Tomfohr et al. 2004), or by using agarose gels to allow the molecules to diffuse prior to binding to the surface (Mai, Fok et al. 2009), or even through laser-assisted adsorption (LAPAP) (Bélisle, Correia et al. 2008). Characterization of the resulting gradients is fraught with many pitfalls, including (i) background fluorescence that makes it difficult to quantify low intensity, (ii) quenching (Giepmans, Adams et al. 2006), (iii) photobleaching and (iv) vignetting (Petty 2007), all of which may compromise the accuracy of measurements.

Quantitative surface bound gradients can be produced by digitalizing the gradient which is achieved by patterning spots of proteins with increasing size (von Philipsborn, Lang et al. 2006), decreasing spacing, (Coyer, Garcia et al. 2007) or combining both techniques (von Philipsborn, Lang et al. 2006). With such patterns, quantification of the

gradient is straightforward and can be calculated based on the surface density of the pattern so it is therefore highly accurate. Microcontact printing has been used to pattern proteins as spots (Bernard, Delamarche et al. 1998) because it is easy to use and cost effective.

Microcontact printing:

Microcontact printing was first developed as an alternative to photolithography to easily and inexpensively pattern gold microfeatures by transferring thiols on gold, where they self-assemble into a monolayer, through a soft polymeric stamp with topography. The gold is then protected from an etchant by the thiol layer (Kumar and Whitesides 1993). This technique was later adapted to proteins resulting in the patterning of proteins on glass (Bernard, Delamarche et al. 1998). Using this technique, the patterning of multiple proteins was easily accomplished by stamping multiple stamps inked with various protein solutions on a same area for example (Bernard, Renault et al. 2000). In addition, due to being a rapid and facile technique, microcontact printing has widely been implemented in the field of cell biology to study a wide range of issues, including, stem cell differentiation (Ruiz and Chen 2008), cell co-culture (Kidambi, Sheng et al. 2007), cell adhesion (Brock, Chang et al. 2003) and cell migration (Dertinger, Jiang et al. 2002). The limitation first presented by the technique is that the feature size must be greater than a single micron and the second is that individual features can't be too far from one another. These two limiting factors cannot readily be resolved because the soft, elastomeric stamps used in microcontact printing collapses when the spots are spaced too far apart or are too small in size (Perl, Reinhoudt et al. 2009). Lift-off microcontact printing which uses flat stamps does not suffer from these mechanical constraints, and it

has been used to pattern nanospots (Renault, Bernard et al. 2002) and more recently gradients with a spot size in the nanometer range (Coyer, Garcia et al. 2007). The original method required a expensive silicon (Si) master patterned using an electron beam with the inverse nanoscale level of resolution pattern which was employed to lift-off undesired proteins from a flat stamp, and was then printed against the target substrate to form the desired pattern. Although this method allows recycling the e-beam patterned Si master, during each passage it is being coated with displaced proteins, some of which adhere irreversibly and cannot be removed by cleaning, leading to a gradual and irreversible deterioration of the master after as few as tens prints. This technique was recently used to pattern nanoarrays of viruses (Solis, Coyer et al. 2010), but no cell response to proteins obtained using this method has been reported. In addition to microcontact printing as a tool to create protein nanopatterns, a number of techniques have been developed that can yield greater resolution, but these improvements come at a greater cost and there is a significant loss in throughput.

Modern techniques for nanopatterning of proteins:

As previously mentioned, microcontact printing is a relatively straight forward approach for patterning proteins at the nanoscale level of resolution; however it is not the only available technique that can successfully yield protein nanopatterns. Several research groups have made use of printers to deposit protein spots at nanoscale levels of resolution or generate the desired patterns through the use of a nanochannel, also known as nanopen (Taha, Marks et al. 2003). Other groups have further enhanced the pattern accuracy by using an Atomic Force Microscope cantilever to either deposit proteins individually (Wadu-Mesthrige, Xu et al. 1999) or scrape off proteins in undesired

locations (Wilson, Martin et al. 2001). The drawback of these three techniques is that they are extremely time consuming and quite expensive. More recently, with the increased proliferation of standard microfabrication techniques for biological applications, several groups have opted to etch protein patterns by electron beam lithography (Harnett, Satyalakshmi et al. 2001). The wide adoption of this technique is once again limited by its high cost. Microcontact printing, on the other hand, does not require expensive equipment, is not time consuming and is not limited in size or geometry when applying the new liftoff technique.

A major limitation of microcontact printing that remains is the single inking solution limit per print. To obtain a pattern composed of multiple inking solutions, the printing of multiple inks can be conducted on the same area subsequently, however this requires the precise alignment of the stamps, which has been accomplished with some complex devices, but only resulted in limited success (Choonee and Syms 2010; Trinkle and Lee 2011).

Rationale

The project presented here focuses on the development of a facile, rapid and inexpensive method to generate geometric protein gradients at the nanoscale level of resolution. We decided to work on the conception of this technique for several reasons. The first is that a number of these complex gradients are present throughout the organism and play essential roles in development as well as potentially during regeneration of the nervous system, yet their mechanism remains unclear. There is a lack of currently available gradient generators that can be tailored and controlled to the extent that we desire for further experiments. Secondly, current methods available to replicate these

gradients in vitro have significant drawbacks that prevent the use of such gradient generators for our application, mainly due to the inaccurate quantification and control of surface-bound gradients. Thus, to obtain the protein nanogradients desired to study surface-bound chemotrophic gradients essential in neural development, we decided to focus on the development of a surface patterning method that allows for the creation of protein nanopatterns. First, we optimized one of the most standard surface patterning techniques, microcontact printing, at the micrometer level of resolution. Secondly, due to the high protein content in the cell media, we had to obtain specific cell response to the patterned protein by neutralizing the surface background, the non-printed portion surrounding the printed areas. We then showed that microcontact printing was applicable to neurobiology by creating island co-cultures of neurons and astrocytes, a technique widely used to study synapse function. We then extended our findings to the sub-micron level of resolution and developed a novel nanocontact printing process. Finally, nanogradients were used to study the commissural neuron response to the netrin-1 gradient present across the spinal cord by creating a surface bound netrin-1 gradient in vitro and seeding commissural neurons.

Chapter 2: Microcontact Printing

Since 1998, when microcontact printing was adapted to pattern protein microfeatures, the technique has been modified greatly, usually with a very limited interpretation of the underlying reasoning as well as the implications of the variations on the obtained results. In order to obtain the best possible protein patterning results using microcontact printing, we decided to investigate every component of the printing process in order to obtain a fully optimized process.

Fabrication of a Master through Microfabrication

Masks were drawn in the design software Clewin (Wieweb Software, Hengelo, Netherlands). The drawings were then sent to FineLine Imaging (Colorado Springs, CO, USA) for chrome etching of the glass plates. In the McGill Nanotools microfabrication cleanroom, four inch borosilicate glass wafers (Montco Silicon Technologies, San Jose, CA, USA) were cleaned in acetone (Sigma-Aldrich, Oakville, ON, Canada), isopropanol (Sigma-Aldrich, Oakville, ON, Canada) and distilled water for 10 minutes each. The wafers were then dipped into Hydrofluoric acid (Sigma-Aldrich, Oakville, ON, Canada) for 1 minute before being rinsed in distilled water and drying under a stream of Nitrogen gas. Once the wafers were completely cleaned, they were coated with SU-8 2015(MicroChem, Newton, MA, USA), for bigger features such as the stripe patterns, using a site coater (Siteservices, Santa Clara, CA, USA) and spun into a thin layer of 15 µm at 1900 rpms for 45 seconds. The wafer was then soft-baked on the same machine for 3 minutes at 95°C. Using chrome etched masks containing the desired negative design (FineLine Solutions, Winnipeg, MB, Canada), the wafer was inserted into a

photolithography exposure machine (EVG, Albany, NY, USA) and separated from the mask by 1μm before being exposed to a single dose of 220 mJ/cm². After the exposure, the wafer was baked once more at 95°C for 4 minutes on a hot plate (Fisher Scientific, Ottawa, ON, Canada). Following the post-bake, the wafer was developed in SU-8 developer (MicroChem, Newton, MA, USA) for 4 minutes before being rinsed in isopropanol. To complete the fabrication process, the wafer was first dried by spinning on a spin coater (Laurell, North Wales, PA, USA) for 5 minutes by increasing the speed from 500 rpm to 2500 rpm followed by a 5 minute hard bake at 150°C (Stoelting, Wood Dale, II, USA). For smaller features such as the 1-5 μm dots, Shipley S1813 (Microchem, Newton, MA, USA) was used as a photoresist by spin coating a 2.5 μm thin layer at 1400 rpm. The photoresist was then soft baked for one minute at 115°C, exposed to one dose of 120 mJ/cm², developed in MF319 (Microchem, Newton, MA, USA) for 90 seconds and hard baked at 90°C for 90 seconds.

Microcontact Printing Technique Optimization

PDMS mixing:

Our lab uses a Poly(dimethylsiloxane) (PDMS) mixer (Dow Corning, Corning, NY, USA) which is designed to accurately mix, resulting in the homogeneous reacting of an ethylene terminated PDMS prepolymer with a poly(dimethylhydrosilane) cross linker (Sylgard 184, Dow Corning, Corning, NY, USA) in a 10:1 ratio. However, earlier findings suggested that the mixer is insufficient to yield a homogeneously mixed PDMS solution (Sloan T., Juncker D., Charron F., unpublished results). This incomplete mixing resulted in wavy surfaces as well as sticky PDMS after curing, but more importantly inconsistent stamps obtained following the mixing process. It was indicated to us, that the

mixing was insufficient and that complete mixing of the PDMS and thorough curing was critical to obtain nonsticky stamps reproducibly (Delamarche E., personal communication). To apply this, in addition to the mixer, the PDMS was manually mixed for a period of 3 minutes, followed by a thorough degassing process and then cured thoroughly for a period of 24 hours. The resulting stamps lacked waviness and all sticky portions of stamps were eliminated.

PDMS extraction:

After determining that the proper mixing resulted in the casting of homogenous PDMS, we noticed that when contact printing, particulate matter was transferred in the areas of contact (Figure 5). This suggested that the PDMS should be extracted to remove all

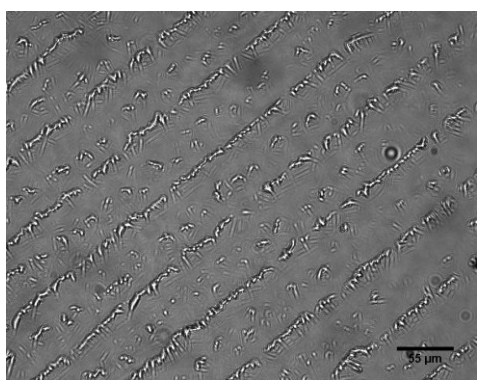


Figure 5: Residues transferred through non-extracted microcontact printing stamps. Bright-light microscopy image of a clean glass slide after microcontact printing of stripes of fluorescent antibody where the residues are visible in the stripe patterns and between the stripes whereas if the printing process what clean, nothing should be visible as the transferred proteins are too small to visualize in this manner, scale bar 55 µm.

residual unpolymerized PDMS particles and oils. The two most commonly used extraction techniques use toluene and ethanol. Due to the heightened toxicity of the toluene and with no clear advantage over ethanol, we decided to extract the stamps with ethanol for a period of 24 hours followed by 6 hours baking at 60°C to evaporate all residual ethanol. This extraction resulted in the elimination of transferred trace particles in the printing process.

Stamp Size:

Next, we investigated the ideal stamp size. As the size of the stamps that were utilized was increased, the likelihood of feature collapse and bubble entrapment increased. In addition, the size of the 1.2 mm diameter coverslips used for neuronal cell culture limited the maximum stamp size. We found that 0.5 cm by 1 cm was advantageous over larger stamps since the tweezers used to handle the stamps can only be opened a limited distance which is perfectly suited for this dimensionality.

Inking Solution:

Having determined the ideal stamp size, fabrication and sterilization methods, we examined the inking solution quantity, concentration and its incubation period. In the past to minimize the amount of protein used to cover the stamp, research groups have used a pipette to spread the solution all over the stamp (Ding, Zhou et al. 2006) or have altered the surface chemistry of the polymer (Xu, Taylor et al. 2003) to reduce its hydrophobicity. Instead, we chose to cover the protein drop with a plasma activated hydrophilic coverslip that spread the drop evenly onto the surface of the PDMS stamp. We determined that the minimum amount of ink required to fully coat the surface of the stamp, using the coverslip spreading technique, was 10 µl. To optimize the concentration of proteins used, we used a fluorescent secondary antibody (chicken anti-goat Alexa Fluor 488, Invitrogen, Burlington, ON, Canada). This fluorescent antibody served as a tracker employed in further experiments. The ideal concentration was determined to be 25 μg/ml of protein solution which yielded highly fluorescent homogenous patterns that could easily be discerned under a fluorescent microscope with 1 sec exposure. Even though 25 µg/ml, was determined to be the optimum inking solution for this biomolecule to visualize it, the concentration of the patterned protein to obtain cell response will differ. The response of the cell to the protein will vary based on the patterned protein as well as the cell used. We determined the optimum concentration of netirn-1 patterned for commissural neurons to respond. Neurons successfully sensed patterned netrin-1 at half the concentration of the optimized visualized protein (12.5µg/ml). Other proteins required much higher concentrations to obtain a successful inking of the stamp as well as subsequent transfer. One such protein that we patterned is the highly negatively charged glycosaminoglycan heparin (Nelson and Cox 2004), which required four times more concentrated solutions than that of optimized visualized protein (100 µg/ml). Due to these significant differences in protein adsorption to the stamp and the substrate and because of the applications for which microcontact printing is being used, the concentration will have to be optimized for each biomolecule.

Incubation:

Next, we investigated the optimum incubation time. Incubation times in past reported microcontact printing techniques have varied drastically, ranging from less than 5 minutes (Shen, Qi et al. 2008) to over 2 hours (von Philipsborn, Lang et al. 2006). We tested a number of incubation periods and printed the stamps on a cleaned glass substrate. We found that shorter incubation times resulted in lower binding of fluorescent proteins to the stamp and lower subsequent transfer onto the substrate resulting in lower fluorescence emission. This low fluorescence requires longer exposures that may lead to greater denaturation of the patterned protein. We also found that longer incubation times resulted in the protein drying which again may result in denaturation and further transfer inconsistencies in the stamping process. We therefore chose to incubate our protein

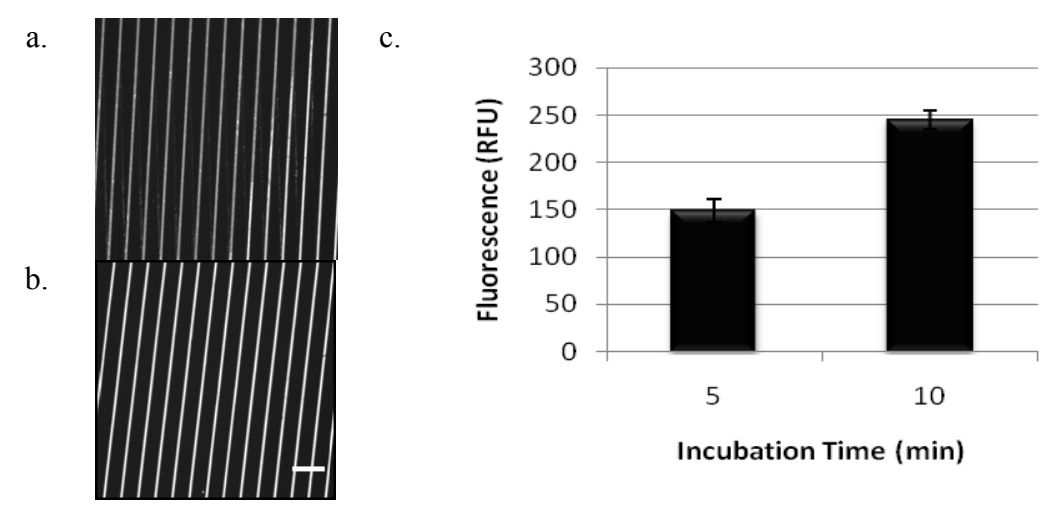


Figure 6: Effect of incubation time on protein transfer. Incubation test showing an incubation of (a) 5min and an optimum incubation of (b) 10min with (c) the quantification of the relative fluorescence of a printed fluorescent antibody at the two incubation time periods, scale bar $50 \mu m$.

solution for 10 minutes for all our work given the results obtained (Figure 6). In addition, to minimize the drying, humid kimwipes were placed in the closed petri dish during incubation.

Washing:

Different wash buffers and wash times were employed to remove unbound proteins and we found that a wash time of 15 seconds was sufficient to remove most unbound protein. Further washing had no added effect. We also found that a solution of 1x PBS was ideal to remove unbound proteins. However, because the strong salt concentration can affect imaging after salt crystallization, the PBS must be washed off with double distilled water with another 15 second wash as the optimum washing time to eliminate residual salts. Reducing the wash time of either rinsing solution resulted in non homogenous protein transfer or protein clumping, while increasing the wash time had no significant effect within the 1 minute time limit of our process.

Drying:

To properly transfer the protein to the substrate, no water molecules can be present as they will preferentially be transferred onto the hydrophilic substrate over the protein and thereby conflict with the conformal binding of the stamp to the substrate. To remove the wash water coating the surface of the PDMS stamp, a stream of compressed nitrogen gas is blown over the surface of the stamp to displace residual water droplets. We observed that with longer drying times, residues were left on the pattern (Figure 7) and cell responses were diminished probably due to the denaturation of the patterned proteins.

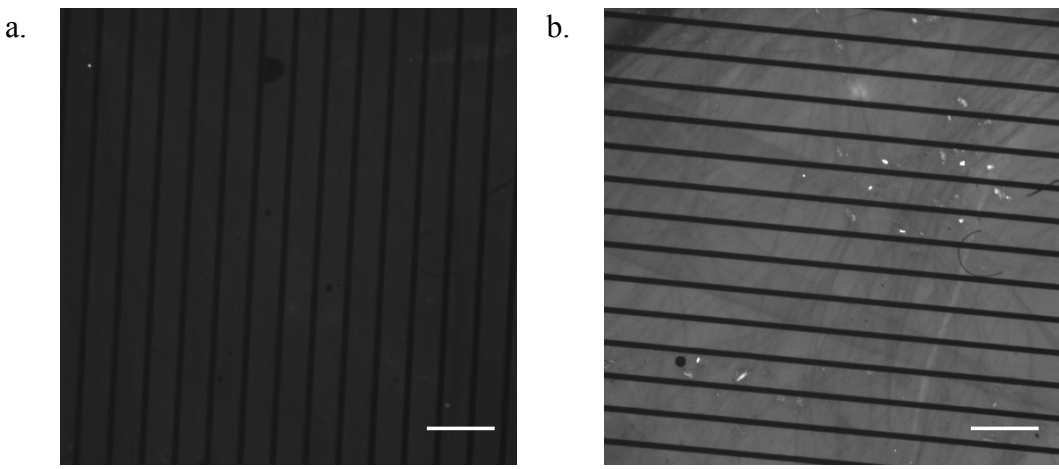


Figure 7: Effect of drying times on protein transfer with a quick (a) 5 second high-pressure air flow and (b) 15 second high-pressure air flow, scale bar 100 μm.

Substrate:

We considered the effect of plasma treating the substrate to raise the surface energy of the substrate. Protein typically transfers onto a higher energy substrate so we expected the transfer to be reduced when occurring onto a glass slide with no increased energy level (Bernard, Delamarche et al. 1998; Chen, Dressick et al. 2002). Consistent with this, we observed that protein transfer did occur, but at a reduced rate. Protein transfer on the uncharged glass slide was approximately $64 \pm 6.5\%$ of the protein transferred when transferring to a plasma activated glass slide (Figure 8).

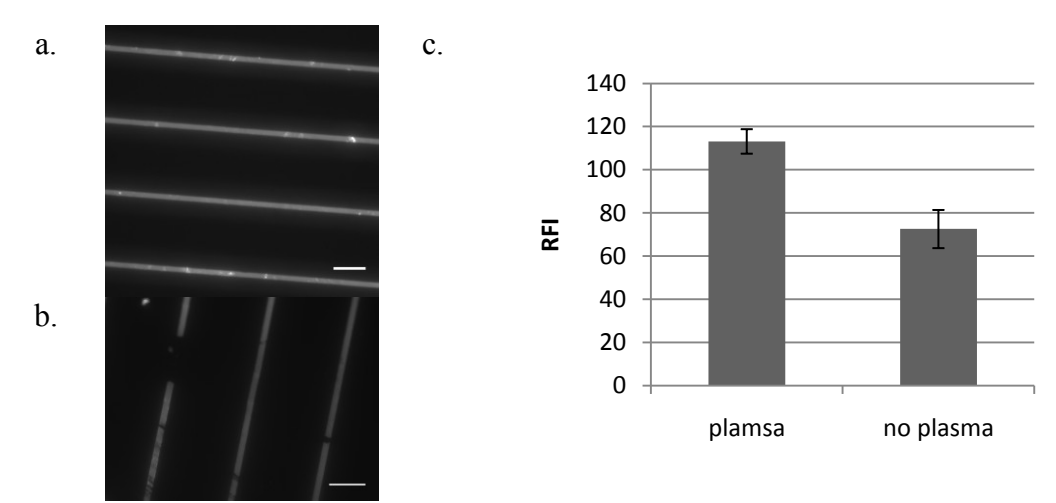


Figure 8: Effect of Plasma treatment of the substrate onto protein transfer with a (a) plasma activated substrate versus (b) a native slide (c) quantified showing relative fluorescent units, scale bar 50 μm.

Printing:

In previous papers, the contact time between the stamp and the final substrate has varied widely, with times ranging from milliseconds (Helmuth, Schmid et al. 2006) to half an hour (Lee, Huie et al. 2002). We found that the optimum time for protein transfer was 15 seconds because such a short periods of time allowed the stamp to remain humid and presumably prevented the protein on its surface from completely drying out. Additionally, we wanted to look at the protein transfer from the stamp surface to the substrate to understand how the protein transfer occurs and to what extent. To do so, fluorescent antibodies were printed under an inverted fluorescent microscope. The results of this experiment showed that 100% of the protein is transferred from the contact site onto the substrate during the printing process. It is important to note that the ridges of the features on the PDMS stamp can serve as protein reservoirs so they can transfer additional protein during a second print when additional force is applied to the stamp, but, the protein is restricted to the ridges and therefore cannot yield nano lines (Figure 9).

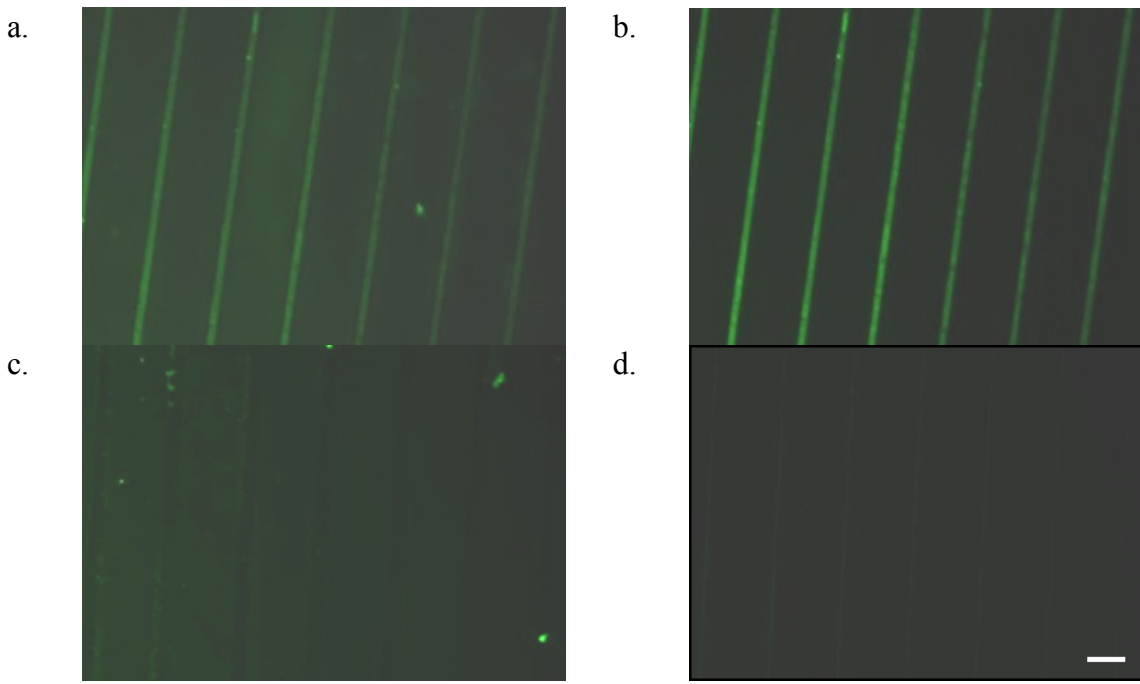


Figure 9: Quantification of protein transferred onto the substrate from the PDMS stamp during the microcontact printing process. (a) The PDMS stamp is shown contacting the glass substrate and transferring the protein, (b) next, the stamp is separated from the substrate where the protein remains, while (c) the protein on the contacted area of the stamp is removed. When the stamp is contacted with the substrate a second time, (d) residual protein from the sides of the features is transferred onto the glass, scale bar $50 \ \mu m$.

To obtain a complete understanding of protein deposition in the microcontact printing process, we conducted scanning near-field optical microscopy (SNOM) using an MFP-3D-BIO atomic force microscope (AFM) (Asylum Research, Santa Barbara, CA, USA) mounted on an Olympus IX-71 inverted optical microscope (Olympus, Markham, ON, Canada). We employed SNOM tips to image the samples by fluorescence microscopy and topography simultaneously in a tapping mode (LeDue, Lopez-Ayon et al. 2009). Through this method we realized that fluorescence microscopy is not the best indicator of homogenous protein deposition (Figure 10) though it seems that the protein deposition is homogenous by fluorescence analysis, we see with AFM that the common coffee ring phenomena (Hu and Larson 2006) is encountered here as well. Though this is not a significant issue because the protein transfer remains successful, it is something to

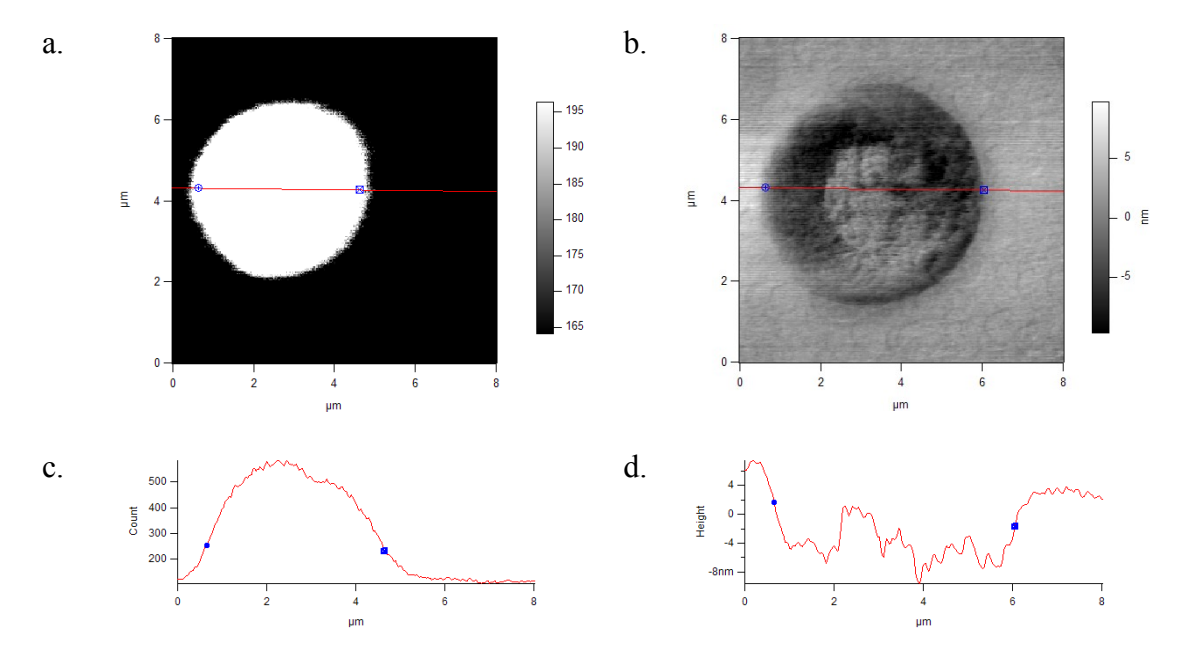


Figure 10: SNOM images of 5 μ m spot of fluorescent secondary antibody patterned through microcontact printing imaged through (a) fluorescence microscopy as well as (b) atomic force microscopy. In both cases, the red line with the two blue dots indicates the location where the cross-section was conducted to yield the respective graphs of (c) relative fluorescence and (d) topography.

be aware of because cells may respond to the fluctuations of protein concentrations across the patterned features. We hypothesize that the coffee ring has been drastically reduced from those shown here with the currently applied optimized technique (presented below), but experiments to confirm this have not been conducted as yet.

Co-localization of Marker Fluorescent Antibodies for Visualization:

To reduce the background that results from immunodetection of the patterned proteins, we decided to use a co-localization approach that has previously been reported (Liu, Loerke et al. 2009). In this approach, a secondary fluorescent antibody is mixed with the protein inking solution and eliminates the need for an expensive specific antibody for the patterned protein. To verify that the secondary antibody did not diffuse from the patterned area, an experiment was conducted in which patterned fibronectin was colocalized with a fluorescent antibody and detected with a FITC-tagged fibronectin-

specific antibody (Figure 11). The result clearly show that the result obtained with the colocalization and those obtained with the fibronectin specific antibody are the same, but

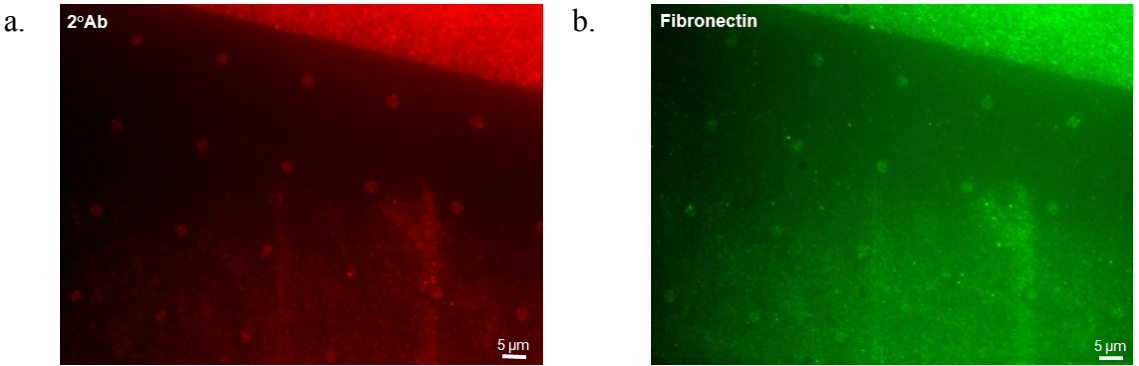


Figure 11: Fluorescent images of the co-localized antibody with the protein of choice. Microcontact printed fibronectin visualized fluorescently by mixing a fluorescent antibody (a) in the staining solution and (b) by applying a fibronectin specific antibody.

background noise is drastically reduced by using the co-localization approach. In addition, to suit the co-localization with the staining of specific cell components that might not as easily be labelled in a different color; we developed a palette of co-localizing antibodies that were always mixed at a concentration of 25 μg/ml in the inking solution. The palette was composed of chicken anti-goat Alexa Fluor 488 (Invitrogen, Burlington, ON, Canada) for green patterns, donkey anti-sheep Alexa Fluor 532 (Invitrogen, Burlington, ON, Canada) for red patterns and goat anti-mouse Alexa Fluor 350 (Invitrogen, Burlington, ON, Canada) for blue features, but the co-localization antibodies are not limited to those mentioned and can be adapted to different organisms and other emissions.

Optimized Microcontact Printing Technique

Mask and nanowafer Design:

Masks with micron features were designed and fabricated as described above in this chapter, while nanopatterns designed in Clewin were sent to INRS (Institut National de la

Recherche Scientifique, Laval, QC, Canasa) for electron beam (e-beam) lithography and deep reactive ion etching.

PDMS:

The pre-polymer and cross linker were mixed in a 10:1 ratio with the help of a mixer-pouring device and manual mixing to ensure thorough mixing. Once a homogenous solution was achieved, the wafer was prepared by depositing a monolayer of 97% Perfluorodecyltriethoxysilane (Sigma-Aldrich, Oakville, ON, Canada) and evaporating in a vacuum chamber (Bel-art, Pequannock, NJ, USA) for 30 minutes. Following the silanization of the wafer, a layer of ~6mm of 1:10 PDMS was manually mixed and deposited on the wafer. To remove bubbles that result from manual mixing, the coated wafer was placed in a dessiccater for 10 minutes. Any remaining surface bubbles were then blown off with a gentle stream of compressed nitrogen gas before curing the PDMS in an oven (VWR, Ville Mont-Royal, QC, CANADA) for 24 hours at 60°C to allow polymerization to occur. To obtain stamps with no topography and an atomically flat surface for liftoff nanocontact printing, PDMS was cured atop a clean Si wafer without any photoresist deposition.

Stamp manufacturing:

Upon completion of PDMS polymerization the cured polymer was peeled off of the wafer and cut into small, easily handled squares by using a scalpel (Fisher Scientific, Ottawa, ON, Canada). To remove low molecular weight PDMS and residual pre-polymer still present throughout the cured PDMS, the squares of PDMS were then extracted in 70% Ethanol for 24 hours and baked at 60°C for 4 hours. In addition to removing

impurities, the ethanol incubation step sterilizes the stamps and renders them appropriate for further use in biological experiments.

Microcontact printing:

Stamps were examined under the microscope to identify and discard defective stamps. Desirable stamps were placed in 70% ethanol for 5 minutes in an ultrasonic bath to sterilize the stamps once more. Once sterile, the stamps were dried under a flow of nitrogen gas. After drying, the stamps were inked with 10µl of solution. To minimize the amount of solution utilized in the experiments, a plasma (Plasmaline) treated coverslip (Carolina Biologicals) was placed on the drop of solution to spread out the solution. The solution was left at room temperature for 5 minutes to bind to the surface of the stamp. Once incubation was complete, the stamp was rinsed for 15 seconds in 1x PBS (Fisher Scientific, Ottawa, ON, Canada), followed by a 15 seconds double distilled water wash (Millipore, Billerica, MA, USA). After washing, the stamp was quickly blown dry with a strong jet of nitrogen gas. The stamps were then immediately contacted with a plasma-activated substrate for 5-15 seconds. If the patterned substrate was not meant for immediate imaging purposes, the pattern could be saved for several months if stored in 1x PBS and kept in a dark place at 4°C.

Conclusions

Here we successfully optimized the microcontact printing procedure to minimize the time of each print and maximize throughput. While conducting the optimization, we also minimized the drying of the protein, the quantity of the protein solution required and the time of contact. In doing so, we succeeded in creating a rapid process that accurately and reproducibly patterns proteins in a predetermined manner (Figure 12). The process developed can produce prints within 15 minutes and it can produce multiple prints simultaneously. Prints for a 24-well plate can be completed within 30 minutes. The new optimized process competes with some of the so-called rapid microcontact printing techniques (Shen, Qi et al. 2008) and yet yields more reproducible and homogeneous prints. Although it is not the fastest procedure currently available, the other methods require expensive equipment (Helmuth, Schmid et al. 2006; Khanna 2008). The cost of this process remains low and is widely accessible to the general scientific community because it does not require expensive equipment.

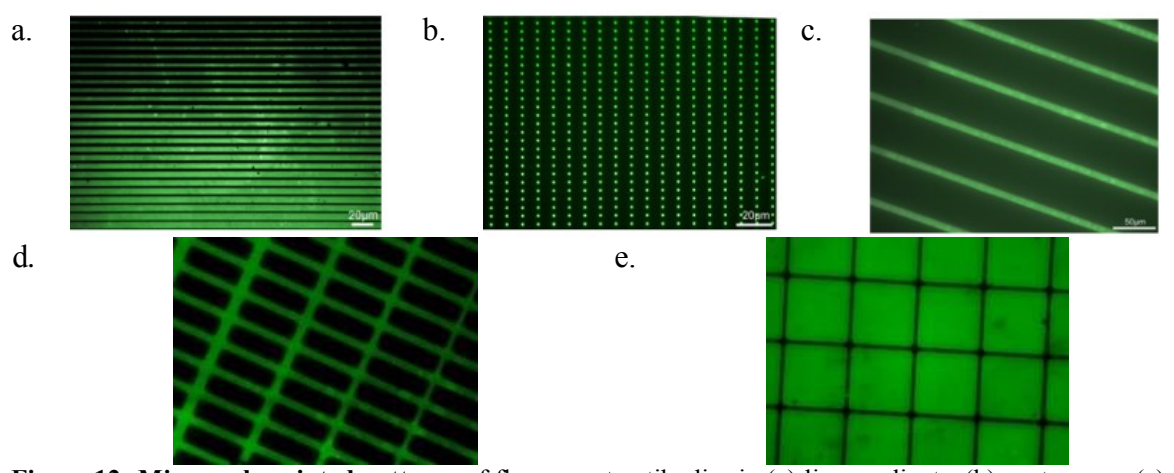


Figure 12: Microscale printed patterns of fluorescent antibodies in (a) line gradients, (b) spot arrays, (c) stripes, (d) gradient grid and (e) large squares geometrical arrangements.

Chapter 3: Cellular Response to Patterns

Following the successful patterning of protein micropatterns using microcontact printing, we wish to show that cells do respond to this level of magnitude in size before drastically reducing the feature size and the number of proteins encompassed within that feature for the cell to respond to. As mentioned in the introduction, numerous studies have patterned proteins to investigate, for example, the cell's binding abilities, motility, or differentiation; however, the cell response in many of these studies was never shown to be caused exclusively by the surface-bound protein. To ensure that the responses observed in our experiments will be caused by the printed proteins, we examine how the background, the area where protein was not transferred through the printing process, affects cell reaction and employ a rapid backfilling process to tailor the background in a controlled fashion that enables us to adjust background adhesion so as to maximize the cell response to the targeted protein patterns.

Experimental Methods

PEG Backfill:

To create a biologically inert surface where the proteins present in the serum cannot bind to the substrate, we utilized poly-L-lysine grafted polyethylene glycol (PLL-g-PEG). In order to allow the PLL chains to bind to the substrate, a solution of PLL(20)-g[3.5]-PEG[2] (SurfaceSolutions, Grande Prairie, AB, Canada) at a concentration of 10μg/ml in PBS was incubated for 15 minutes before washing off unbound PLL-g-PEG with 1x PBS.

Cell cultures:

C2C12, HEK293, U87, and astrocyte cells were cultured in flasks in 10% fetal bovine serum (Invitrogen, Burlington, ON, Canada) and 5% Pennicillin/ Streptavidin (Invitrogen, Burlington, ON, Canada) Dulbecco's Modified Eagle Medium (Invitrogen, Burlington, ON, Canada). The cells were trypsinized (Invitrogen, Burlington, ON, Canada) prior to being seeded on patterned substrates. Cells were grown in a temperature-controlled incubator (Thermo Scientific, Neppean, ON, Canada) at 37°C with 5% CO₂.

Commissural neuron cultures:

Spinal commissural neuron cultures were obtained from E14.5 rats (Moore and Kennedy 2008) and cultured for a period of 2 days in neurobasal/FBS culture medium prior to fixing the neurons.

Immunocytochemisty:

After satisfactory cell growth was achieved, cells were fixed in 4% PFA solution (4% paraformaldehyde (PFA), 0.0015% 1M NaOH in 1x PBS) for 1 minute. After fixation, the cells were permeabilized in Perm buffer (0.15% Triton X-100 in 1x PBS) for 5 minutes. The samples were then blocked with blocking solution (3% Horse Serum, 0.1% Triton X-100 in 1x PBS) and left overnight in a 4°C dark room. After blocking, a staining solution (1% Horse Serum, 0.1% Triton X-100 in 1x PBS) with antibodies (1:500), phalloidin conjugated to Alexa Fluor 555 (1:250, Invitrogen, Burlington, ON, Canada) and/or with Hoechst stain (1:100, Invitrogen, Burlington, ON, Canada) was added to the samples and placed on a rocking plate (VWR, Ville Mont-Royal, QC, CANADA) for 1 hour. Samples were then washed 3 times for 5 minutes each time in 1xPBS and a

secondary antibody (1:500) solution was applied if required for the specific experiment. After staining and washing, the samples were briefly rinsed in double distilled water before mounting the slides with fluorogel (Electron Microscopy Sciences) and fixing the coverslips with clear nail polish.

Imaging:

Fluorescent imaging was conducted on a customized C1Si inverted confocal microscope (Nikon). Dark field and DIC imaging were conducted on an LV150A Industrial microscope (Nikon).

Cell Culture Technique Optimization:

Once the patterns have been printed, cells must be grown on the substrate and respond specifically to the printed protein pattern. For this response to occur, all other parameters in the three dimensional environment of the cell must be accounted for, otherwise the cells may not respond specifically to the patterned protein (Figure 13).

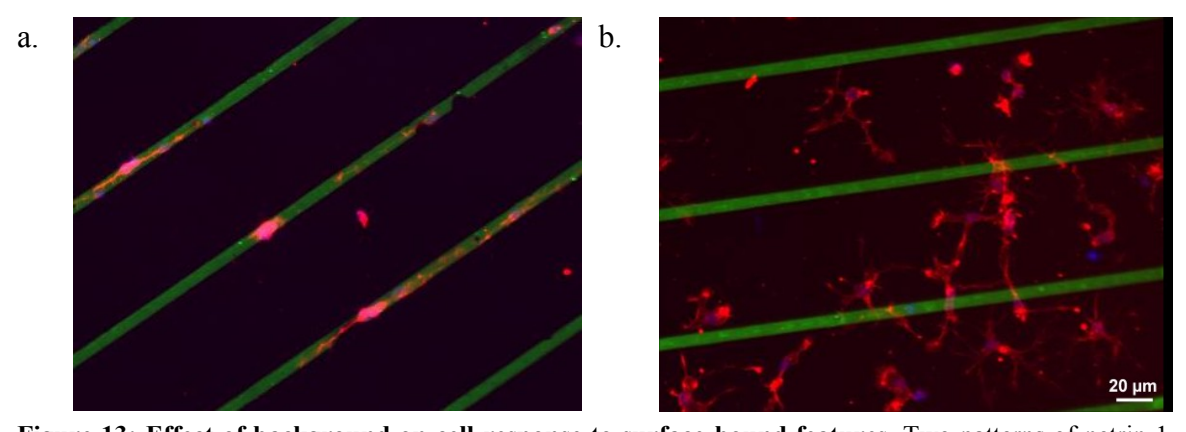


Figure 13: Effect of background on cell response to surface-bound features. Two patterns of netrin-1 stripes co-localized with a fluorescent secondary antibody (green) with commissural neurons seeded and grown on the pattern for a period of two days. (a) The background adhesion was correctly tailored to obtain the proper cell response to the pattern, while (b) the pattern was not considered in the experimental setup and the cells do not respond to the patterned protein.

Cell Media:

One such factor that must be considered is the cell media. Most cell media requires the addition of large quantities of serum. Serum is an essential component of blood which contains all the plasma except for the fibrinogen clotting factors. Serum is widely used in cell culture since it contains many growth factors that facilitate cell growth (Gospodarowicz and Moran 1976), however serum has not yet been fully characterized so all of the proteins present and their effects on cell growth have not been determined thus far. To show the impact that serum concentration has on cell growth we conducted an experiment where Human Embryonic Kidney cells 293 (HEK 293) were grown in environments with various levels of serum in the cell media. To show the specific cell response to the substrate, we coated the coverslips with poly-D-lysine. Polylysine is a small peptide consisting of a polymer of the amino acid lysine (Shima 1977). Two isomers of this molecule exist in which the lysine is either in the D or L conformation. The poly-L-lysine is the natural form that is excreted by bacteria in the environment and can be cultured (Shima and Sakai 1981), but to reduce the price and degradation rate of the polymer, a synthetic version was manufactured in the D form (Tsuyuki, Tsuyuki et al. 1956). The exact mechanism through which cells bind to the polylysine is not understood, but cells have been widely documented to attach to a polylysine substrate and the coverslip prior to cell seeding in solution (Yavin and Yavin 1974). Given the known cellular response to this environment and ease of deposition, we decided to coat the coverslips with this substrate to determine at which serum percentage the cells responded specifically to the polylysine-coated substrate (Figure 14). At a concentration of 1% serum, the cells expand and proliferate whether PDL was coated on the coverslips or not, suggesting that the serum concentration is too high and that proteins present in the serum are covering the PDL. The response of the cells is therefore non-specific to the pattern.

When the serum concentration is reduced, the cells expand and proliferate only when

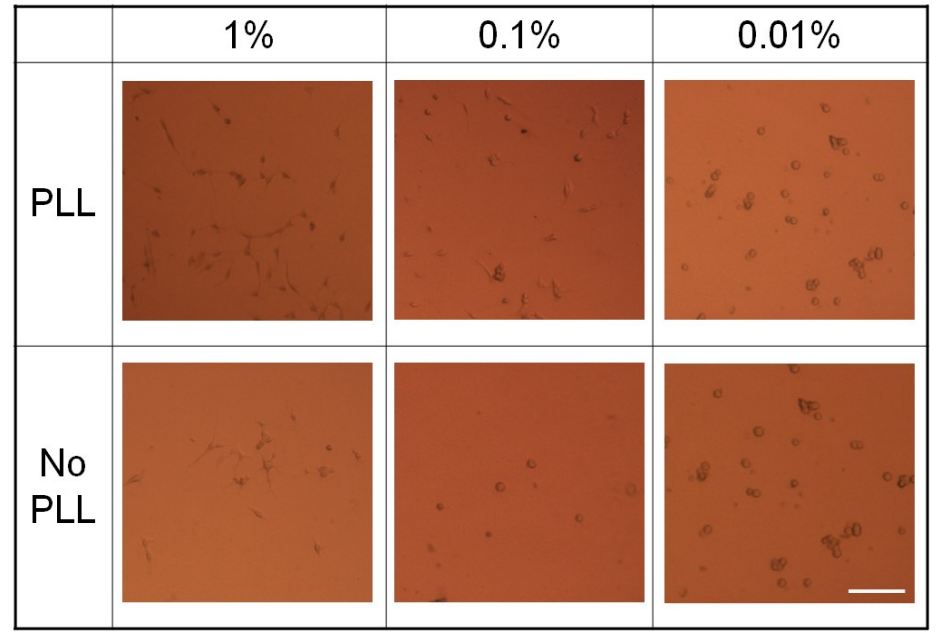


Figure 14: Cell response to patterned protein in different media concentrations. HEK 293 cells seeded and grown on PLL coated or non-coated coverslips to investigate cell response to various serum concentrations. The cells are not stained but visualised through DIC imaging, scale bar $100 \, \mu m$.

PDL is coated on the coverslip. When polylysine is not present, cells do not attach or grow well due to insufficient adhesion to the glass surface. Furthermore if the serum concentration is reduced to 0.01%, even PDL at a concentration of $10~\mu g/ml$ is insufficient to sustain growth and proliferation. These results show that the serum concentration has a tremendous impact on cellular response to patterned proteins.

Background of the Printed Protein:

To further illustrate the effect of the environment on cell growth and response, we studied the background of surface-bound protein on the coverslips in between patterned protein stripes. By background we mean the non-contacted area where protein was not transferred through the microcontact printing, but where protein adsorbs from solution.

As described above polylysine supports cell proliferation. To express the opposite cell response, growth inhibition, we use Polyethylene glycol (PEG). PEG is a polyether compound which binds very strongly to water and prevents the adhesion of protein (Sigal, Mrksich et al. 1998). For our experiments we decided to deposit the polymer in the same manner as the polylysine, in solution (Csucs, Michel et al. 2003). To permit the binding of the molecule to the glass coverslips, we used a commercially available construct of PEG linked to a Poly-L-lysine polymer that readily binds to the glass substrate and thereby facilitates the rendering of coverslips into inhibitory growth substrates.

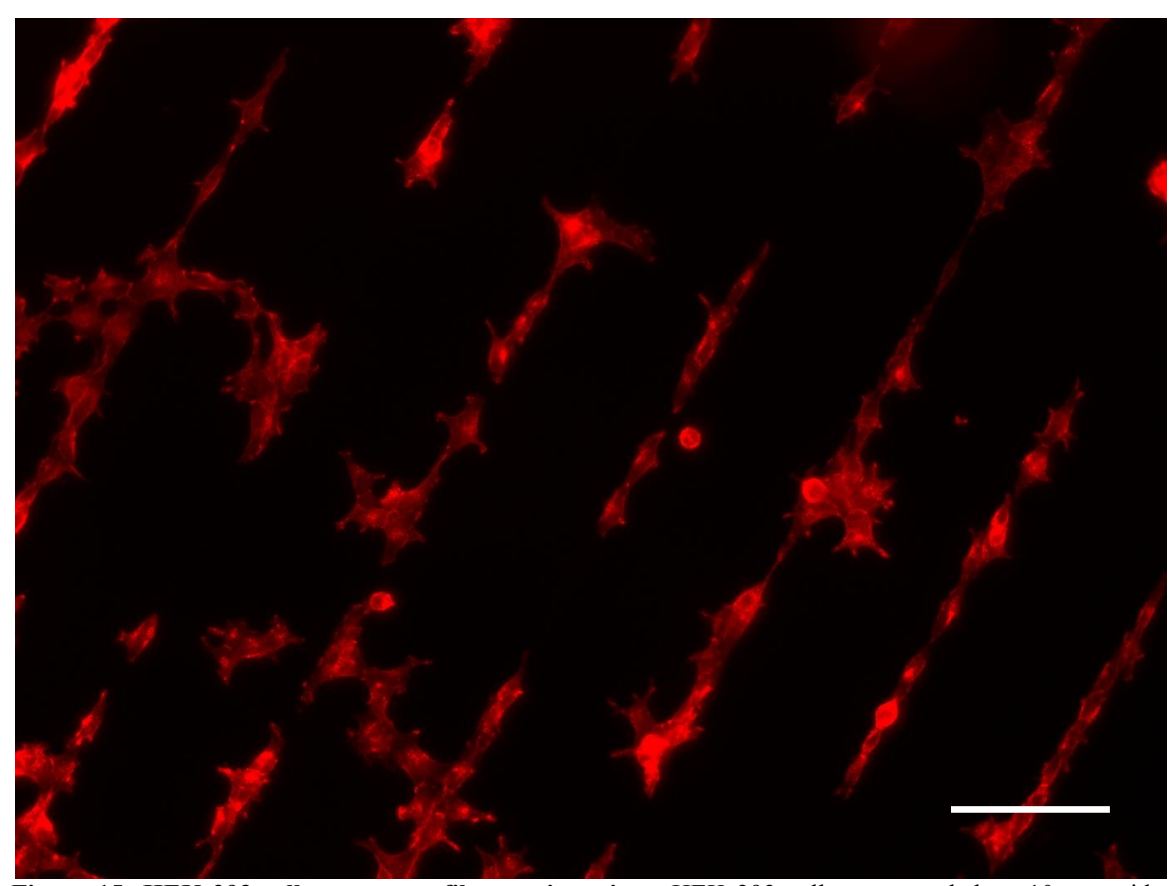


Figure 15: HEK 293 cells grown on fibronectin stripes. HEK 293 cells were seeded on $10 \mu m$ wide fibronectin stripes and grown on the pattern for 18 hours before fixing and staining for filamentous actinusing phalloidin (red), scale bar $100 \mu m$.

To investigate the effect of the background environment on the response of the cells to the stripes, we patterned stripes of fibronectin (FN). HEK 293 cells responded by aligning themselves to $10\mu m$ wide stripes (Figure 15). Consistent with this response, HEK 293 cells express the $\alpha v\beta 3$ integrin receptor and the expression of this receptor mediates FN driven migration (Simon, Nutt et al. 1997).

In order to test the effect of the background on cell response, we printed stripes of FN and then backfilled the stripes by applying a solution of various ratios of PEG-g-PLL and PLL. The morphology of the cells and the number of cells capable of adhering to the stripes and background differed depending upon the ratio between adhesive and repulsive surfaces, (Figure 16). From these experiments, it is clear that cells seeded on highly repulsive backgrounds were restricted to the stripes, while cells grown on a more permissive background proliferate all over the surface and showed no preference for the patterned stripes.

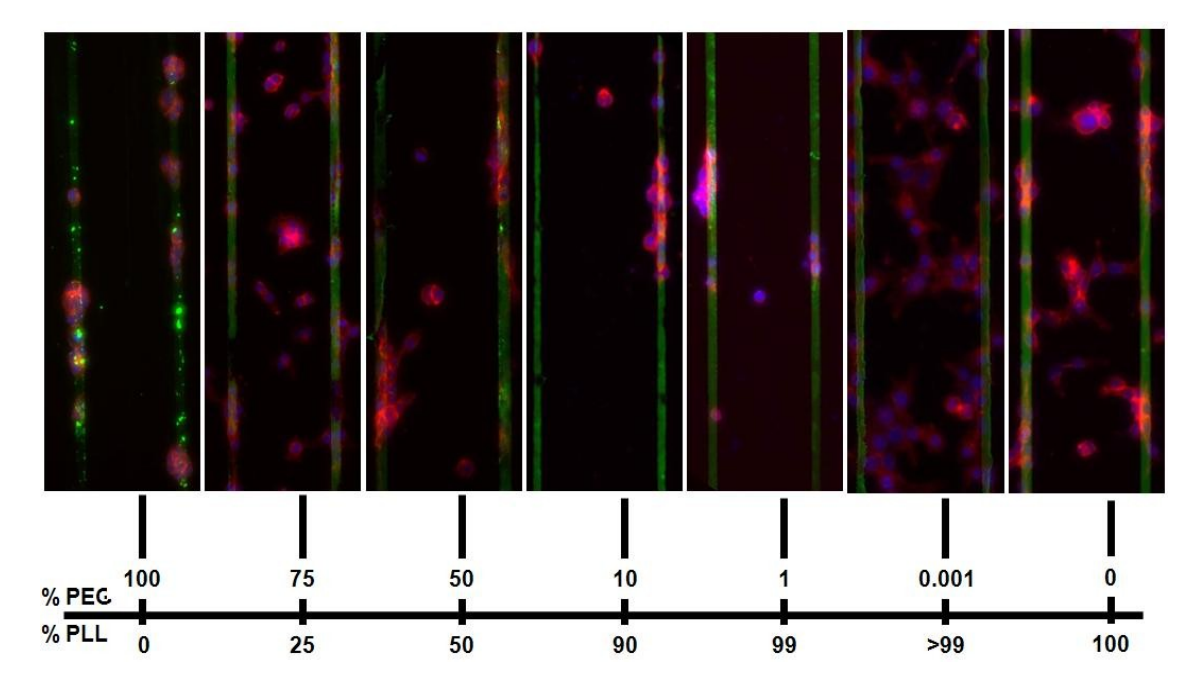


Figure 16: Response of HEK 293 cells to fibronectin stripes with altered background. HEK 293 cells seeded and grown on fibronectin stripe patterns backfilled with solutions of various PLL: PLL-g-PEG ratios grown in 0.1% serum media for 18 hours.

Based on these results and previous literature describing the cells used in our studies, we decided to use a 10 µg/ml concentration of PEG-g-PLL applied for 15 minutes on a shaking table to backfill the patterned proteins and grow the cells in 10% serum media to obtain the best cellular response (Csucs, Michel et al. 2003). Though cells are aligning onto the stripes, this may not necessarily indicate a specific interaction between the integrin receptors present on the surface of the cell with the patterned fibronectin. The stripe alignment of the cells could be due to differing charges between the patterned surface and the backfilled surface. To test whether the interactions are specific, we utilized specific markers for focal adhesions. Focal adhesions are the adhesive structures that cells make with the extra cellular matrix (ECM) in which the primary receptor-ligand binding event leads to the recruitment of specific proteins such as paxillin, zyxin, or focal adhesion kinase (FAK), to the site of binding. This complex allows the cell to generate force to move around the surface (Balaban, Schwarz et al. 2001). To test this we patterned stripes of geltrex (Invitrogen, Burlington, ON, Canada), a solution used for 3D cell culture similar to Matrigel[©], which has previously been demonstrated to drive cell adhesion (Moroi, Okuma et al. 1992). Geltrex is composed largely of laminin and collagen IV which both signal the cell through a number of receptors, among them integrin α1 (Calderwood, Tuckwell et al. 1997). This should recruit paxillin to the site of adhesion among a number of focal adhesion markers (Seo, Russell et al. 2010). We then grew C2C12 myoblast cells on the pattern and visualized paxillin using immunocytochemistry. The literature indicates that paxillin is an appropriate downstream indicator that integrin receptors are binding to the components of the geltrex stripes. The results indicate that the cell aligns with the stripes and shows a

response similar to that observed in previous experiments with fibronectin. We also see that the targeted paxillin proteins that mark the location of focal adhesions through spots of increased fluorescence, are located on the stripes and that the areas of the cells that are not atop the stripes do not form focal adhesions since they do not show any localized spots of heightened fluorescence. Background fluorescence could be reduced by transfecting the cell to express an engineered paxillin protein that is fluorescently labelled, but characterizing the consequences of overexpressing paxillin would require extensive work. The results obtained support the conclusion that specific cell-substrate interactions lead to the alignment of the cells with the stripes (Figure 17).

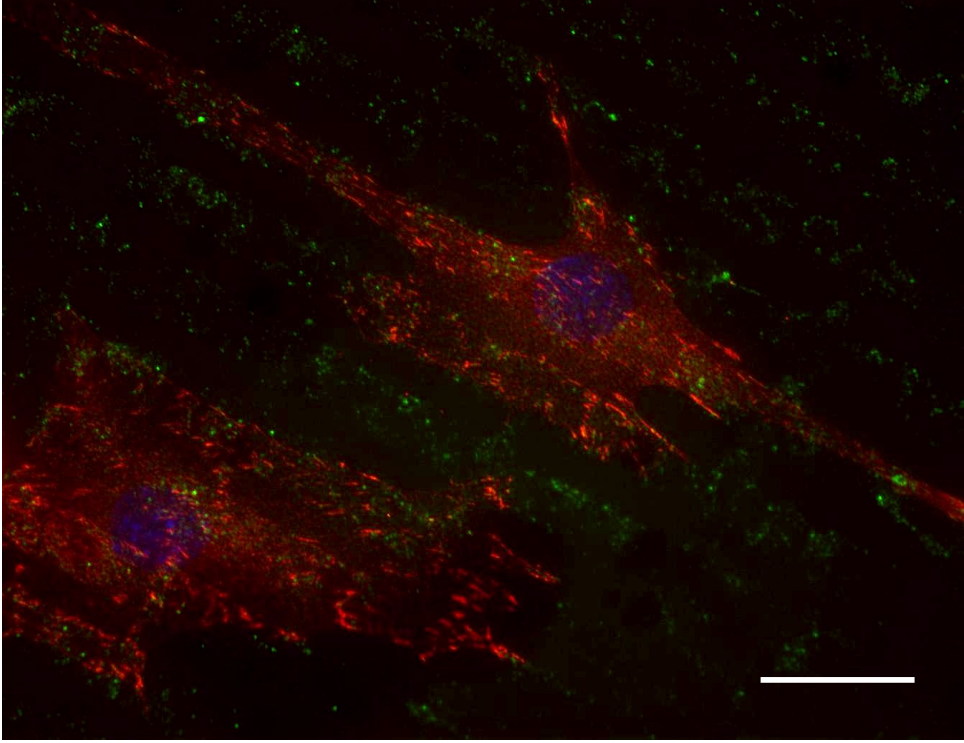


Figure 17: Stripes of Geltrex initiate the formation of focal adhesions. C2C12 cells seeded and grown on geltrex stripe patterns backfilled with PLL-g-PEG ratios grown in 0.1% serum media. The punctate staining of the geltrex stripes is the result of the gelated substance which does not favour homogenous mixing with our fluorescently labelled secondary antibody. The C2C12 cells were grown for 18hours on the substrate and stained with Hoechst and paxillin, scale bar is $25 \, \mu m$.

Results of cell response to patterned protein

Before examining primary cells, such as neurons, that require extensive care and are much more expensive to work with, we investigated the response of cell lines to a variety of protein patterns following optimization. Multiple cell lines were investigated as well as a number of proteins that yield various cell responses.

HEK 293 cell are repelled by Sparc stripes:

SPARC (secreted protein acidic and rich in cysteine), also known as osteonectin, is an ECM glycoprotein (Bornstein 1995) that plays a significant role in cell-matrix interactions during development, cellular differentiation, and cell migration (Lane and Sage 1994). Even though SPARC is present in the ECM, it does not induce cell attachment, but instead results in cell rounding (Sage and Bornstein 1991) and prevents cell spreading (Sage, Vernon et al. 1989). In addition, SPARC has been shown to disrupt focal adhesions through a mechanism that remains unclear at this point (Goldblum, Ding et al. 1994). These properties of SPARC make it an interesting subject to determine whether the microcontact printed proteins remain active following printing and if they will result in cell repulsion as predicted by prior findings. SPARC was successfully patterned at a concentration of 100 µg/ml in a stripe pattern. In order for the cells to have attachment sites on the coverslip, we did not conduct the PLL-g-PEG backfill technique and instead allowed serum derived proteins to bind to the surface and facilitate cell attachment between stripes. HEK 293 cells were preferentially aligned between the stripes of printed SPARC. In the control condition, where we patterned stripes of the secondary antibody used to detect the SPARC, the cells did not respond to the stripes (Figure 18). However cell staining was not successful because the SPARC antibody not only reacted with substrate bound SPARC, but also stained the cells as well suggesting cross reactivity or the expression of HEK 293 cells of SPARC on their surface.

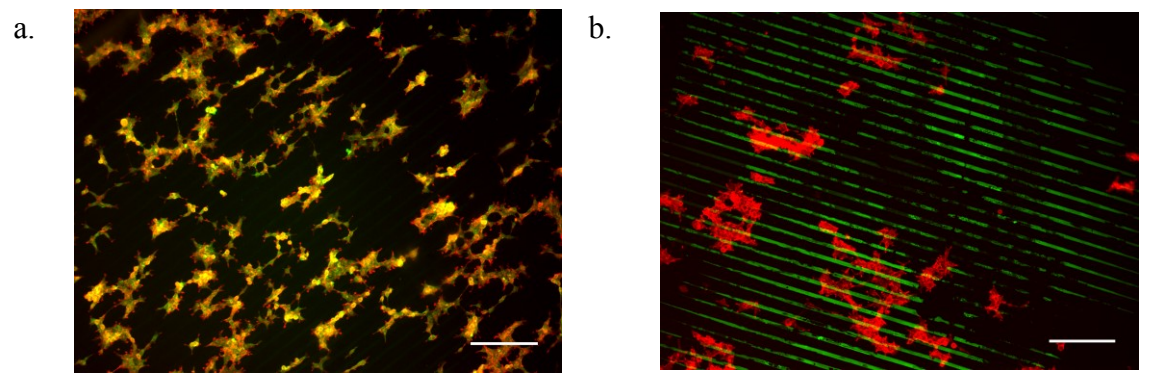
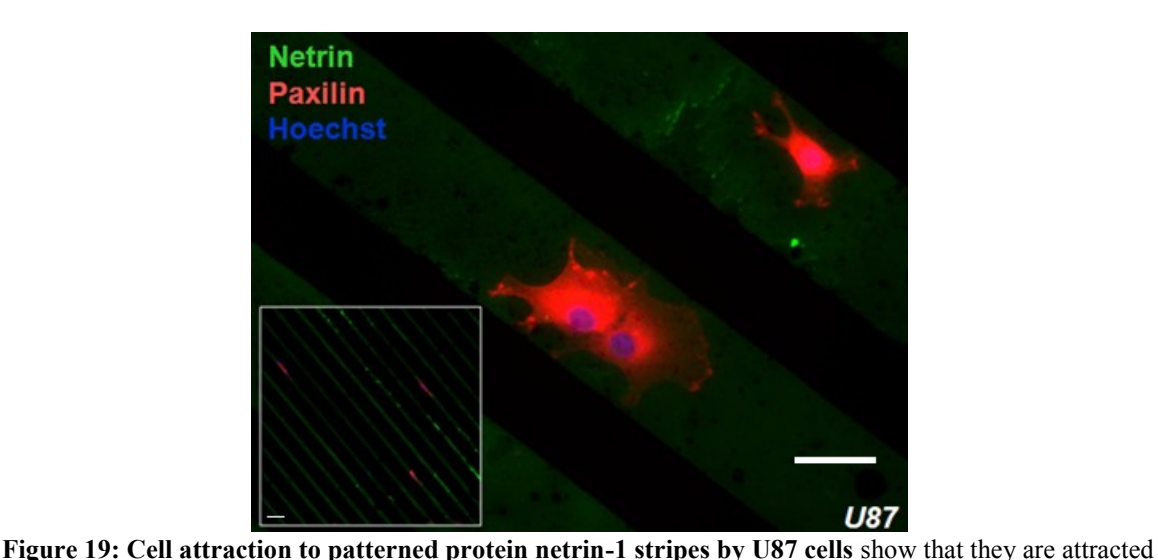


Figure 18: HEK 293 cell response to patterned SPARC protein. HEK 293 cells grown for 18 hours on microcontacted printed (a) SPARC and (b) secondary antibody stripes grown in 10% serum solution, scale bar is $100~\mu m$.

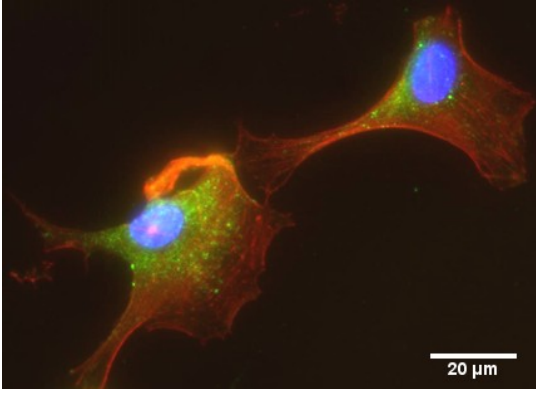
Cell line attraction to netrin-1 stripes:

In order to make sure that the patterning process could also successfully pattern attractive proteins and mediate the desired cell response, netrin-1 was pattered at a concentration of $25 \mu g/ml$ in stripes. To obtain the desired response, cells that express the proper receptors for netrin-1 had to be seeded on the pattern. We first chose to work with U87 cells, a human glioblastoma cell line (Martuza, Malick et al. 1991). Previous work conducted in the lab that indicates that these cells express the netrin-1 receptor DCC and respond in an attractive manner to netrin-1 (Jarjour et. al, unpublished). The cells responded as expected by adhering preferentially to the netrin-1 stripes, and in addition they also generated focal adhesions (Figure 19), but the size of the focal adhesions was quite small so the motility of these cells was limited.

To focus our attention on a single cell line and conduct live imaging experiments of motile cells, we switched our attention to C2C12 cells, a cell line that has been widely employed to study the formation of focal adhesion (Tu, Huang et al. 2001). C2C12 cells



to netrin stripes and grow preferentially on these stripes while making focal adhesions as shown by the accumulation of paxillin, a focal adhesion marker, on the printed stripes. Inset shows large view of cells segregated on stripes while image shows close-up on three cells, scale bars are 25 µm and 50 µm for inset. are a suitable target for our netrin-1 driven experiments since they express the netrin-1 receptor neogenin (Kang, Yi et al. 2004; Bae, Yang et al. 2009). To confirm that netrin-1 receptors are expressed by the C2C12 cells, we stained the cells with an antibody against DCC which revealed strong DCC expression at the cell surface (Figure 20). However, the antibody used does not differentiate between DCC and neogenin, so the signal might be due to expression of neogenin rather than DCC. In any case, the results confirm that the cell does express a receptor for netrin-1 and suggests that the cells may respond to the



netrin-1 patterns. In an attempt to obtain more conclusive results, a western blot analysis

Figure 20: DCC expression in C2C12 cells. C2C12 cells were seeded on PLL coated glass and grown for 18 hours before staining the cells for DCC (green) expressed in cells stained with Hoechst (blue) and phalloidin for filamentous actin(red).

was conducted. Preliminary results suggest that, as previously reported, the cell line expresses large amounts of neogenin as well as more reduced expression of DCC.

Once it was determined that netrin-1 receptors were expressed by C2C12 myoblast cells, we tested netrin-1 patterned stripes, backfilled with PLL-g-PEG and investigated the cell response over time by conducting a time lapse imaging experiment (Figure 21). To reduce the cytotoxic effect of fluorescence imaging, the images were taken in DIC. A fluorescence image of the patterned protein was taken at the beginning and at the conclusion of the time-lapse imaging to identify the location of the features as well as their displacement over the time period. No significant displacement was

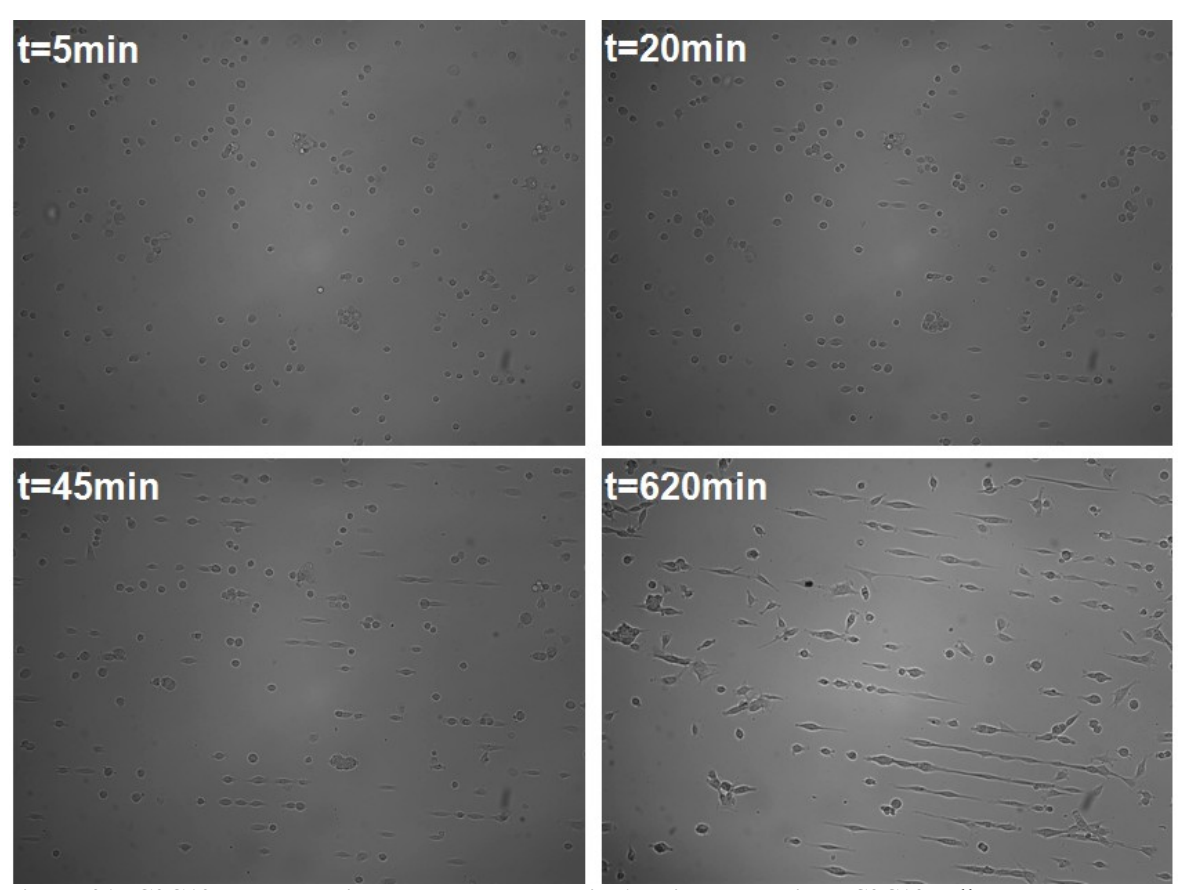


Figure 21: C2C12 cell attraction to patterned netrin-1 stripes over time. C2C12 cells were grown on netrin-1 10 μm wide stripes backfilled with PLL-g-PEG in 10% serum solution for extended periods of time with images being captured in bright field every 5 minutes over a period of 10.5 hours.

observed using our setup except when multipoint imaging was conducted. We therefore only conducted single point imaging. In the image presented we do not overlay the stripe pattern as the location of the stripes becomes apparent due to the cell response in the time-lapse video. Indeed, the C2C12 cells exhibited a very strong response that commenced as soon as they contacted the glass substrate. By 45minutes almost all the cells were localized on netrin-1 stripes and most cells had begun extending processes. In addition, as cells replicated over time, they maintained their attachment to the netrin-1 stripes and remained responsive to the pattern for as long as sufficient room for all the cells remained on the stripes. When the stripe surface area became over-saturated with cells, the cells pushed each other off the stripes into the background region. The slight displacement of the aligned cells on the image observed in this experiment at t=620 minutes was caused by the media replenishment which requires the opening and closing of the petri dish lid.

Primary cells respond to netrin-1 patterns:

Once the response of cell lines to microcontact printed netrin-1 features was established, we examined the response of neurons to netrin-1 micropatterns. To optimize the background and maximize the cell response to the printed protein, we patterned stripes of netrin-1 and backfilled with different ratios of PLL to PLL-g-PEG as described above. We then grew commissural neurons on these patterns for 2 days. With the 100% PLL-g-PEG backfill, the neurons are clearly restricted to the netrin-1 stripes and do not migrate off the stripes. As PDL was added to 25% of the backfill solution, neurons remained on the stripes, however some successfully migrate away from the stripes. At the 50:50 ratio, the neurons no longer respond specifically to the stripes (Figure 22).

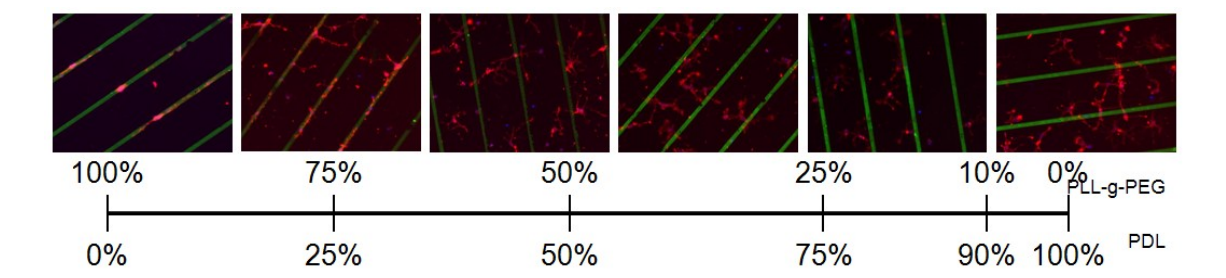


Figure 22: Differing response of Commissural neurons to netrin-1 stripes based on the varying background. Stripes of $10 \mu m$ in width of netrin-1 were backfilled with different ratios of PLL and PLL-g-PEG ranging from 100% to 0% before growing the neurons on the patterned substrate for 2 DIV.

Once optimized, the response of cultured embryonic rat spinal commissural neurons to patterned protein can be studied (**Figure 23**). The neurons clearly respond by extending their axons along the netrin-1 stripes. No somas could be found that were not located on the netrin-1 stripes within the entire patterned area. This suggests that the somas either migrated onto the stripes or the somas that were located elsewhere and did not find a sufficient attachment point were not able to mature successfully and washed off

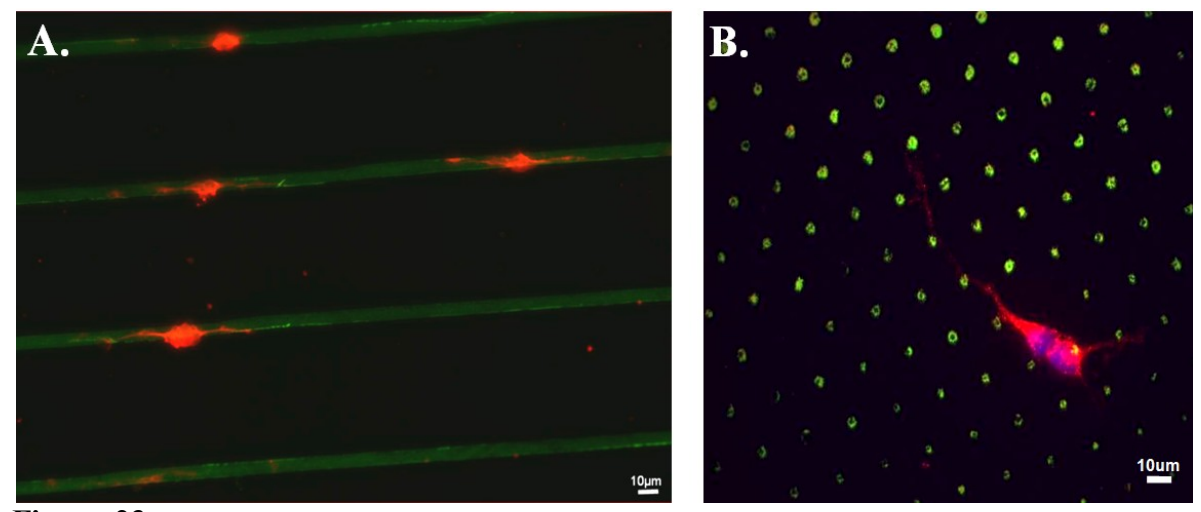


Figure 23: Commissural neuron response to netrin-1 micropatterns. (A) Attraction of neurons to 10μm netrin-1 stripes and (B) Commissural axon following 3μm netrin-1 spots. The netrin-1 was detected with an anti myc FITC bound antibody(abcam). The commisural neurons were stained for filamentous actin with phalloidin bound to AlexaFluor555 and with Hoechst, a nuclear stain. Coverslips were additionally covered with poly-D-lysine prior to cell plating for the spot pattern.

during the fixation procedure. To further investigate the cell response, an array of $5 \mu m$ spots in diameter of netrin-1 was coated with a layer of polylysine. The somas

successfully attached to the substrate coated with polylysine and extended axons through the background and appeared to follow the netrin-1 spots as they extended. These results suggest that the somas not located on the netrin-1 stripes did not form sufficient attachment and were washed off, while binding of the axon to the netrin-1 spots was sufficient to attach the neuron to the coverslip during the washing. While intriguing, these results must be repeated using live imaging to provide more conclusive results.

Conclusions

Here we applied a backfilling technique to adapt the non-patterned background in order to obtain the highest cell response to the surface-bound protein. Using this PLL-g-PEG backfill we then successfully obtained cell response to a number of patterned proteins with positive as well as negative charge. Furthermore we also obtained specific cell response of seeded cells as shown by the expression on the cell surface of focal adhesion markers. Lastly we obtained neuronal cell response to surface-bound netrin-1 microfeatures. Using the presented technique we ensure that the cell response is specific as well as the highest attainable.

Chapter 4: Application of Microcontact Printing to Neuroscience- Neuronal Island Co-cultures

Since the earliest days of cell culture, researchers have attempted to reduce the complexity of the conditions in vitro. Microisland cultures techniques were developed to limit the numbers of cells making synaptic connections, or in the extreme, to study autaptic synapses made by one neuron onto itself (M.M. Segal 1998). Furshpan et al. initially generated microisland cultures where single neurons were isolated on a bed of heart cells. To create these islands of dissociated cardiac myoblasts and fibroblasts, a solution containing collagen was applied to a nonwetting polystyrene surface, causing the collagen solution to form beads. Drying created islands of collagen protein between 300-500 µm in diameter, which were then used to segregate heart cells due to their preferential adherence to the protein islands. These islands of heart cells were then used as a substrate for subsequent growth of neurons (Furshpan, MacLeish et al. 1976; Furshpan, Landis et al. 1986). This technique of using a non-wetting background has been widely applied in studies of synaptogenesis and synapse function (Masuko, Nakajima et al. 1992; Cardozo 1993). Later, the background was changed to a thin layer of agarose gel, to reduce stress resulting from drying the protein during the patterning process, whereupon the protein solution was sprayed to create microdroplets by using a microatomizer (Bourque and Trudeau 2000; Jomphe, Bourque et al. 2005). More recently the process has been facilitated by directly spraying a collagen solution onto cleaned untreated glass coverslips (Fasano 2008). Even though this technique drastically reduces preparation time by eliminating the agarose preparation, it still requires extensive groundwork to optimize the thin layer chromatography reagent sprayer as well as produces significant waste due to the inefficiency of the spraying. Additional techniques have been developed in the meantime to create other types of cell cocultures to allow better controlled isolation regions; however these techniques remain quite complicated and require extensive training as well as equipment (Goubko and Cao 2009).

The extension of the application of microcontact printing technology to protein patterning has primarily resulted from developing methods to print smaller patterns at increasingly higher levels of resolution. In contrast, here we use microcontact printing to create relatively large islands, 150 µm in diameter, composed of either poly-D-lysine, fibronectin, laminin or netrin-1. By backfilling the patterned substrate with PLL-g-PEG, cells can be restricted to the patterned protein spots. We first seeded astrocytes onto island arrays and grew them to confluence on each spot. A low concentration of hippocampal neurons was then seeded onto the pattern, which readily allowed islands containing one or a few neurons to be obtained. The application of microcontact printing to generate microisland cultures substantially increases the reproducibility of obtaining appropriately patterned substrates.

Experimental Methods

Stamp Preparation:

Arrays of 12 x 12 circles of 150 µm in diameter with pitch of 300 µm in X and Y direction were designed in Clewin® (Wieweb Software, Hengelo, Netherlands). Upon completion, the files were sent to Lasex (San Jose, CA, USA), which laser etched the pattern into 125 micron thick polyethylene terephthalate (PET). PDMS was prepared by reacting an ethylene terminated PDMS prepolymer with a poly(dimethylhydrosilane)

Sylgard 184 cross linker (Dow Corning, Corning, NY, USA). The prepolymer and cross linker were mixed in a 10:1 ratio, respectively, with the help of a mixer pouring device (Dow Corning, Corning, NY, USA) as well as manual mixing to ensure thorough mixing. Once complete mixing was achieved, the plastic protective layer was removed from the glue side of the PET mask and the mask glued onto a clean glass slide. To ensure proper adhesion and complete removal of bubbles, the flat side of a razor blade was pressed onto the surface of the mask. In order to shape the stamps, a 16-well slide module (Grace Biolabs, Bend, OR, USA) was attached to the slide with a silicone gasket (Grace Biolabs, Bend, OR, USA). To facilitate the removal of the PDMS, a monolayer of Perfluorodecyltriethoxysilane, 97% (Sigma-Aldrich, Oakville, ON, Canada) was deposited onto the surface of the assembly by evaporation in a dessicator (Bel-art, Pequannock, NJ, USA) for 30 minutes. Following silanization of the complex, 250 µl of the mixture were added to each well. To remove bubbles resulting from manual mixing, the construct was first centrifuged at 1600 rpm for 5 minutes and then placed in a dessiccator for 10 minutes. Any bubbles remaining at the surface were blown off with a gentle stream of compressed nitrogen gas before curing the PDMS in an oven (VWR, Ville Mont-Royal, QC, Canada) for 24 hours at 60°C to activate the Pt catalyst driven polymerization. When the PDMS was completely polymerized, the gasket was separated from the glass slide and the sealing layer peeled off of the gasket exposing the cured polymer stamps. Each stamp was then extracted with tweezers, from the gasket and slide module. To remove low molecular weight PDMS and residual prepolymer present in the cured PDMS, the PDMS squares were extracted using 70% ethanol for 24 hours followed by baking for 4 hours at 60°C to remove all ethanol by evaporation. In addition to removing impurities from the ethanol incubation, this step also sterilized the stamps for biological studies.

Microcontact printing:

The quality of the stamps obtained was investigated under a microscope, and those that contained visible defects were discarded. The desired stamps were then placed in an ultrasonic bath containing 70% ethanol for 5 minutes, to sterilize the stamps once more, and then dried under a flow of nitrogen gas. After drying, the stamps were inked with 10 μl of a mixture of poly-D-lysine (5 μg/ml, PDL, 70-150 kDa, Sigma-Aldrich, Oakville, ON, Canada) and netrin-1 (12.5 µg/ml, obtained as described in (Serafini, Kennedy et al. 1994; Shirasaki, Mirzayan et al. 1996). To minimize the amount of solution utilized in the experiments, an air plasma (Plasmaline, Tegal, Petaluma, CA, USA) was used to remove the surface layer of organic compounds as well as simultaneously oxidizing the surface of the glass coverslips (Carolina Biologicals, Burlington, NC, USA) thereby rendering them highly hydrophilic and allowing the spreading of the solution on the surface of the PDMS stamp once placed on the stamp. The solution was left at rt (~23° C) for 5 minutes in order for it to bind to the surface of the stamp. Once the incubation was complete, the stamp was rinsed for 15 sec with 1x PBS (Fisher Scientific, Ottawa, ON, Canada) and washed for 15 sec in double distilled water (Millipore, Billerica, MA, USA). After the two washes, the stamp was quickly dried with one strong blow of compressed nitrogen gas. The stamps were then contacted immediately with a plasma activated glass coverslip for 5 sec, then peeled off, and the printed coverslip immediately submerged in 1x PBS.

PEG backfill:

To create a biologically inert surface where the proteins present in the serum cannot bind to the substrate, poly-L-lysine linked polyethylene glycol (PLL(20)-g[3.5]-PEG[2], Surface Solutions, Grande Prairie, AB, Canada) at a concentration of 10 μ g/ml in PBS was incubated for 15 minutes before washing off any unbound PLL-g-PEG with 1xPBS.

Astrocyte seeding and culture:

Astrocytes were obtained from mixed glial cultures derived from newborn rat brain as described (Jarjour, Manitt et al. 2003), and seeded at a concentration of 50,000 cells per coverslip. The cells were then grown at 37°C in 5% CO₂ for two days in high glucose DMEM (Invitrogen, Burlington, ON, Canada), 10% Fetal Bovine Serum (Invitrogen, Burlington, ON, Canada) and 1% Penicillin/Streptomycin (Invitrogen, Burlington, ON, Canada).

Hippocampal neuron seeding and culture:

Hippocampal neurons were obtained from newborn rat pups as described (Kaech and Banker 2006) and were seeded at a concentration of 2,500 cells per coverslip. The cells were then grown at 37°C in 5% CO₂ for five days in neurobasal media (Invitrogen, Burlington, ON, Canada), 1% B27 (Invitrogen, Burlington, ON, Canada), 0.5% N2 (Invitrogen, Burlington, ON, Canada), and 0.25% L-glutamine (Invitrogen, Burlington, ON, Canada).

Immunocytochemistry:

Cells were fixed with 4% PFA for 1 minute, permeabilized with triton-X 100 for 5 minutes and blocked with horse serum (Invitrogen, Burlington, ON, Canada) overnight at 4°C. Astrocytes were labelled with phalloidin conjugated to Alexa Fluor 555 (1:250,

Invitrogen, Burlington, ON, Canada) and with Hoechst stain (1:100, Invitrogen, Burlington, ON, Canada). Protein spots were colocalized with a secondary chicken antigoat antibody conjugated to Alexa Fluor 488 (polyclonal, 1:500, Invitrogen, Burlington, ON, Canada). Astrocytes were also stained with a mouse monoclonal GFAP antibody (monoclonal, 1:500, Sigma, Oakville, ON, Canada) detected with a secondary fluorescent donkey anti-mouse antibody conjugated to Alexa Fluor 555 (polyclonal, 1:500, Invitrogen, Burlington, ON, Canada). Neurons were stained with a rabbit neuronal intermediate filament specific antibody (monoclonal, 1:500, Millipore, Billerica, MA, USA) detected with a secondary fluorescent donkey anti-rabbit antibody conjugated to Alexa Fluor 488 (polyclonal, 1:500, Invitrogen, Burlington, ON, Canada). Neuronal dendrites were labelled using a chicken MAP2 specific antibody (polyclonal, 1:1000, GeneTex Inc., Irvine, CA, USA) and a secondary goat anti-chicken conjugated to Alexa Fluor 633 (polyclonal, 1:250, Invitrogen, Burlington, ON, Canada).

Imaging:

Phase contrast microscopy was conducted using an axiovert 40CFL (Carl Zeiss Canada, Toronto, ON, Canada). Standard epifluorescence microscopy was performed using 60 × objective and immersion oil on a C1Si inverted fluorescence microscope (Nikon, Saint-Laurent, QC, Canada).

Neuronal Co-culture Development:

Choosing the proper inking solution:

In order to create an adhesive substrate for the astrocytes to proliferate on, a number of proteins can be patterned through microcontact printing, including polylysine, fibronectin, laminin and netrin-1. To find the best inking solution that will result in the

most homogenous astrocytic islands, we printed all four of these biomolecules and compared their ability to recruit astrocytes to these microislands (Figure 24). Cells were fixed and stained for nuclear components using Hoechst and the number of cells for 10 different islands of each protein type was counted to determine the best substrate to create

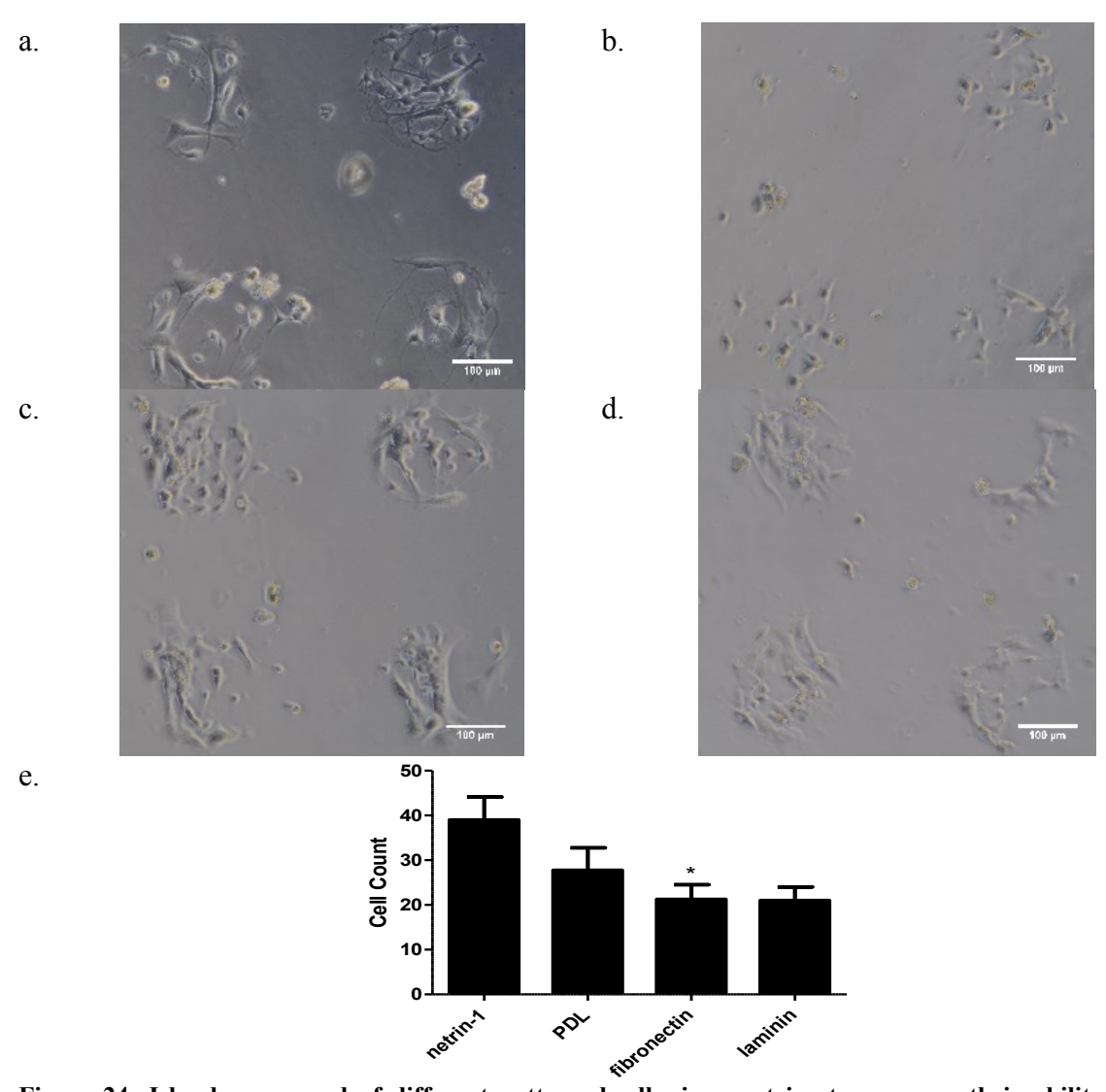


Figure 24: Islands composed of different patterned adhesion proteins to compare their ability to recruit astrocytes. Newborn rat astrocytes grown for 2 DIV on protein islands composed of (A) netrin-1, (B) PDL, (C) fibronectin, or (D) laminin. (E) Cell nuclei were visualized with Hoechst stain. Cell number per island and standard deviation were quantified for n = 10 islands. Scale bar corresponds to $100 \ \mu m$.

the islands. The results indicate that a substrate of netrin-1 best promoted the formation of homogeneously covered islands. On average 39 cells were present per island. PDL, Laminin and Fibronectin had fewer cells with a mean of 28, 21 and 21 cells/island

respectively. The recruitment of astrocytes to the fibronectin islands came as a surprise since it had previously been reported that fibronectin lost its biological activity in the microcontact printing process (von Philipsborn, Lang et al. 2006). Our ability to pattern proteins that were previously reported to be impossible to pattern suggests that our microcontact printing technique has been optimized, compared to previous methods. The differences in cells recruited to the islands might be somewhat skewed since the protein concentration inked on each stamp varied based on the protein. This difference may only be of minor significance as the protein absorbed to the stamp surface might be the same even though one concentration is higher than another.

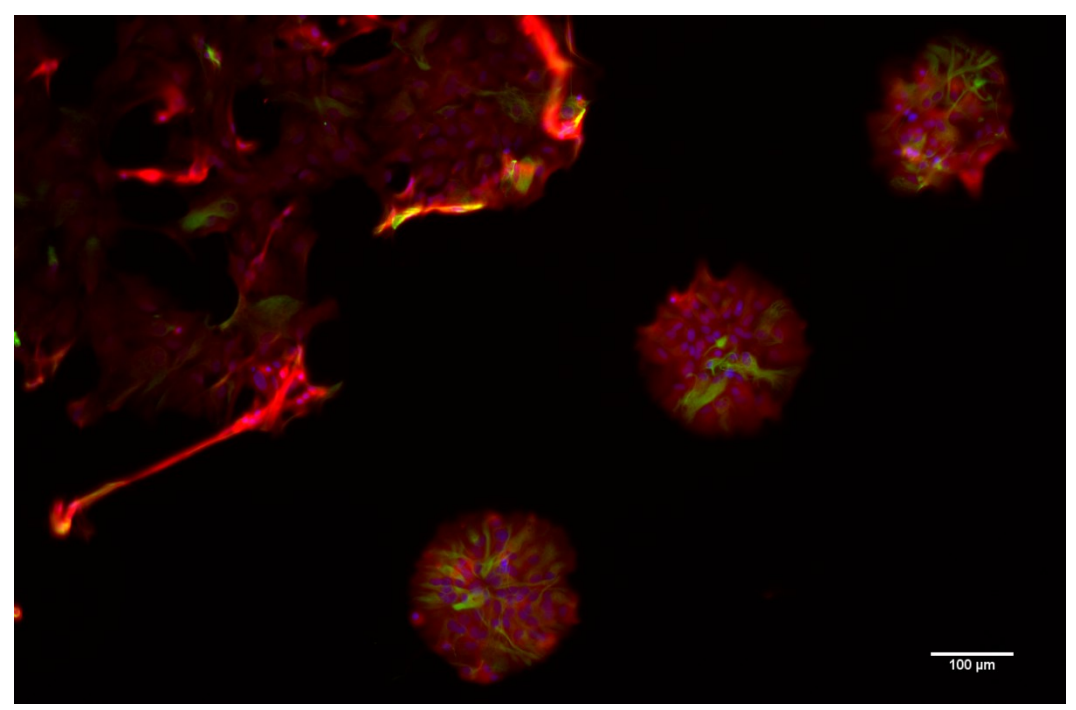


Figure 25: Immunofluorescent image of hippocampal neurons grown on an astrocyte monolayer covering printed islands of netrin-1. GFAP (green) labels astrocytes and Hoechst stain labels nuclei (blue). At the top left of the image, overgrowth of the astrocytes resulted in loss of isolation of the protein islands, where the cells have extended past the island boundaries. Scale bar corresponds to 200 μm.

Seeding optimal cell densities:

We found that regardless of the printed protein, the quantity of cells seeded was a critical step in obtaining the desired island co-cultures. If too many astrocytes were seeded, the

astrocytes proliferated past the boundaries of the protein islands and formed bridges between the islands that eventually led to extensive overgrowth that created a continuous lawn of cells extending over the background and the protein islands (Figure 25). However, if too few cells were seeded, they did not succeed in covering the entire protein island leading to patchy islands which limited the attachment of neurons that were subsequently seeded. Ideally, astrocytes created a homogenous lawn of cells that were limited to the boundaries of patterned protein. If astrocytic coverage of the islands was insufficient at the end of the 36-48 hour growth period, the astrocytes could be cultured longer and would continue proliferating. Once confluence on islands was achieved, the media was then changed to the neuronal media which is depleted of serum and growth factors, and therefore inhibits further astrocytic growth.

Similarly to astrocytes, the number of neurons grown on the astrocytic islands had to be carefully monitored since at too high density, they would also overgrow the islands. Determining the correct number of cells seeded on the islands is even more critical for neurons since the seeded cells will not divide. If too few neurons were seeded, most islands did not have any neurons growing on them and therefore no synaptic studies could be conducted. However, if too many neurons were seeded, the numbers of neurons proliferating on the islands would exceed the desired ratio of a single neuron per island (Figure 26). We found that for the island design employed in our work, an array of 12 x12 150 µm in diameter islands, seeding 2,500 neurons resulted in 1-2 neurons per island.

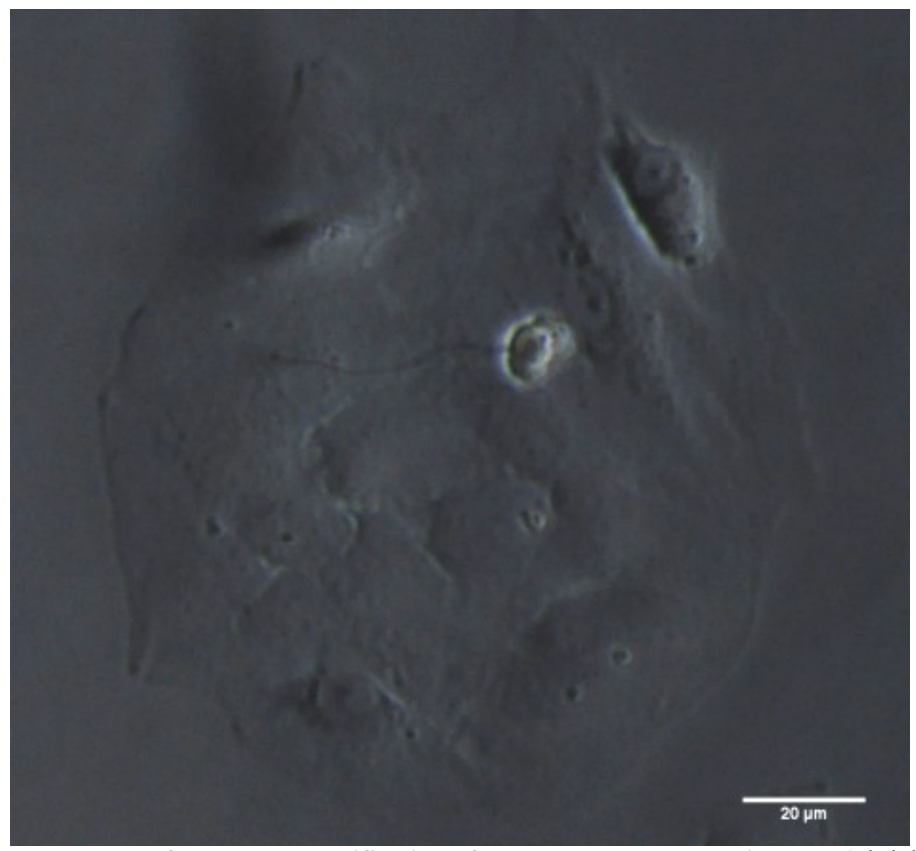


Figure 26: Importance of accurate quantification of neurons seeded on the islands. A brightfield DIC image shows a single hippocampal neuron grown on an astrocytic island seeded on a netrin-1 spot.

Staining for neuronal markers:

To monitor the growth of astrocytes and neurons on the islands, as well as the differentiation of the neuronal precursor cells, a number of markers were employed to differentiate between the astrocytes and the neurons and also between the axonal and dendritic portions of the neurons. The challenging factor with using three different markers is that for each a primary and a secondary antibody must be used and all the organisms from which the antibodies were obtained must be carefully considered so that there is minimal crosstalk between the different antibodies. Improper optimization of the antibody pairs employed for the staining may result in crosslinking of the antibodies and yield misleading results (Figure 27).

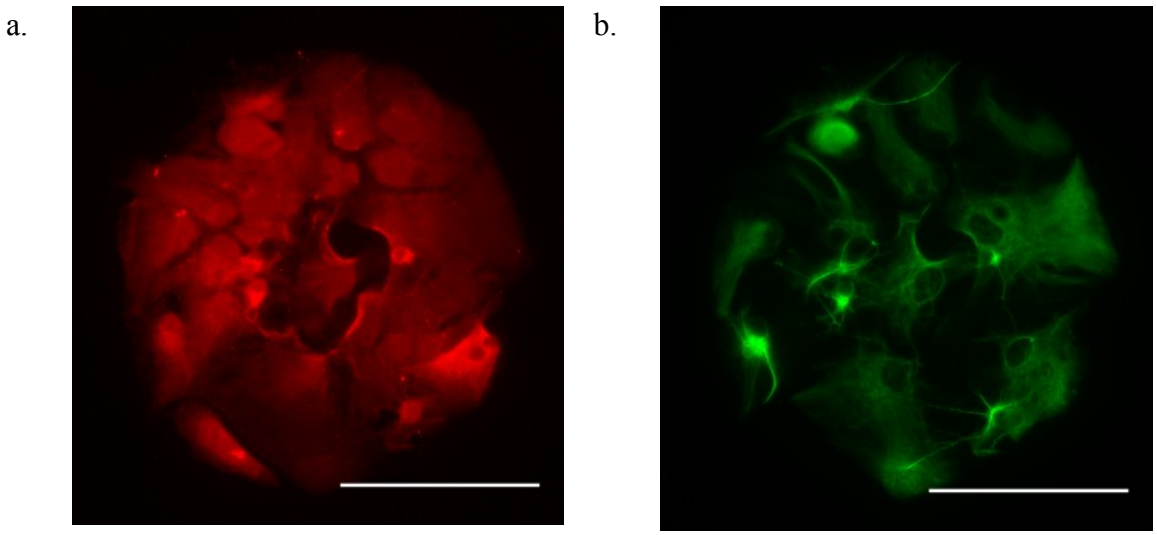


Figure 27: Fluorescent image of hippocampal neurons grown on astrocytes covered netrin-PDL island. Image showing the astrocytic cells stained with (a) the astrocyte marker GFAP (red) and (b) with the axonal marker NFM (green), scale bar 100 μm.

Time in vitro required for neurons to polarize and form synapses:

Neuronal progenitor cells require sufficient time for the cells to differentiate into mature polarized neurons. Consistent with previous studies (Tovar and Westbrook 1999), we found that hippocampal neurons extended long axons by day 7. The growth time should be adjusted based on the desired application of this technology and the literature consulted for the neuronal cell type grown to determine its growth course and the ideal fixation time.

Conclusions:

Here we introduced a method that utilizes the optimised microcontact printing process that we developed to provide a valuable tool to rapidly, easily and inexpensively yield neuronal island co-cultures. We have shown that astrocytes can be segregated to of PDL, netrin-1, fibronectin or laminin, over a period of at least 9 days. Furthermore, we showed that the islands, once covered with astrocytes support the growth and differentiation of embryonic rat hippocampal neurons (Figure 28). This method increases

the reproducibility of the pattern generated and reduces the time required to generate reliably patterned substrates.

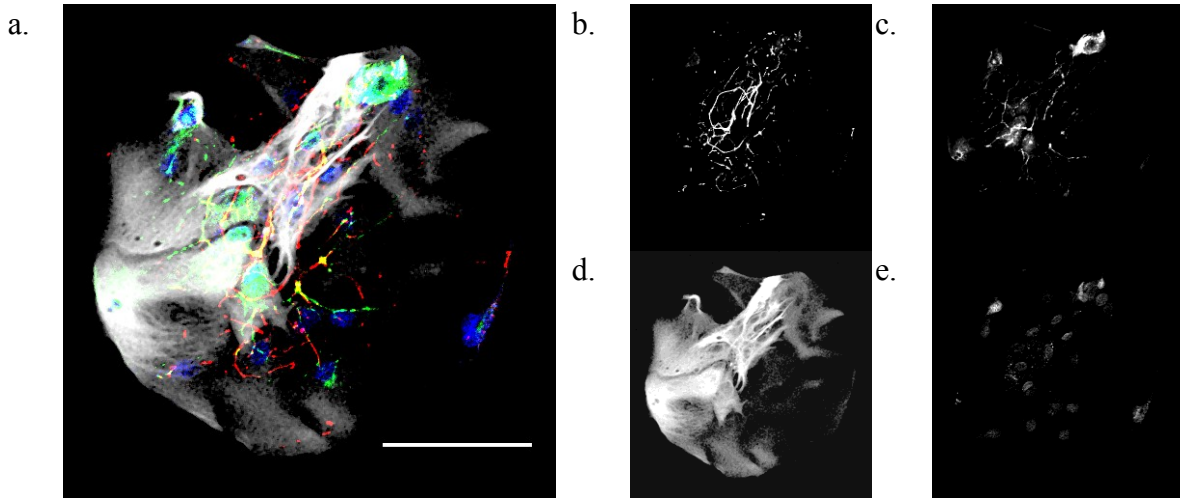


Figure 28: Fluorescent image of hippocampal neurons grown on astrocytes covered netrin island. (a) Merged image showing the neuronal cells stained with the axonal marker NFM (red), the dendritic marker MAP2 (green), the astrocyte marker GFAP (grey) and the nuclei (blue). The split images are also shown for the individual stains obtained using (b) NFM, (c) MAP2, (d) GFAP and (e) Hoechst, scale bar is 50 μm.

Chapter 5: Development of Nanocontact Printing Process to study cellular responses to nanogradients

Cells navigate by integrating signals derived from discrete binding of signalling proteins to individual receptors that are typically a few nanometers in diameter and interact with single proteins. There is thus a great interest in creating deterministic *in vitro* patterns to address how the density and distribution of proteins control intracellular signalling and cell navigation. Investigation of these issues in vitro has been limited by the lack of available and affordable methods. One of the more affordable techniques is nanocontact printing (Coyer, Garcia et al. 2007; Pla-Roca, Fernandez et al. 2007), in which features can be printed at a scale that more closely resembles the actual expression of the proteins in vivo. The generation of digitalized gradients is of particular interest as mentioned in the introduction. One problem that has limited the use of this technique is the collapse of the feature when utilizing PDMS (Perl et al., 2009).

Materials and Methods:

Nanowafer fabrication:

A six inch silicon wafer was coated with e-beam resist and a dot design patterned by electron beam lithography (VB6 UHR EWF, Vistec), followed by 100 nm reactive ion etching (System100 ICP380, Plasmalab) into the Si. After cleaning, the wafer was coated with an anti-adhesion layer by exposing it to Perfluorodecyltriethoxysilane (Sigma-Aldrich, Oakville, ON, Canada) in vapour phase in a desiccator (Bel-art, Pequannock, NJ, USA).

Scanning Electron Microscopy (SEM):

SEM micrographs were obtained on an S-4700 FE-SEM (Hitachi). Samples were coated with an Au/Pd sputterer (Hummer) to a layer of 100 nm in a period of 50 seconds.

Atomic Force Microscopy (AFM):

AFM of the nanowafer was conducted on a NanoScope IIIa (Digital Instruments), while AFM of proteins was conducted on a MFP-3D-BIO (Asylum Research mounted) in tapping mode (Schirmeisen, Holscher et al. 2005).

Nanoarray and Digital Nanodot Gradient (DNG) Design:

Spot arrays and gradients were designed in Clewin Pro 4.0 (Wieweb software, Hengelo, Netherlands). A first wafer was designed by Mateu Pla-Roca with nanospot arrays. An array of nine different patterns was designed where each pattern was comprised of 1x10⁸ spots, however, the spot diameter varied from one array to the next with diameters of 50 nm, 100 nm and 200 nm. The three nanospot arrays of each diameter differed in the pitch which was either 500 nm, 1000 nm or 1500 nm. The gradient wafer was first designed with 100 nm spots, but due to visualization issues covered below; the gradients were redesigned and the diameter was doubled to 200 nm. To ensure biological relevancy, the maximum spacing was limited to 10 µm which is commensurate to cell size; if spacing is too large, cells will not be able to sense the gradient. An array of 64 gradients was designed where each gradient was between 200 and 400 μ m long depending on the slope, 400 μ m wide, and occupies an area of 6.3×4.5 mm² on the wafer. The parameters of the 64 gradients were varied. Various parameters such as the formula employed to generate the gradient, the slope, or even the direction of the gradient were changed (Table 1, Figure 29). The gradients that follow an arithmetic slope have a standard formula of y = mx + b where m is the slope and it varies from 0.05 to 0.4. Geometrical gradients follow the equation $y=10 \times D^i$, where D varies from 1 to 0.85. The spacing of the spots in X and Y was calculated as the square root of the slope of m=0.05 and composed of 40 boxes each 10 μ m wide. The number of spots within each gradient varied based on the design, but reached up to 494,083 spots. Two dimensional gradients were constructed based on a series of boxes that are each composed of an array of spots without any slope, however the width of the boxes is relatively short and therefore result in an overall density gradient.

Table 1: Parameters of a few representative gradients

Gradient type	Slope	Formula	Dimensions (µm)	Number of spots
Arithmetic	=0.05	$\delta = yC + dt$	400 x 400	8,600
Arithmetic	m=0.4	$\delta = yC + dt$ $c - c^{n+1}$	400 x 195	16,000
Geometric	-	$f = \frac{1-c}{1-c}$	400 x 400	9,800
Geometric	-	$f = \frac{c - c^{n+1}}{1 - c}$	400 x 250	107,400
2D	-	$\frac{d\delta}{dA} = C$	400 x 400	494,083
2D	-		400 x 200	31,932

Slope \type	Arithmetic	Geometric	2D
Low			

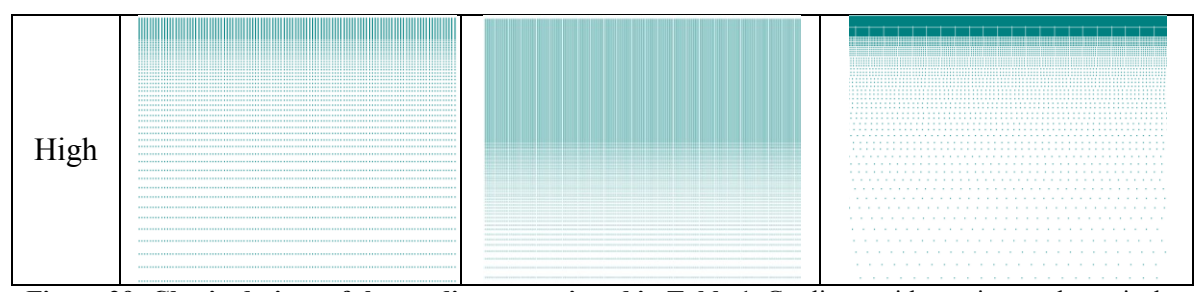


Figure 29: Clewin designs of the gradients mentioned in Table 1. Gradients with varying mathematical designs (arithmetic, geometric and 2D) and with different slopes (high and low) are shown.

Develop a stamp replication method:

Since the wafers were obtained through electron beam lithography, the price of the wafers renders conventional lift-off microcontact printing (Renault, Bernard et al. 2002; Coyer, Garcia et al. 2007) unpractical since in that previously developed technique, the wafer is used to remove protein coating a polymeric stamp from specific areas through contact induced transfer. Unfortunately, once the protein is transferred, it cannot be fully cleaned off of the silicon surface and therefore prevents the return of the wafer to its original clean state once contaminated. In order to render the nanopatterning process cost efficient, we must use a stamp replication process to mass produce inexpensive, disposable replicas that can easily be obtained for the liftoff printing process (Figure 30). To obtain these replicas we will use a double replication process that will first yield an

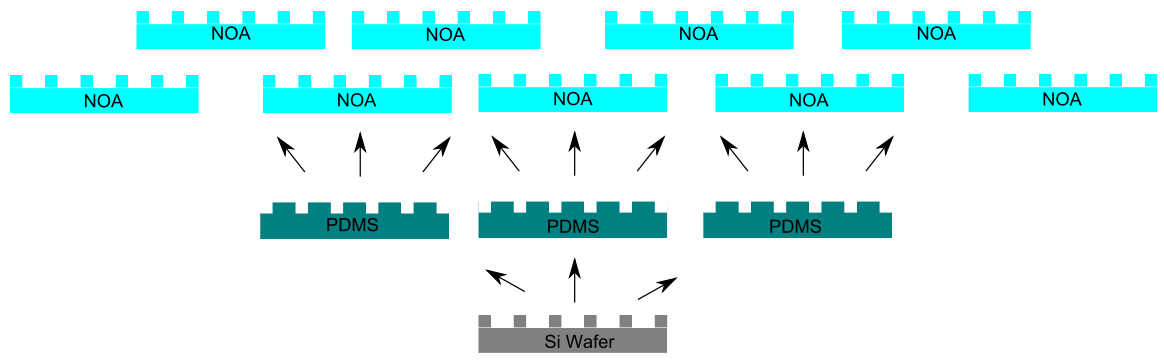


Figure 30: Diagram of how the intended mass production of disposable replicas will take place. A single Silicon wafer with topography etched into the Si wafer through electron beam lithography is replicated into numerous flexible PDMS intermediate stamps with the opposite topography. The PDMS replicas are then employed to yield up to 20 NOA replicas each.

intermediate replica adorned with the opposite of our desired pattern. Through a second replication step using the intermediate replica as a mold, we will obtain identical replicas to the original wafer pattern that we can then use in the lift-off experiment.

Intermediate stamp:

A number of critical parameters had to be maintained by the intermediate replica to yield a secondary replica that will maintain the nanopattern present on the original wafer. Such parameters include a clean deposition and separation of the material from the wafer. A material that will maintain the imprinted topography over time in order to make numerous secondary replicas of the intermediate replica is needed. Finally, the material should be easily separated from the silicon wafer. In order to find the best material we investigated mainly three different polymers (Table 2). We will cover the advantages and disadvantages of each polymer below.

Table 2: Polymers for the intermediate replica

	Deposition	Polymerization	Height	Hardness (Shore D)
NOA 63	Liquid	UV	0.5 cm	90
Parylene	Evaporation	Heat	5 μm	70
PDMS	Liquid	Heat	0.5 cm	50

NOA 63:

Norland Optical Adhesive 63 (NOA 63) is a clear liquid photopolymer that will polymerize when exposed to UV light. The curing of the polymer is very rapid when using a high intensity UV light and therefore yields replicas very rapidly. Since this polymer is primarily used in an industrial setting for adhesive purposes, one of its challenges is the detachment of the replica from the wafer once cured. A variety of polymers are available from Norland Products Inc., but due to the stiffness of the polymer and the limited deformation occurring during the curing process, the 63 version of this

product is the most appropriate for our application. In order to detach the polymer from the wafer, we tried to partially polymerize the stamp and detach it by inserting a pair of tweezers under the polymer and pushing it off. However, using this technique, the wafer could be damaged by scraping the surface with the tweezers and the separated replicas are deformed which will diminish the accuracy of the replicated nanofeatures.

Parylene:

The second polymer investigated for the intermediate replica in our replication process is parylene. Parylene is a vapor deposited poly(p-xylylene) polymer that is frequently used as an insulator in the field of electrical engineering micro- and nanofabrication. More recently it has been used as a mask to pattern proteins at nanoscale resolution (Tan, Cipriany et al. 2010). Due to the vapour evaporation required to deposit this polymer on the wafer, a special machine is required that is quite costly and the evaporation to set the polymer takes a lot of time. In addition to the machinery limitations, the polymer is deposited in very thin sheets, usually at the sub micron range, which renders the peeling of the intermediate replica quite complicated due to thin membrane tearing. We increased the deposition to 5 µm which requires close to 6 hours and yet does not prevent the formation of tears. In order to maintain the planar surface of the parylene after detaching it from the wafer, we coated the full wafer with the UV curable NOA 61. Through UV exposure, polymerization takes place and results in high surface stress and heating of the Silicon wafer. As a result of the heating and high stress, the NOA replica sometimes simply popped off of the wafer surface while maintaining the micron layer of parylene on its surface. We successfully made NOA 63 secondary replicas out of the parylene intermediate replica after silanating the surface (Figure 31).

Investigating the surface by using light microscopy, we concluded that the nanopatterns were well maintained, however the process was not very robust and the reliability of the process was very limited and quite time consuming due to the slow evaporation process.

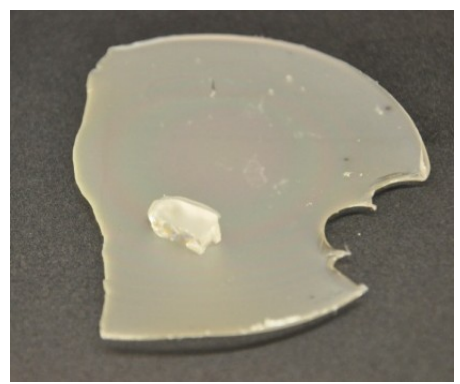


Figure 31: Image of a parylene intermediate replica and a second NOA63 replica. The intermediate replica is composed of a layer 5 μm thick of parylene detached from the Si wafer through the curing of NOA 61 on its surface. A cubic secondary replica made out of NOA 63 was obtained by curing NOA 63 on the side of the parylene containing the topography and detaching it.

PDMS:

The last polymer thoroughly investigated as an intermediate replica candidate in our replication process is PDMS. As mentioned above, PDMS is a soft polymer that is heat cured. The major issue with this polymer was that it seems to lose its uniformity as secondary replicas were made (Figure 32). This also seemed to have a tremendous affect on the quality of the prints that resulted from the use of later obtained stamps from the

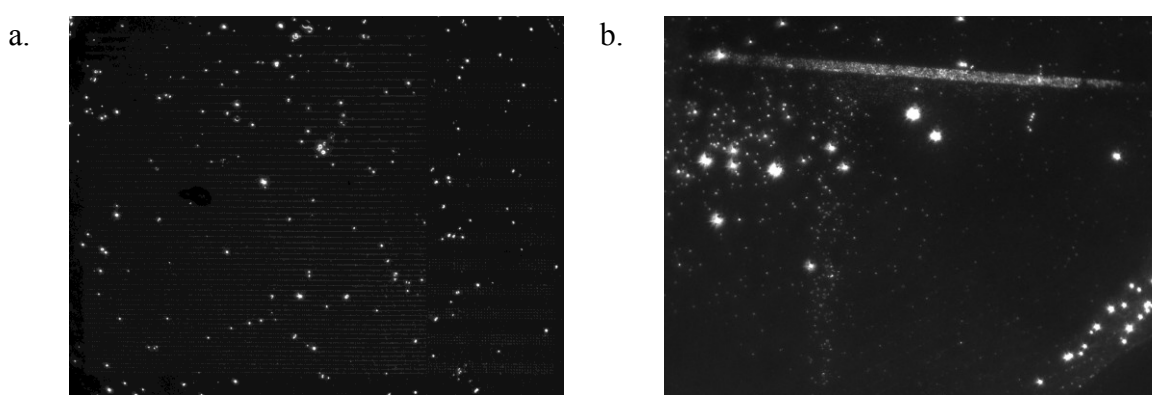


Figure 32: Degradation of the PDMS intermediate replica though replication. The loss in quality of the PDMS intermediate replica after multiple castings of NOA replicas was shown by printing fluorescent antibodies with (a) a newly obtained PDMS intermediate replica and (b) a replica obtained from a PDMS replica that had already produced 20 NOA replicas. The printed pattern is a single nanogradient.

same intermediate replica. In order to retard the degradation of the intermediate stamp, the curing protocol mentioned in Chapter 2 was utilized which allowed the replica of a single intermediate replica into 20 secondary replicas, before any drastic degradation of the intermediate PDMS occured.

Secondary replica:

For the secondary replica, the same requirements as for the intermediate replica are essential. In addition, the stamp must be atomically flat to facilitate conformational contact with the inked PDMS stamp and thereby obtain a homogenous liftoff across the surface of the stamp. Additionally, to maintain the nanostructures imbedded at the surface of the stamp during the contact period of the lift-off printing, the material utilized should be quite rigid. Given all these requirements and the previous work conducted to identify the perfect polymer for the intermediate replica, the Norland optical Adhesive 63 is the most appropriate to be used in creating secondary replicas for the following reasons. (1) NOA 63 is one of the stiffest Norland adhesives that given, (2) its fast curing UV exposure facilitates high throughput manufacturing of replicas, and (3) it has one of the lowest stresses during curing and therefore best maintains the nanotopography. We found that this double replication technique is actually quite common to replicate nanofeatures (Xia, McClelland et al. 1997).

Optimized stamp replication technique:

The wafer was replicated by producing an accurate polymer copy of the features of the Si wafer in a double replication using poly(dimethylsiloxane) (PDMS) and a UV sensitive polyurethane (Figure 33). Firstly, a ~ 6 mm layer of 1:10 PDMS (Dow Corning, Corning, NY, USA) was poured on the wafer inside of a Petri dish, followed by removal

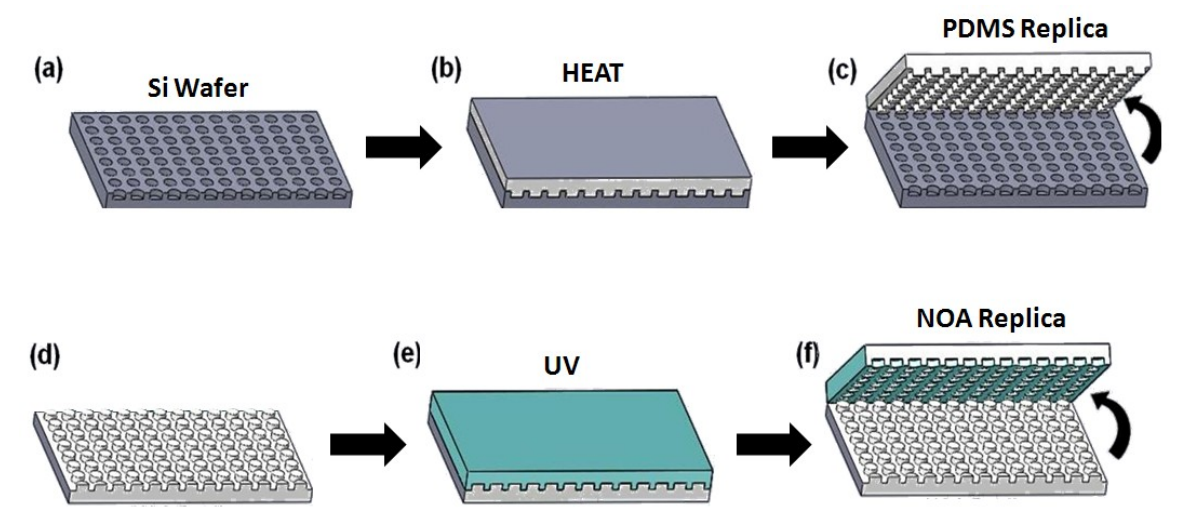


Figure 33: Schematic of the double replication procedure of a Si wafer with nanometer-scale patterns made by e-beam lithography. (a) The structured Si wafer is coated with a silane release layer and covered with a PDMS layer which is degassed to remove all trapped air bubbles. (C) Upon heating, the cured replica is separated from the master. (D) The intermediate replica is covered with a liquid photo curable adhesive that is pressed flat with a Teflon-covered glass slide. (E)Upon exposure to UV light, the original pattern is obtained.

of bubbles under a vacuum in a dessicator for 10 minutes. Next, the PDMS was cured in an oven for 24 hours at 60 °C (VWR, Ville Mont-Royal, Montreal, QC, Canada) and then peeled off of the wafer. To remove low molecular weight PDMS and un-crosslinked extractables, the PDMS replica was bathed in 70% Ethanol for 24 hours and then baked at 60 °C for 4 hours. In order to obtain a second replica, a large drop of UV sensitive polyurethane (Norland Optical Adhesive 63 (NOA); Norland Products, Cranbury, NJ) was cured by exposing it to 600 W (Uvitron International, Inc., West Springfield, MA) for 50 s. Upon curing of the NOA, the PDMS was simply peeled off yielding an NOA master. SEM and AFM images of the original Si master, the intermediate and final replicates were conducted to confirm that the features are maintained throughout the process (Figure 34). We replicated the Si

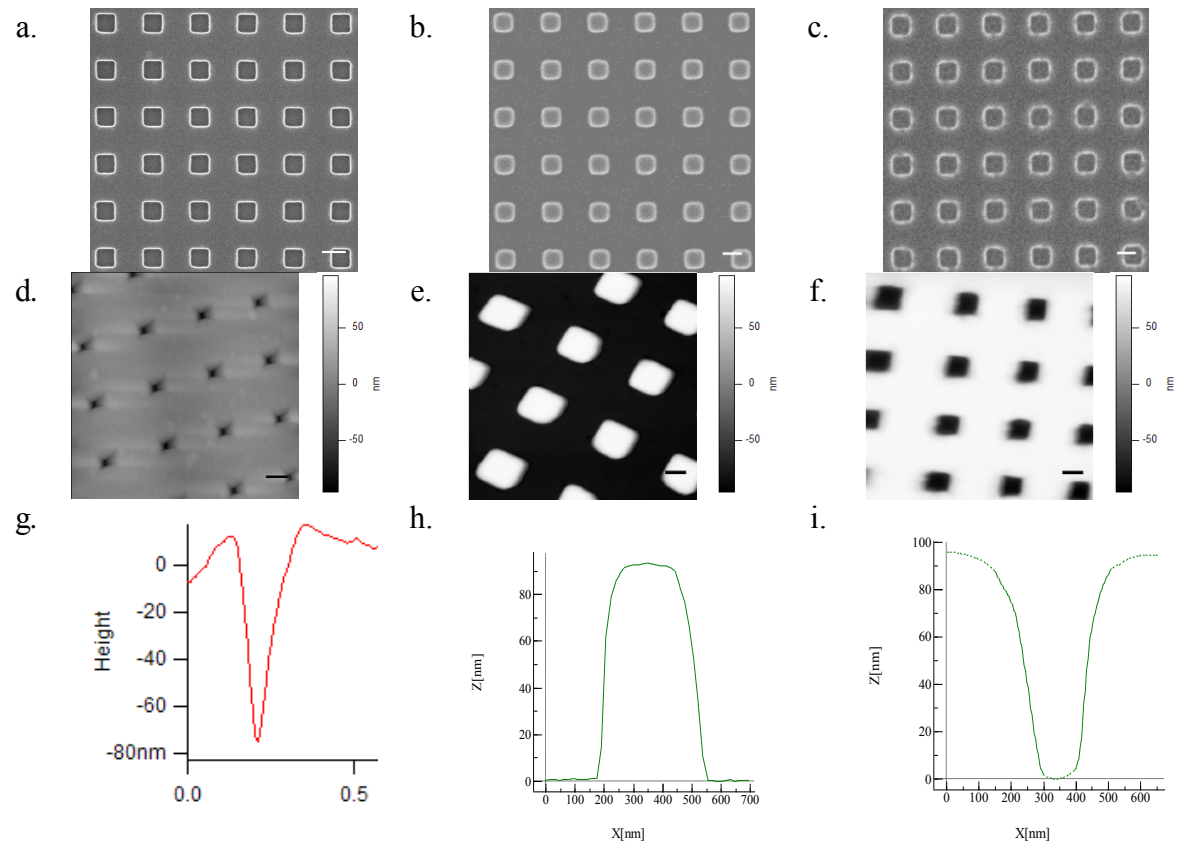


Figure 34: Images of the original master and of the replicas (a-c) SEM images of the pattern on(a) the silicon wafer, (b) the intermediate replica and (c) the second photoadhesive replica. (d-e) AFM micrographs of the topography on (d) the Silicon wafer, (e) the intermediate replica and (f) the second photoadhesive replica. Scale bar for (a-f) is 200 nm. (g-i) Topography graphs of individual features are shown for the entire process from the respective (d-f) AFM micrographs.

wafer over 20 times into PDMS, and individual PDMS replica were replicated into NOA tens of times. Since it takes only ~ 1 minute for the second replication process, hundreds of NOA copies from a single Si master can rapidly be produced.

Creating a cost efficient liftoff printing method for nanoscale levels of resolution:

Once the photopolymer stamps were obtained, we then conducted the lift-off printing process (Figure 35). We have chosen the lift-off process (Renault et al., 2002)

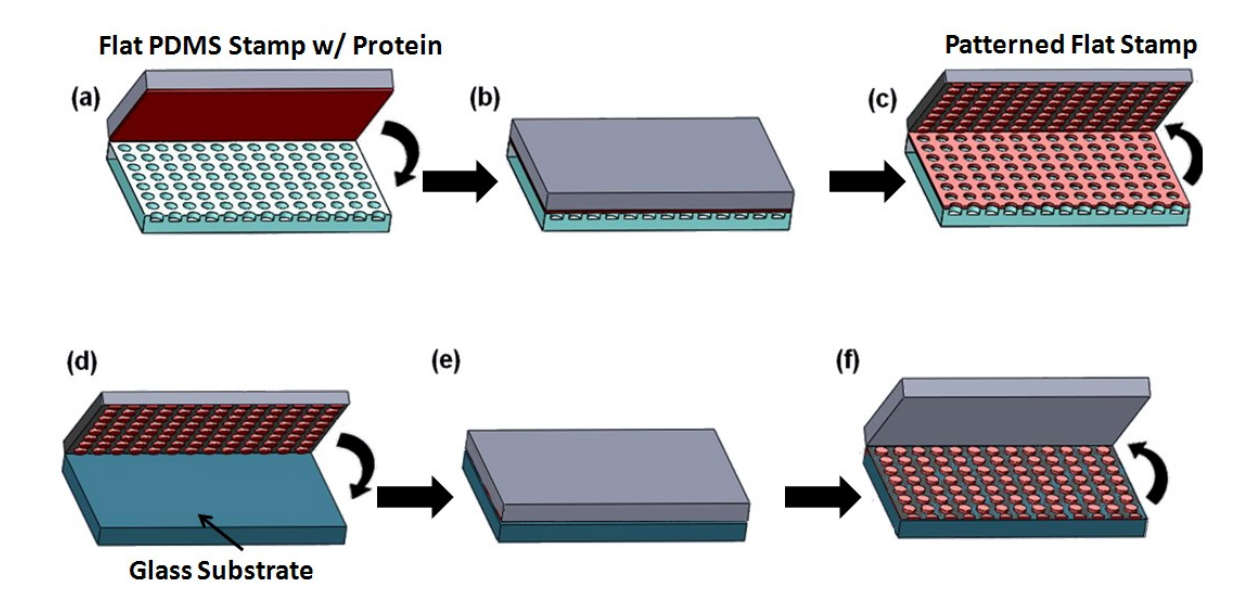


Figure 35: Schematic of the lift-off printing process. (1) The planar elastomer is incubated with protein, while the NOA replica is plasma activated. (2) The planar elastomer covered with a self-assembled monolayer of proteins is placed in contact with the nanotemplate. (3) Upon release, proteins on the elastomer are confined to the opposite pattern from the nanotemplate. (4) A glass substrate is plasma activated and (5) placed in contact with the planar elastomer onto which the protein has been patterned and (6) upon separation, the proteins are transferred to the substrate.

due to the extremely small size of the features that we are attempting to pattern, as well as the high aspect ratio which renders direct microcontact printing impossible due to feature collapse. As a matter of fact, whereas PDMS is regularly selected for printing large features, the scale of our application generates additional unique challenges. For instance, the pillars may not stay completely straight and buckle, or the roof may also collapse due to the heavy weight applied (Perl et al., 2009), both result in incomplete pattern replication. The lift-off technique is the approach we selected to address all these issues. In the first step, proteins are incubated on an atomically flat stamp and patterned by targeted protein removal through contact with the secondary replica stamp with topography on its surface. Once the proteins are patterned on the flat stamp, they can be transferred onto the desired substrate by contact between the flat stamp and the desired substrate. In our process, an extremely flat piece of PDMS is obtained by curing PDMS

on a clean silicon wafer. The obtained stamps are cut and sterilized in the above manner. Once the stamps are sterile, the protein solution can be incubated on the surface following the above mentioned method. Once the incubation is complete, subsequent washes with 1x PBS and double distilled water are conducted. After the washes, the surface is rapidly blown dry under a stream of nitrogen gas and the stamp is immediately placed in contact with a plasma activated NOA replica for 5 seconds. To ensure proper contact between the stamp and the replica, the PDMS is applied to the NOA stamp at an angle and contact is progressively applied from one end to the other. The PDMS stamp is then separated from the replica and immediately transferred onto a plasma treated coverslip for 10 seconds. Once the protein patterns are transferred onto coverslips, the coverslips are instantly immersed in PBS and kept in the dark until further experiments are carried out.

After developing the stamp replication process as well as the liftoff printing

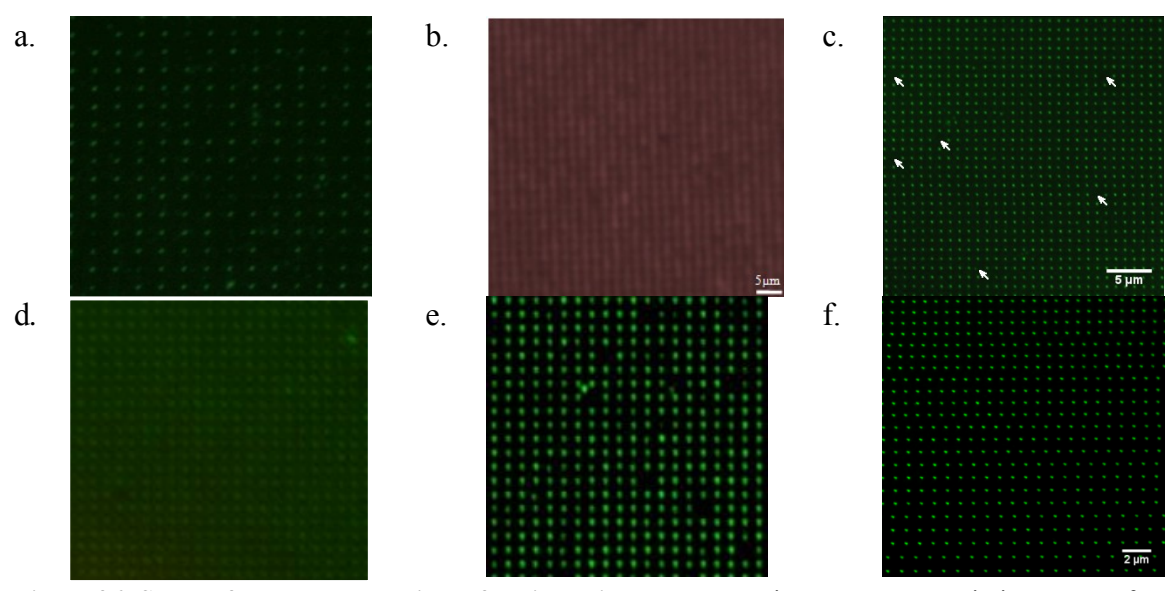


Figure 36: Successful nanoarray prints of various biomolecules. Using nanocontact printing arrays of 200nm spots in diameter with a pitch varying from 500 nm to 1500 nm of (a) IgG, (b) biotinilated antibody with streptavidin Cy-5, (c) FITC PLL, (d) fibronectin, (e) netrin-1, and (f) RGD peptides were obtained. process, both techniques were used to generate protein nanoarrays onto glass coverslips.

We printed a variety of proteins whose transfer was confirmed by detection using specific

fluorescently-bound antibodies or use of engineered proteins that have a bound fluorophore and visualized through fluorescence microscopy (Figure 36).

To further study the arrangements of our nanospots and obtain a better understanding of the efficiency of our developed nanopatterning process, we utilized AFM (Figure 37). We studied arrays of secondary fluorescent antibody as well as

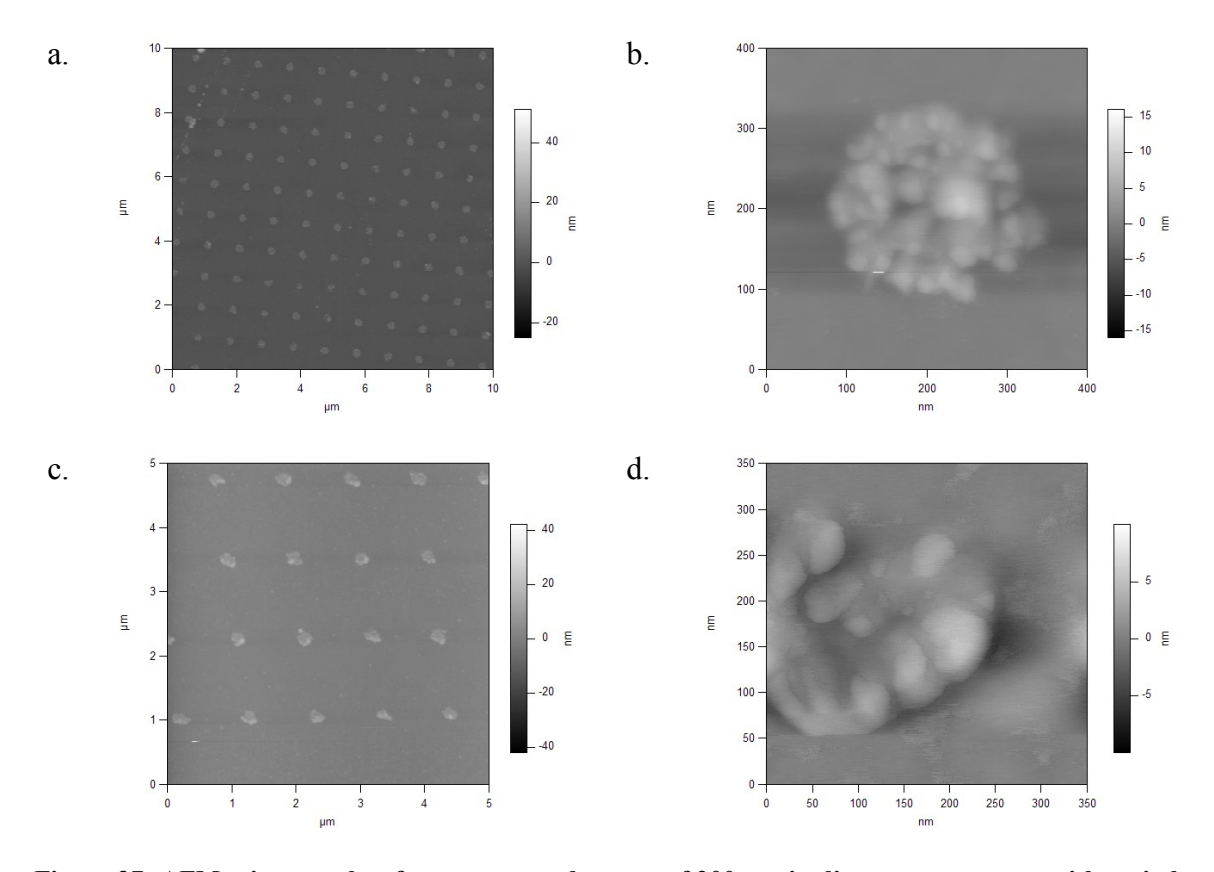


Figure 37: AFM micrographs of nanopatterned arrays of 200 nm in diameter nanospots with a pitch of 1 μm composed of antibody and netrin-1. AFM was employed to image nanoarrays of (a-b) chicken anti goat alexa fluor 488 fluorescently labelled antibodies and (c-d) netrin-1 mixed with the fluorescently antibody at a 1:20 ratio. The images show a (a, c) $(5 \ \mu m)^2$ scan of an array of spots and (b, d) higher magnification $(350 \ nm)^2$ scan of a single nanospot. Sample in air taken using an AC240 cantilever from Olympus. The 512 pixels \times 512 pixel image was collected at 1s/line in tapping mode. Amplitude of 40 nm, resonance frequency of 70 kHz.

nanoarrays of netrin-1. In both patterns it was clearly visible that the majority of the transferred protein matter was limited to the spots, even though few elevations, that are hypothesized to be single proteins, could be found outside the spot boundaries. The

diameter of the dots was established using an image recognition algorithm ("analyze particle" function in Image J) for 16 spots and found to be $210 \text{ nm} \pm 18 \text{ nm}$, thus closely matching the original design. The variation can be attributed to minor changes during replication or of proteins that are only partially contacted and did not lift off. Furthermore, through the results obtained by AFM we determined the maximal height to be 5nm. The exact quantification of individual proteins is complicated by the interactions among proteins, therefore the exact number can not accurately be obtained by counting the number of globules composing individual nanospots. To obtain accurate quantification of the proteins on single nanospots, photobleaching methods previously employed for this purpose should be repeated (Renault, Bernard et al. 2003).

Once the nanopatterning was determined to be successful, we repeated the optimized replication and printing process using the nanogradient wafer in order to start studying cell response to these patterned gradients. Our original gradient wafer had 100 nm in diameter features as reported above, and we successfully patterned fluorescently labelled gradients of antibodies (Figure 38). However, as illustrated in Figure 38, the



Figure 38: Gradient composed of 100 nm diameter spots of fluorescent antibody. The nanocontact printed gradient shows a corner of the gradient where the density of 100 nm in diameter spots is at the highest and as the distance is increased along the gradient, in the x direction in the image, the density of fluorescent antibody decreases, scale bar is 3 μ m.

fluorescence on the spots and on the background is not that clearly differentiated. This is due to the small number of fluorescent antibodies present on each spot that emit a limited amount of fluorescence. To allow the visualization of these spots, high exposure imaging must be used which raises a number of issues such as photobleaching and also results in an increased background. To eliminate these issues and facilitate finding the patterned gradients on the large area of the coverslips, we doubled the diameter of the spots from 100 nm to 200 nm. The doubling of the diameter results in an increase in area from 7,854 nm² to 31,416 nm² and thereby increases the number of proteins present on the spot by a factor of four which drastically raises the emitted fluorescence, decreases the speed of photobleaching of the nanospots and also significantly increases the ease of locating the nanopatterns on the large coverslips. Using the wafer containing the 200 nm diameter spots, we were much more successful at creating and locating our desired patterns (Figure 39). As seen on the images, the background is drastically reduced and the gradients can also be detected with a significantly lower exposure time thereby better preserving the fluorescent patterns. On some of the images, bright fluorescent spots or dark spots in the patterns can be seen. The bright fluorescent spots are most likely the result of dust particles or polymeric residues that are undesirably transferred. The dark spots are the results of air bubbles that get trapped when either contacting the PDMS stamp with the replica stamp during the lift-off process or when contacting the PDMS with the substrate during the print. The non-contacting areas are thought to be the result of irregularities in the surface smoothness. AFM to prove this hypothesis has not yet been conducted.

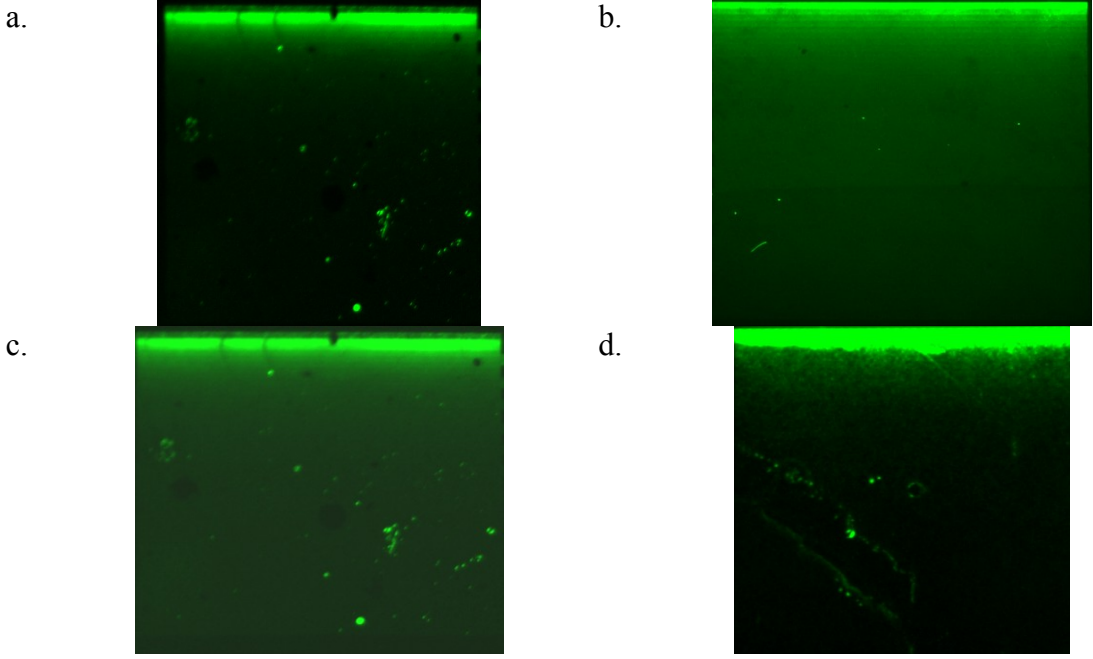


Figure 39: 200nm nanogradients of a variety of biomolecules. Using the nanocontact prining technique and the redesigned Si wafe nanogradients of (a) fluorescent antibody, (b) RGD, (c) netrin-1 and (d) geltrex were patterned on a glass substrate.

Cell Response to Protein and Peptide Nanopatterns

We then chose to apply our experiments to the field of cellular biology and more specifically axonal motility and guidance. Due to the complexity of working with primary neurons, we chose to first conduct our work using cell lines where we could more easily obtain an understanding on whether the cells respond to the protein nanopatterns without having to account too greatly for the sensitivity of the neurons to fluctuations within the experimental setup.

Cell line response on nanopatterns

Based on our success using C2C12 myoblasts and their proven response to netrin-1 patterns, we chose to continue our work with these cells at the nanoscale level of resolution. We first attempted to grow cells on nanoarrays of netrin-1 and compared the cell response to secondary antibody arrays on which the cells should not respond. In fact,

not only did the cells not respond to the antibody arrays, but they were incapable of adhering to the surface and were therefore washed off during the fixation process. Imaging these antibody nanopatterns presented arrays that were completely depleted of cells. On the other hand, when cells were grown on fibronectin arrays, the cells grew long filamentous protrusions and made structures like focal adhesions on these spots (Figure 40). The difference in cell numbers present on the patterns is sufficient to conclude that cells do respond to the nanopatterned protein.

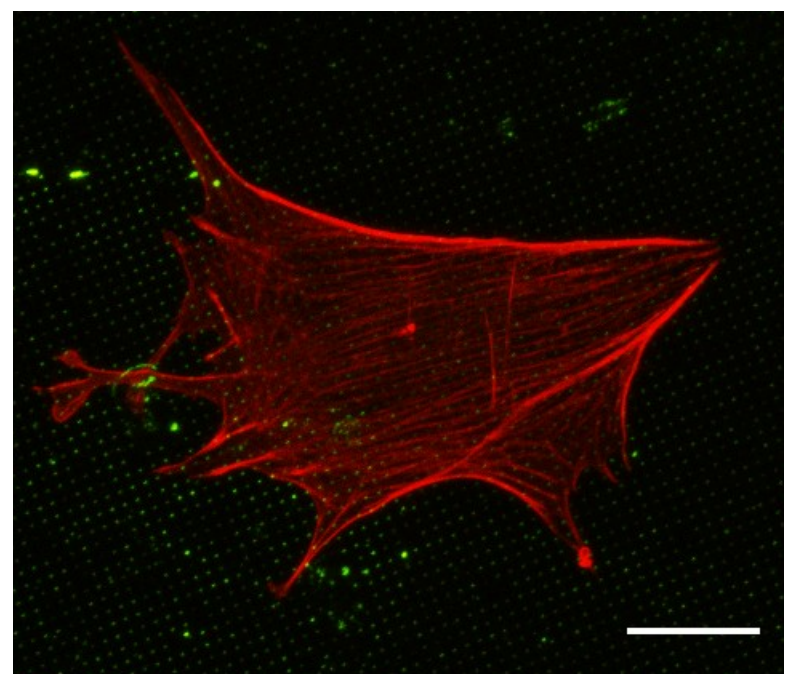


Figure 40. C2C12 cell on a fibronectin nanoarray. Confocal image of a C2C12 myoblast cell stained for filamentous actin with phalloidin grown on a nanoarray of 200 nm spots with 1000 nm pitch of colocalized fluorescent antibody and fibronectin, scale bar is $10 \, \mu m$.

We further continued our study of C2C12 myoblast cell response to nanopatterns by growing these cells on netrin-1 nanogradients that were backfilled according to the method presented in Chapter 3. C2C12 cells demonstrated a significant response by aligning to the edges of the higher density portions of the gradient as well as by directing the leading edge of their cytoskeleton towards the higher density portions of the gradients (Figure 41).

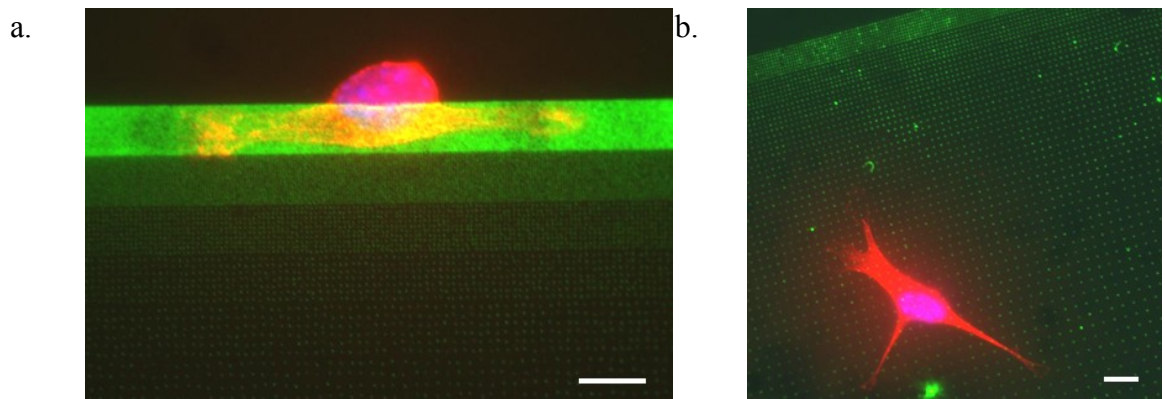


Figure 41: C2C12 cells grown on netrin-1 nanogradients. Nanocontact printing was employed to pattern gradients of substrate-bound netrin-1 (green) nanogradients upon which C2C12 myoblasts were seeded. After 18 hours of culture the cells were fixed and stained for filamentous actin (red) and the nuclei (blue). The cells showed response to the pattern through (a) alignment along the edges of the gradient and (b) the directionality of the cell leading edges which point toward the increasing direction of the gradient, scale bars are 10 μm.

To acquire more convincing evidence that the cells indeed respond to the netrin-1 nanogradients, we conducted time-lapse imaging experiments as described in chapter 3. A 4 gradient array was imaged for a period of eight hours. One of the 4 gradients had a faulty design that did not reproduce aside from the outline of the gradient, so this outlined area served as a negative control. Over that period of time it was clear that the cells migrated up the gradients to the higher density portions and remained there. We quantified this data by splitting the main body of the gradient into three equal areas (high, medium and low density). We then counted the number of cells present in each section at each point in time and divided by the total number of cells present on the gradient at that time point to obtain a percentage of cells present in that section. This quantification was then repeated for only two out of the three other gradients present in the imaged array because the 4th gradient served as a negative control in that the main body of the gradient was not transferred in the printing step. The quantification showed very strong migration of the C2C12 cells over the first 45 minutes of the experiment after which the cell movement stabilized (Figure 42).

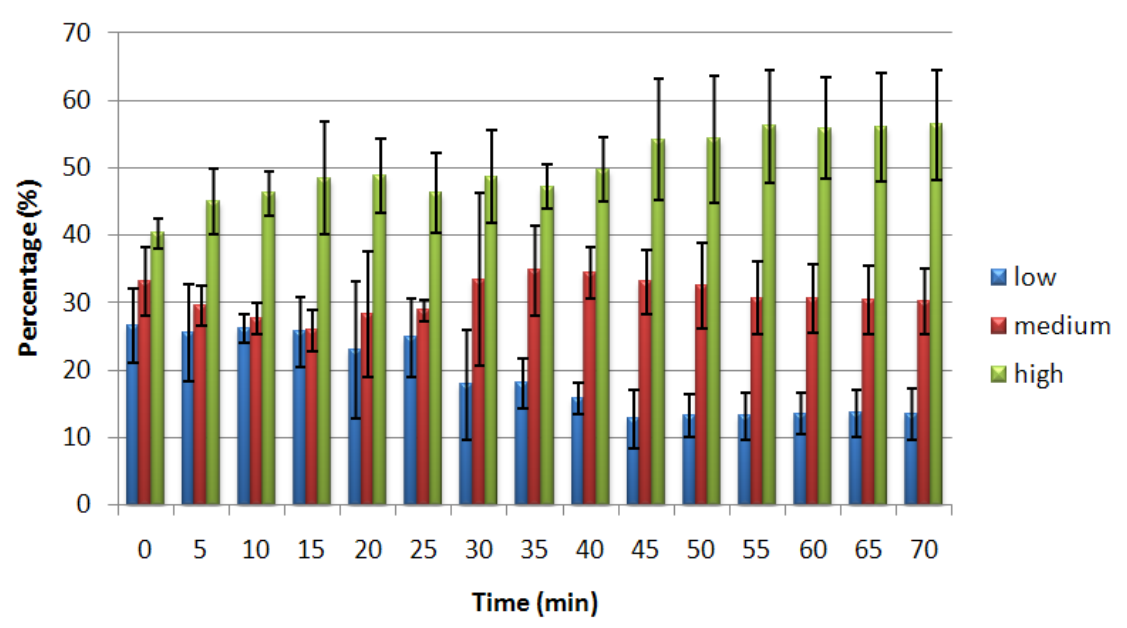


Figure 42: Number of C2C12 myoblasts cells in each of 3 high, medium and low density areas of the DNG over time. C2C12s were grown on a peptide gradient for a period of 50 minutes and imaged at 5 minute intervals. For the analysis, the cells were counted in each section and divided by the total number of cells present on the gradient at that specific point in time to obtain a percentage of cells present in that section at that point in time. The process was repeated for every time point and for three different gradients to obtain a standard deviation. The p-value for the results obtained was p=0.0001 and was obtained through the analysis of variances. It was also found that the gradient accounted for 79.09% of the variances.

Unfortunately with the method employed to image this migration we were unable to start the imaging exactly at the time of cell seeding, but started within 5 minutes. This short time difference accounts for the difference in cell density at t=0 which is in fact t=3-5 minutes. The p-value for the results obtained was p=0.0001 and was obtained through application of an analysis of variances. The gradient accounted for 79.09% of the variance.

Neuronal response on nanopatterns

Once the nanogradients were demonstrated functional with the C2C12 myoblast cell line, we investigated the gradient's effect on neurons by printing nanopatterns of netrin-1. As previously stated, the optimization of the background had to be conducted to obtain the strongest neuronal response to the pattern. Even though previously conducted with microfeatures, we repeated this work with gradients to see if the response was

similar and indeed we witnessed an even stronger response where neuronal migration was limited to gradients with 100% PLL-g-PEG, while neurons seeded on nanogradients with a 25% PLL background, were already successfully proliferating between gradients where no netrin was localized (Figure 43). This experiment needs to be repeated to identify the point between 0% PLL-100%PLL-g-PEG and 25% PLL-75% PLL-g-PEG which is sufficient to allow the neuronal soma to attach to the surface yet only proliferate in the presence of netrin-1 to obtain the best possible response to the gradient.

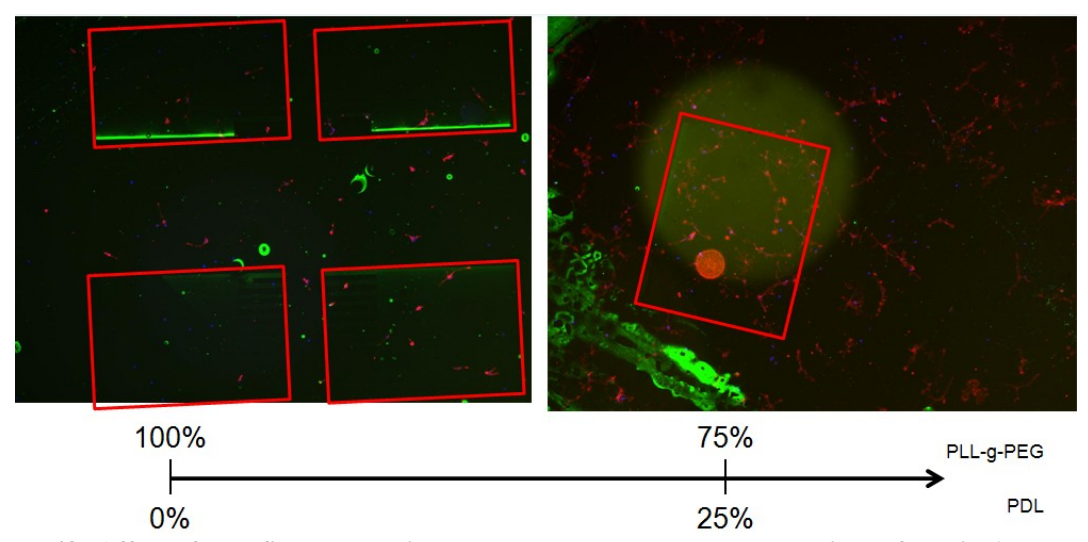


Figure 43: Affect of backfill on commissural neuron response to nanogradient of netrin-1. Patterned nanogradients of netrin-1 (green) were backfilled with different ratios of PLL and PLL-g-PEG. Commissural neurons were seeded and grown on the gradients for 2 DIV before being fixed and stained with phalloidin (red) and Hoechst (blue).

However, even with 100% PEG backfill, a significant response was seen even though it was limited to the higher density portions of netrin-1 gradients. This may be due to the cell somas not being able to attach anywhere else on the patterns because the protein density is simply too low elsewhere on the gradient to sustain somatic attachment. In the areas that the somas do attach to the gradient, the axons extend from the cells and follow the edge of the gradient. In the case of linear gradients; secondary neurites budding off of the axon even seem to follow the aligned netrin spots (Figure 44).

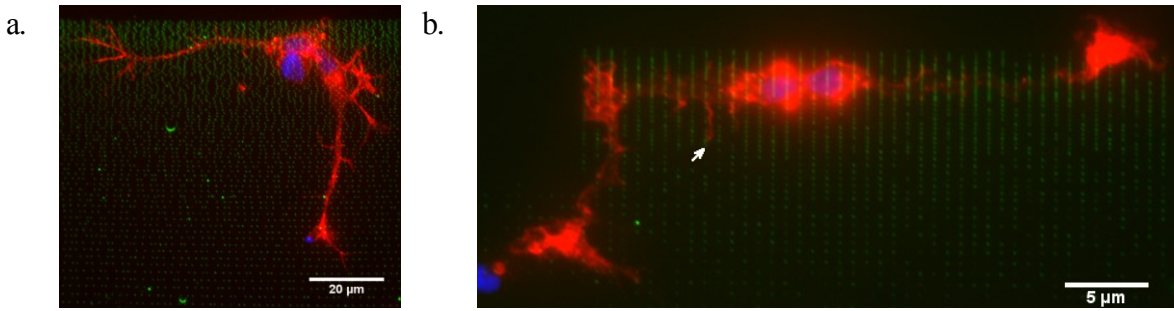


Figure 44: Commissural neurons grown on netrin-1 nanogradients. Commissural neurons grown on netrin-1 nanogradients showing strong response by (a) the extension of the axons following the edge of the gradient as well as (b) the formation of secondary neuritis that seem to follow the lines of spots (arrow).

Conclusions

Here we report the development of a new nanopatterning technique composed of a two step process. The first step consists of a replication process that results in the rapid manufacturing of inexpensive, disposable lift-off stamp replicas of an electron beam obtained nanopattern etched on a silicon wafer. Following the stamp replication process, we used the replica stamps in a liftoff printing process that can pattern arrays of digitally designed protein nanopatterns to feature sizes down to 100nm. We then applied this process to C2C12 myoblast cell migration where we determined the time required for cells to respond to the nanogradients by using time lapse imaging. We further tested our patterning process by growing more sensitive primary neurons on the patterns and successfully obtained a response.

Chapter 6: Discussion

The present study aimed to develop, characterize and implement a simple and reproducible patterning technique to create accurate protein patterns. This printing process was first optimized to obtain a microcontact printing technique that even though limited to feature sizes exceeding single microns, can easily and rapidly be conducted to obtain accurate and reproducible protein micropatterns. A technique was then developed to obtain cell specific responses to these features by backfilling the background with a PEG solution. Despite the size limitations of the microcontact printing technique, this process was successfully implemented to create a neuronal island co-culture with astrocytes. In order to decrease the feature size and create protein nanopatterns, the process was adapted and implemented by creating nano dot gradients that myoblast cells as well as neurons could sense and respond to.

Microcontact Printing

Since the first direct printing of antibodies was reported (Bernard, Delamarche et al. 1998), microcontact printing has widely been implemented to cell biology (Feng, Hou et al. 2004). Although widely applied, the techniques employed have varied drastically without any in depth analysis of how these variations affect the results. In the technique that we developed we implemented a process that yields micropatterns of protein reliably within 15 minutes. Prior techniques have suggested that these patterns could be created within 5 minutes by eliminating all wash steps (Shen, Qi et al. 2008), however we found that the results obtained by following this protocol were sporadic and interspersed with undesired residues that are eliminated using our procedure. Despite the 15 minutes time period required for experimentation this procedure remains significantly shorter than

most microcontact printing procedures which range from 30 minutes to 2 hours (von Philipsborn, Lang et al. 2006). Our technique closely follows this last technique; however we found that by using a hydrophilic coverslip we did not have to cover the stamp with inking solution, rather the solution was evenly spread by applying a coverslip. Furthermore, we found that adding a 1x PBS wash prior to the double distilled water wash resulted in a background decrease, hypothetically through the presence of the salts within the solution that bind to unbound proteins and facilitate their flushing off of the stamp surface. We continued conducting a water rinse following the PBS rinse to remove the salt crystals from the wash solution that would otherwise interfere with the printing and subsequent imaging. Lastly we found that the optimal printing time was 5 seconds which resulted in the complete transfer of protein without extensive denaturation, yet did not necessitate any intricate equipment that has previously been required to conduct fast microcontact printing (Lis, Peremans et al. 2009).

The optimized technique was employed to successfully pattern biomolecules with a positive charge such as PDL or PLL (Erbacher, Roche et al. 1997) onto glass substrates. This method works quite efficiently since the positively charged amine side group of the individual lysine amino acids interact with the negatively charged PDMS surface (Beattie 2006). However we also successfully patterned highly negative molecules such as heparin. The reason for which this occurs is unclear since in the past, to pattern negatively charged molecules such as DNA, extensive adaptation has been required to flip the charge at the surface of the stamp and on the glass to drive the transfer (Lange, Benes et al. 2004). Here, significant molecular transfer occurred using the same process

as we used to print positively charged inks by simply increasing the ink concentration 4 fold.

One of the remaining limitations of the presented technique is the limited control over the homogeneity of the proteins printed. As shown through AFM of microspots in Chapter 2, the height of the protein across the 5 µm cross section of a spot varies significantly from a monoloayer of proteins (~5 nm in thickness) to a multilayer (> 8 nm in thickness). This lack of control became even more apparent in Chapter 5 when AFM was conducted on 200 nm spots. The variance in spot area varied greatly due to positioning of the proteins on the flat PDMS stamp before liftoff. In addition this variance in spot area also suggests that the number of proteins present on each spot varies, which might result in some axonal preference for one spot over another, due to the uneven repartition of proteins over the spots. One possible solution to decreasing this variance would be to sufficiently dilute the proteins in the inking solution, which upon printing would result in single proteins on each spot. For further precision, the nanospots could be patterned with an AFM tip. However, despite the excellent precision offered by this technique, the throughput would be low.

Additionally, here we facilitated the visualization of patterned protein by mixing the protein of choice with a fluorescent non-specific antibody in the same ink. The protein and the antibody did not diffuse from the printed area meaning that the co-printed fluorescent particles are good indicators of the localization of the printed protein. Furthermore through this process we show that we greatly reduce the background noise that usually results from antibody detection of the printed protein. It is important to note

that the protein and the antibody were mixed in a 1:1 ratio by weight, but the molecules are not the same size. The marker antibodies are 150 KDa, while for example netrin-1 is 75 KDa, so the actual molar ratio is 2 netrin-1 proteins: 1 antibody. The ratio might further differ if one molecule has more exposed charged group that will result in a higher binding affinity of that molecule to the PDMS than the other. The consequences of these details could be further investigated at a later time, but we decided to apply the technique to cell response studies instead.

Specific Cell Response

Protein patterns obtained through microcontact printing have frequently been used to study cell adhesion and cell motility. The integrity of proteins following the patterning process has been questioned (Lee, Lim et al. 2003), however there is no simple way to show that the patterned proteins remain biologically active. One way to obtain an idea of the conservation of the protein structure is by investigating the cellular response to the patterned protein (Kam and Boxer 2001). This technique, even though widely accepted, is not an adequate indicator of whether the patterned proteins are inducing a response in the cells of interest. An issue with this line of thought is that the cell response is not necessarily induced exclusively by the printed protein; rather the response might result from the binding of proteins present within the growth media to either the printed proteins or the glass background (Horbett and Schway 1988). In addition to the growth factors in the serum containing media, cells secrete chemotrophic factors that may also bind to the glass or pattern and drive the cell response (Tjia, Aneskievich et al. 1999). In order to prevent the adhesion of solubilised proteins to glass surfaces, PEG was used because the long chains prevent the adsorption of protein through steric stabilization (Mrksich and Whitesides 1996). The deposition of PEG has been applied to fill background and restrict cells to patterned stripes (Csucs, Michel et al. 2003), however this may result in further complications. Mainly, a cellular response might be due to the inability of cells to adhere to PEG rather than a response to the patterned surface (Winblade, Nikolic et al. 2000). The ideal situation in this case is to have a background that will sustain limited cell attachment, yet not push the cells onto the patterns. At the same time, the cells should preferentially grow on the stripes and for this to occur the affinity of the cells for the patterned protein should exceed that for the backfilled molecules. Not accounting for this nonspecific response of cells to the background might lead to very misleading interpretations of the results.

The quick experiment that we carried out using the stripe assay and varying ratios of PLL-g-PEG to PDL offers a rapid method to define the most favourable background to obtain optimum cell response to patterned substrates. This method can be applied to different printed proteins as shown with netrin-1 and Fibronectin, with different cells as shown with C2C12 cells and primary commissural neurons (which both have very different growth media) and can be conducted on different patterns ranging from large microscale patterns (10 µm stripes) to nanopatterns (200 nm gradients). The great dexterity of this technique yields a strong tool. Moreover, our future goals aim to strengthen this technique by employing time lapse imaging on a multi-well plate to simultaneously image cell growth on a number of patterns where the background differs from strongly attractive to strongly repulsive. The combination of our backfill ratio gradient with time lapse imaging should provide keen insight into how cells behave on different backgrounds.

Neuronal Island Co-cultures

The creation of neuronal microisland co-cultures is an important tool to study interactions between neurons, and between neurons and their supporting cells. The importance of support cells such as astrocytes is that they provide an environment more similar to that in which the neurons proliferate *in vivo* (Bruckenstein and Higgins 1988). Such support cells provide a three dimensional matrix into which neurons can attach. In addition, astrocytes secrete various growth factors (Furukawa, Furukawa et al. 1986). By replicating this environment *in vitro* we provide a more realistic environment that can be utilized to better understand the role of support cells in neuronal function.

Standard microcontact printing typically requires a laborious process in a clean room environment to yield a Si wafer with topography. This wafer is then used as a mold onto which PDMS is cast and cured to produce stamps for the microcontact printing process. While this process is reliable and reproducible, it has been a limiting factor for many labs because it requires a clean room environment as well as microfabrication expertise. To alleviate this limitation, we designed an inexpensive method to create microcontact printing stamps that does not require a cleanroom or photolithography. This process is rendered possible by the production of laser etched adhesive masks marketed by Lasex. These masks are glued onto a clean glass slide before being covered with a 16-well slide module. PDMS is then poured into the wells and cured for 24 hours before yielding stamps with 118 ± 2.98 µm wide pillars.

We employed microcontact printing to pattern arrays of protein islands 150 µm in diameter composed of netrin-1, laminin, fibronectin, or PDL. To visualize the printed pattern, a fluorescent secondary antibody was mixed in the printing ink, revealing an

array of islands of the expected size (Fig. 2). In the past, fibronectin has been utilized as a substrate to seed cells, but this extracellular matrix protein was reported to lose its biological activity as a result of the microcontact printing process causing denaturation (von Philipsborn, Lang et al. 2006). In contrast, we show that using the microcontact printing process we developed we successfully patterned all of the above mentioned proteins, and astrocytes clustered on the protein islands, demonstrating that the patterned proteins remained active after printing. By staining with Hoechst, we quantified the number of cells that were located on each spot of the four different patterns. Surprisingly we found that PDL, even though widely used in cell biology was the worst substrate to create well-covered islands, whereas netrin-1 was the most effective protein substrate. Even though PDL patterning resulted in patchy astrocytes islands, better coverage could be obtained by increasing the number of astrocytes seeded or increasing the culture time. To limit cell adhesion and proliferation between the protein islands, protein absorption from the serum containing media was prevented by backfilling with PLL-g-PEG after printing.

To obtain a dense monolayer of astrocytes on the surface of the protein spots that does not extend past the boundaries of the islands, the cell density, as well as the incubation time, was optimized. We found that plating 50,000 cells on a 1.5 cm² substrate surface area, and incubating for 2 DIV yielded the required coverage. Furthermore, by adjusting the density of neurons seeded on the coverslip, in many cases, one individual neuron per astrocyte island. Specifically, in the conditions described here, seeding 2,500 hippocampal neurons per coverslip yielded optimal results. Four days after plating the neurons, a total of 6 DIV, the cultures were stained with Hoescht dye to label nuclei, and

immunolabeled for glial fibrillary acidic protein (GFAP), a specific marker of astrocytes (Rodnight, Goncalves et al. 1997). The dendrites of neurons growing in these cultures were selectively immunolabeled using an antibody against MAP2 (Caceres, Banker et al. 1984), and the axons labeled using an antibody against NFM (Chan, Yabe et al. 2003).

The method described can be applied effectively, using the standard microcontact printing technique, to create neuronal microisland co-cultures. This protocol should be readily applicable to a wide variety of cells.

Nanocontact Printing Process

We also developed a versatile nanocontact printing process that utilizes a twostep stamp replication followed by lift-off printing. We demonstrate that the technique
can readily be employed to pattern a wide range of proteins at the nanoscale level of
resolution. Although not tested directly, we suspect patterning negatively charged
proteins will not be replicable at this level of resolution. With the drastic decrease in
protein transfer associated with negatively charged molecules, it is likely that the
reduction of transfer on the liftoff stamp followed by a second weak transfer onto the
glass will result in very weak patterns that lack the robust reproducibility we
demonstrated with positively charged proteins. As in the past for negatively charged
molecules such as DNA, the technique that we present here might be alterable to yield a
more reliable protein transfer that maintains the ease of the technique at the nanoscale
level of resolution (Lange, Benes et al. 2004).

The application of an NOA patterned hard stamp obtained through a two-step replication process for lift-off printing is the first reported use of a polymer to remove proteins from a flat PDMS stamp for further protein nanocontact printing. In the past, all

lift-off printing was conducted by employing an e-beam patterned Si wafer as a lift-off stamp (Renault, Bernard et al. 2002; Coyer, Garcia et al. 2007). This process is quite expensive since the protein binds irreversibly to the Si wafer that was obtained through the expensive process of e-beam lithography. This irreversible fouling of the wafer results in the degradation of the yielded patterns. By mass producing stamps rapidly and inexpensively we drastically reduce the cost of lift-off and render the technique more widely accessible to the general scientific community.

The technique presented here was shown to otherwise follow the qualities of microcontact printing mentioned in Chapter 2 as well as most of its limitations. The patterned proteins remain bound to the substrate for extended periods of time as long as the samples remain stored in a cool dark environment. We also think that this technique can be employed with other patterning techniques to pattern multiple inks. It may even be possible to print multiple times on the same substrate; however both of these ways of obtaining multiple patterns on a same substrate need to be tested. One major challenge that occurs at this scale of resolution is the need for precise alignment. Given that the ink is transparent or fluorescent, visual alignment would have to be conducted using a fluorescent microscope and mechanical micromanipulators. This approach has not been exploited yet to our knowledge, however what has been done to control the overlap of two prints is the development of devices that control the placement of the pattern of the stamp as well as the location of print of the stamp on the substrate (Choonee and Syms 2010; Trinkle and Lee 2011).

Digital Nanodot Gradients and Cell Migration

In order to create surface-bound gradients that can be exactly quantified and patterned through the above mentioned nanocontact printing process, we created DNG's with varying spacing between individual 200 nm spots. The implementation of this digitalized approach enables the exact quantification of the gradient through a controlled design. Additionally by employing this approach we could reach the highest dynamic range, the ratio between the lowest and highest concentration in the gradient, reported to date.

The dynamic range of previously reported gradient generators has been between 0.5 and 2 orders of magnitude (OM) for microfluidic generators that yield solution gradients (Jeon, Dertinger et al. 2000; Dertinger, Chiu et al. 2001; Abhyankar, Lokuta et al. 2006), 1.4 OM for a static gradient such as the ones formed in a Boyden chamber (Shimizu, Minakuchi et al. 1997) and 2 OM for a gradient formed by "diffusible printing" molecules in a gel (Rosoff, Urbach et al. 2004). Goodhill and colleagues produced gradients in gels by inkjet printing various protein concentration features and allowing diffusion to create an unstable gradient with about 2.1 OM. Using this technique, they created gradients with 6 OM by printing overlapping gradients with a range of inking concentrations of NGF (Rosoff, Urbach et al. 2004; Mortimer, Pujic et al. 2010). The main challenge with fluidic driven gradients is that the driving mechanism for this technique, diffusion, leads to the rapid degradation of the high dynamic range of the gradient and limits the lifetime of the gradient.

For surface bound gradients, a dynamic range of 1.14 OM was reached using microfluidics (Caelen, Bernard et al. 2000), 2 OM using an agarose gel (Mai, Fok et al. 2009), and 3 OM using the LAPAP technique (Bélisle, Correia et al. 2008); however the

dynamic range of surface-bound gradients in general has remained difficult to quantify owing to limitations in fluorescence microscopy mentioned in Chapter 1.

Quantitative surface bound gradients produced by digitalization through microcontact printing have been limited to a dynamic range of a factor of 25 (1.25 OM) (von Philipsborn, Lang et al. 2006). This is limited compared to diffusible gradients; however it cannot readily be increased because of microcontact printing collapse when the spots are spaced too far apart (Perl, Reinhoudt et al. 2009). In order to increase the dynamic range, liftoff microcontact printing was employed to pattern discrete surface bound nanogradients of spots down to sub-100 nm scale that range in density by a factor of 64 across the gradient (1.64 OM) (Renault, Bernard et al. 2002; Coyer, Garcia et al. 2007).

With the method presented here and the designed DNG made of 200 nm spots spaced between 0 and 10 µm apart we reached a dynamic range of 3,140, or 3.5 OM. The 3.5 OM could be further extended for other applications. For our application in neuroscience, individual spots were not spaced further than 10 µm because the cells we used do not reach that far. To further extend the dynamic range it may be possible to adjust the number of proteins on individual spots, as was reported for diffusion gradients (Rosoff, Urbach et al. 2004). If the number of proteins on individual spots was reduced from 35 to single proteins, this would to 109,900, or 5.0 OM in our designed DNGs. Creating single protein nanospots would be of particular interest since it was shown that neurons could respond down to 10⁻² nM concentrations of chemotrophic factors and more importantly turn in response to 0.1% protein differences over the width of the growth cone (Mortimer, Pujic et al. 2010).

Patterning nanogradients *in vitro* is critical to understand how the organism functions. A limited number of gradients have been demonstrated *in vivo*, yet those identified have proven to play crucial roles in development, immune response, and regeneration as discussed in the introduction. Even less is known about the absolute concentration of these gradients and how they affect the way cells interpret the information detected. We hypothesize the response is dose dependant *in vivo*. By patterning gradients *in vitro* we can test assumptions about mechanisms used by cells to respond.

Future Directions

Overall, the optimized technique presented exhibits many advantages over currently employed microcontact printing methods. Furthermore, the backfill optimization technique that we describe here could be widely applied to overcome nonspecific cell responses to either PLL or media-derived surface-bound proteins that are rarely addressed in such studies.

The method we introduced for creating island neuronal co-cultures provides a tool to rapidly, easily and inexpensively yield neuronal island co-cultures. The method presented increases the reproducibility of the pattern generated and reduces the time required to generate reliably patterned substrates. For these reasons, the method described can be applied effectively to create neuronal microisland co-cultures for multiple applications in cell biology.

DNGs will be useful to test the dynamic range over which cells respond to both attractive and repulsive gradients while monitoring the response in real time. Another area of interest will be to test how cells navigate in response to a combination of a surface

bound and a diffusible gradient which may be achieved by enclosing a DNG within a microfluidic device (Wang, Li et al. 2008), or by delivering chemicals using a microfluidic probe (Juncker, Schmid et al. 2005).

In future studies these patterns could be utilized to investigate the response of different neuronal populations to netrin-1 gradients and the signal transduction mechanisms involved. Additionally, the motility of axonal growth cones to gradients of different characteristics could be investigated. Additionally, such patterned gradient could be combined with gradients applied in solution using a microfluidic probe (Juncker, Schmid et al. 2005; Queval, Ghattamaneni et al. 2010) to generate double gradients, or to investigate possible differences in the efficacy of gradients applied as a substrate or in solution.

Conclusion

This project aimed to develop a technique that will allow inexpensive and efficient transfer of protein nanopatterns for neuronal cell response studies. In the process of developing a successful approach to create surface bound gradients, we also optimized microcontact printing as well as developed an approach to optimize the background in order to minimize its affect on cell response. We employed both of these optimized procedures to create neuronal microisland co-cultures using a technique that has several advantages over current methods. Finally we patterned DNGs using a two step stamp replication process to yield a hard NOA replica that was subsequently used for lift-off printing. The obtained DNGs were employed to investigate how C2C12 cells as well as primary neuronal cells migrated on gradients of either RGD peptide or netrin-1. The five methods presented here provide optimized techniques for patterning proteins at different levels of resolutions for a wide range of applications in cellular biology.

References

- Abhyankar, V. V., M. A. Lokuta, et al. (2006). "Characterization of a membrane-based gradient generator for use in cell-signaling studies." <u>Lab on a Chip</u> **6**(3): 389-393.
- Adler, J. and W. W. Tso (1974). "Decision-Making in Bacteria Chemotactic Response of Escherichia-Coli to Conflicting Stimuli." Science **184**(4143): 1293-1294.
- Amarie, D., J. A. Glazier, et al. (2007). "Compact Microfluidic Structures for Generating Spatial and Temporal Gradients." <u>Analytical Chemistry</u> **79**(24): 9471-9477.
- Atencia, J., J. Morrow, et al. (2009). "The microfluidic palette: A diffusive gradient generator with spatio-temporal control." <u>Lab on a Chip</u> 9(18): 2707-2714.
- Atwal, J., K. Singh, et al. (2003). "Semaphorin 3F antagonizes neurotrophin-induced phosphatidylinositol 3-kinase and mitogen-activated protein kinase kinase signaling: a mechanism for growth cone collapse." <u>Journal of Neuroscience</u> **23**(20): 7602.
- Bae, G. U., Y. J. Yang, et al. (2009). "Neogenin Regulates Skeletal Myofiber Size and Focal Adhesion Kinase and Extracellular Signal-regulated Kinase Activities In Vivo and In Vitro." <u>Molecular Biology of the Cell</u> **20**(23): 4920-4931.
- Balaban, N., U. Schwarz, et al. (2001). "Force and focal adhesion assembly: a close relationship studied using elastic micropatterned substrates." <u>Nature Cell Biology</u> **3**(5): 466-472.
- Beattie, J. (2006). "The intrinsic charge on hydrophobic microfluidic substrates." <u>Lab on a Chip</u> **6**(11): 1409-1411.
- Bélisle, J., J. Correia, et al. (2008). "Patterning protein concentration using laser-assisted adsorption by photobleaching, LAPAP." <u>Lab on a Chip</u> **8**(12): 2164-2167.
- Bernard, A., E. Delamarche, et al. (1998). "Printing patterns of proteins." <u>Langmuir</u> **14**(9): 2225-2229.
- Bernard, A., J. P. Renault, et al. (2000). "Microcontact printing of proteins." <u>Advanced</u> Materials **12**(14): 1067-1070.
- Bhatwadekar, A. D., J. V. Glenn, et al. (2008). "Advanced glycation of fibronectin impairs vascular repair by endothelial progenitor cells: Implications for vasodegeneration in diabetic retinopathy." <u>Investigative Ophthalmology & Visual Science</u> **49**(3): 1232-1241.
- Bornstein, P. (1995). "Diversity of function is inherent in matricellular proteins: an appraisal of thrombospondin 1." <u>The Journal of Cell Biology</u> **130**(3): 503-506.
- Bourque, M. J. and L. E. Trudeau (2000). "GDNF enhances the synaptic efficacy of dopaminergic neurons in culture." <u>European Journal of Neuroscience</u> **12**(9): 3172-3180.
- Boyden, S. (1962). "Chemotactic Effect of Mixtures of Antibody and Antigen on Polymorphonuclear Leucocytes." <u>Journal of Experimental Medicine</u> **115**(3): 453-&.
- Brock, A., E. Chang, et al. (2003). "Geometric Determinants of Directional Cell Motility Revealed Using Microcontact Printing†." <u>Langmuir</u> **19**(5): 1611-1617.
- Brose, K., K. Bland, et al. (1999). "Slit proteins bind Robo receptors and have an evolutionarily conserved role in repulsive axon guidance." Cell **96**(6): 795-806.

- Bruckenstein, D. and D. Higgins (1988). "Morphological differentiation of embryonic rat sympathetic neurons in tissue culture* 1:: I. Conditions under which neurons form axons but not dendrites." Developmental Biology **128**(2): 324-336.
- Caceres, A., G. Banker, et al. (1984). "Map2 Is Localized to the Dendrites of Hippocampal-Neurons Which Develop in Culture." <u>Developmental Brain Research</u> **13**(2): 314-318.
- Caelen, I., A. Bernard, et al. (2000). "Formation of gradients of proteins on surfaces with microfluidic networks." Langmuir **16**(24): 9125-9130.
- Calderwood, D., D. Tuckwell, et al. (1997). "The integrin 1 A-domain is a ligand binding site for collagens and laminin." Journal of Biological Chemistry **272**(19): 12311.
- Campbell, K. and A. Groisman (2007). "Generation of complex concentration profiles in microchannels in a logarithmically small number of steps." <u>Lab on a Chip</u> 7(2): 264-272.
- Cardozo, D. L. (1993). "Midbrain Dopaminergic-Neurons from Postnatal Rat in Long-Term Primary Culture." Neuroscience **56**(2): 409-421.
- Carmeliet, P. and M. Tessier-Lavigne (2005). "Common mechanisms of nerve and blood vessel wiring." <u>Nature</u> **436**(7048): 193-200.
- Chan, W., J. Yabe, et al. (2003). "Growth cones contain a dynamic population of neurofilament subunits." Cell Motility and the Cytoskeleton **54**(3): 195-207.
- Charron, F., E. Stein, et al. (2003). "The morphogen sonic hedgehog is an axonal chemoattractant that collaborates with netrin-1 in midline axon guidance." <u>Cell</u> **113**(1): 11-23.
- Chen, M. S., W. J. Dressick, et al. (2002). "Physisorptive inks for microcontact printing applications." <u>Abstracts of Papers of the American Chemical Society</u> **224**: U429-U429.
- Cheng, S., S. Heilman, et al. (2007). "A hydrogel-based microfluidic device for the studies of directed cell migration." <u>Lab on a Chip</u>.
- Choonee, K. and R. R. A. Syms (2010). "Multilevel Self-Aligned Microcontact Printing System." <u>Langmuir</u>: null-null.
- Coyer, S. R., A. J. Garcia, et al. (2007). "Facile preparation of complex protein architectures with sub-100-nm resolution on surfaces." <u>Angewandte Chemie-International Edition</u> **46**(36): 6837-6840.
- Csucs, G., R. Michel, et al. (2003). "Microcontact printing of novel co-polymers in combination with proteins for cell-biological applications." <u>Biomaterials</u> **24**(10): 1713-1720.
- de la Torre, J. R., V. H. Hopker, et al. (1997). "Turning of retinal growth cones in a netrin-1 gradient mediated by the netrin receptor DCC." <u>Neuron</u> **19**(6): 1211-1224.
- Dertinger, S., D. Chiu, et al. (2001). "Generation of gradients having complex shapes using microfluidic networks." <u>Anal. Chem</u> **73**(6): 1240-1246.
- Dertinger, S., X. Jiang, et al. (2002). "Gradients of substrate-bound laminin orient axonal specification of neurons." <u>Proceedings of the National Academy of Sciences of the United States of America</u> **99**(20): 12542.
- Dertinger, S. K. W., D. T. Chiu, et al. (2001). "Generation of gradients having complex shapes using microfluidic networks." <u>Analytical Chemistry</u> **73**(6): 1240-1246.

- Diao, J., L. Young, et al. (2006). "A three-channel microfluidic device for generating static linear gradients and its application to the quantitative analysis of bacterial chemotaxis." <u>Lab on a Chip</u> **6**(3): 381-388.
- Dickson, B. (2002). "Molecular mechanisms of axon guidance." <u>Science's STKE</u> **298**(5600): 1959.
- Dickson, B. J. (2002). "Molecular mechanisms of axon guidance." <u>Science</u> **298**(5600): 1959-1964.
- Ding, L., W. Zhou, et al. (2006). "Direct preparation and patterning of iron oxide nanoparticles via microcontact printing on silicon wafers for the growth of single-walled carbon nanotubes." Chem. Mater 18(17): 4109-4114.
- Drescher, U., F. Bonhoeffer, et al. (1997). "The Eph family in retinal axon guidance." <u>Current Opinion in Neurobiology</u> 7(1): 75-80.
- Dudanova, I., G. Gatto, et al. (2010). "GDNF Acts as a Chemoattractant to Support ephrinA-Induced Repulsion of Limb Motor Axons." <u>Current biology: CB.</u>
- Eccles, S. A. (2005). "Targeting key steps in metastatic tumour progression." <u>Current</u> Opinion in Genetics & Development **15**(1): 77-86.
- Engle, E. (2010). "Human Genetic Disorders of Axon Guidance." <u>Cold Spring Harbor</u> Perspectives in Biology **2**(3).
- Erbacher, P., A. Roche, et al. (1997). "The reduction of the positive charges of polylysine by partial gluconoylation increases the transfection efficiency of polylysine/DNA complexes." Biochimica Et Biophysica Acta-Biomembranes **1324**(1): 27-36.
- Fasano, C., Thibault, D. and Trudeau L.E. (2008). "Culture of Postnatal Mesencephalic Dopamine Neurons on an Astrocyte Monolayer." <u>Current protocols</u> **3**(21): 1-19.
- Feng, X. Z., S. Hou, et al. (2004). "Microcontact printing techniques in bioscience." Chemical Research in Chinese Universities **20**(6): 826-832.
- Fredrickson, C. and Z. Fan (2004). "Macro-to-micro interfaces for microfluidic devices." Lab on a Chip 4(6): 526-533.
- Furshpan, E., S. Landis, et al. (1986). "Synaptic functions in rat sympathetic neurons in microcultures. I. Secretion of norepinephrine and acetylcholine." <u>Journal of Neuroscience</u> **6**(4): 1061.
- Furshpan, E., P. MacLeish, et al. (1976). "Chemical transmission between rat sympathetic neurons and cardiac myocytes developing in microcultures: evidence for cholinergic, adrenergic, and dual-function neurons." <u>Proceedings of the</u>
 National Academy of Sciences of the United States of America **73**(11): 4225.
- Furukawa, S., Y. Furukawa, et al. (1986). "Synthesis and secretion of nerve growth factor by mouse astroglial cells in culture* 1." <u>Biochemical and Biophysical Research Communications</u> **136**(1): 57-63.
- Genzer, J. and R. R. Bhat (2008). "Surface-bound soft matter gradients." <u>Langmuir</u> **24**(6): 2294-2317.
- Gerhardt, H., M. Golding, et al. (2003). "VEGF guides angiogenic sprouting utilizing endothelial tip cell filopodia." <u>Journal of Cell Biology</u> **161**(6): 1163-1177.
- Giepmans, B. N. G., S. R. Adams, et al. (2006). "The Fluorescent Toolbox for Assessing Protein Location and Function." <u>Science</u> **312**(5771): 217-224.
- Gilbert, S., J. Opitz, et al. (1996). "Resynthesizing evolutionary and developmental biology." <u>Developmental Biology</u> **173**(2): 357-372.

- Goldblum, S., X. Ding, et al. (1994). "SPARC (secreted protein acidic and rich in cysteine) regulates endothelial cell shape and barrier function." <u>Proceedings of the National Academy of Sciences of the United States of America</u> **91**(8): 3448.
- Goodman, C. S. (1996). "Mechanisms and molecules that control growth cone guidance." Annual Review of Neuroscience 19: 341-377.
- Gospodarowicz, D. and J. Moran (1976). "Growth factors in mammalian cell culture." Annual Review of Biochemistry **45**(1): 531-558.
- Goubko, C. A. and X. D. Cao (2009). "Patterning multiple cell types in co-cultures: A review." <u>Materials Science & Engineering C-Materials for Biological Applications</u> **29**(6): 1855-1868.
- Gundersen, R. and J. Barrett (1979). "Neuronal chemotaxis: chick dorsal-root axons turn toward high concentrations of nerve growth factor." <u>Science</u> **206**(4422): 1079-1080.
- Gundersen, R. and J. Barrett (1980). "Characterization of the turning response of dorsal root neurites toward nerve growth factor." <u>The Journal of Cell Biology</u> **87**(3): 546
- Gurdon, J. B. and P. Y. Bourillot (2001). "Morphogen gradient interpretation." <u>Nature</u> **413**(6858): 797-803.
- Haessler, U., Y. Kalinin, et al. (2009). "An agarose-based microfluidic platform with a gradient buffer for 3D chemotaxis studies." <u>Biomedical Microdevices</u> **11**(4): 827-835
- Harnett, C. K., K. M. Satyalakshmi, et al. (2001). "Bioactive templates fabricated by low-energy electron beam lithography of self-assembled monolayers." <u>Langmuir</u> **17**(1): 178-182.
- Hatch, A., A. E. Kamholz, et al. (2001). "A rapid diffusion immunoassay in a T-sensor." Nature Biotechnology **19**(5): 461-465.
- Helmuth, J. A., H. Schmid, et al. (2006). "High-speed microcontact printing." <u>Journal of the American Chemical Society</u> **128**(29): 9296-9297.
- Holden, M. A., S. Kumar, et al. (2003). "Generating fixed concentration arrays in a microfluidic device." <u>Sensors and Actuators B-Chemical</u> **92**(1-2): 199-207.
- Horbett, T. and M. Schway (1988). "Correlations between mouse 3T3 cell spreading and serum fibronectin adsorption on glass and hydroxyethylmethacrylate—ethylmethacrylate copolymers." <u>Journal of Biomedical Materials Research</u> **22**(9): 763-793.
- Hu, H. and R. Larson (2006). "Marangoni effect reverses coffee-ring depositions." <u>J.</u> Phys. Chem. B **110**(14): 7090-7094.
- Imondi, R., C. Wideman, et al. (2000). "Complementary expression of transmembrane ephrins and their receptors in the mouse spinal cord: a possible role in constraining the orientation of longitudinally projecting axons." <u>Development</u> **127**(7): 1397.
- Irimia, D., D. A. Geba, et al. (2006). "Universal microfluidic gradient generator." Analytical Chemistry **78**(10): 3472-3477.
- Irimia, D., S. Liu, et al. (2006). "Microfluidic system for measuring neutrophil migratory responses to fast switches of chemical gradients." Lab on a Chip 6(2): 191-198.

- Ismagilov, R. F., A. D. Stroock, et al. (2000). "Experimental and theoretical scaling laws for transverse diffusive broadening in two-phase laminar flows in microchannels." <u>Applied Physics Letters</u> **76**(17): 2376-2378.
- Jarjour, A. A., C. Manitt, et al. (2003). "Netrin-1 is a chemorepellent for oligodendrocyte precursor cells in the embryonic spinal cord." <u>Journal of Neuroscience</u> **23**(9): 3735-3744.
- Jeon, N., S. Dertinger, et al. (2000). "Generation of solution and surface gradients using microfluidic systems." Langmuir **16**(22): 8311-8316.
- Jeon, N. L., S. K. W. Dertinger, et al. (2000). "Generation of solution and surface gradients using microfluidic systems." <u>Langmuir</u> **16**(22): 8311-8316.
- Jomphe, C., M. J. Bourque, et al. (2005). "Use of TH-EGFP transgenic mice as a source of identified dopaminergic neurons for physiological studies in postnatal cell culture." Journal of Neuroscience Methods **146**(1): 1-12.
- Juncker, D., H. Schmid, et al. (2005). "Multipurpose microfluidic probe." Nat Mater 4(8): 622-628.
- Juncker, D., H. Schmid, et al. (2005). "Multipurpose microfluidic probe." Nat Mater 4(8): 622-628.
- Kaech, S. and G. Banker (2006). "Culturing hippocampal neurons." <u>Nature Protocols</u> **1**(5): 2406-2415.
- Kam, L. and S. Boxer (2001). "Cell adhesion to protein micropatterned supported lipid bilayer membranes." <u>Journal of Biomedical Materials Research</u> **55**(4): 487-495.
- Kandel, E. R., J. H. Schwartz, et al. (2000). <u>Principles of Neural Science</u>. New York, McGraw-Hill.
- Kang, J. S., M. J. Yi, et al. (2004). "Netrins and neogenin promote myotube formation." Journal of Cell Biology **167**(3): 493-504.
- Karniadakis, G., A. Be kök, et al. (2005). <u>Microflows and nanoflows: fundamentals and simulation</u>, Springer Verlag.
- Kater, S. and V. Rehder (1995). "The sensory-motor role of growth cone filopodia." Current Opinion in Neurobiology **5**(1): 68-74.
- Keenan, T. M. and A. Folch (2008). "Biomolecular gradients in cell culture systems." Lab on a Chip **8**(1): 34-57.
- KeinoMasu, K., M. Masu, et al. (1996). "Deleted in Colorectal Cancer (DCC) encodes a netrin receptor." Cell 87(2): 175-185.
- Kennedy, T. E., T. Serafini, et al. (1994). "Netrins Are Diffusible Chemotropic Factors for Commissural Axons in the Embryonic Spinal-Cord." <u>Cell</u> **78**(3): 425-435.
- Kennedy, T. E., H. Wang, et al. (2006). "Axon guidance by diffusible chemoattractants: A gradient of netrin protein in the developing spinal cord." <u>Journal of Neuroscience</u> **26**(34): 8866-8874.
- Kent, C. B., T. Shimada, et al. (2010). "14-3-3 Proteins Regulate Protein Kinase A Activity to Modulate Growth Cone Turning Responses." <u>Journal of Neuroscience</u> **30**(42): 14059-14067.
- Khanna, K. (2008). "Analysis of the capabilities of continuous high-speed microcontact printing."
- Kidambi, S., L. Sheng, et al. (2007). "Patterned Co Culture of Primary Hepatocytes and Fibroblasts Using Polyelectrolyte Multilayer Templates." <u>Macromolecular Bioscience</u> **7**(3): 344-353.

- Kim, D., M. Lokuta, et al. (2009). "Selective and tunable gradient device for cell culture and chemotaxis study." <u>Lab on a Chip</u> **9**(12): 1797.
- Kim, S., H. J. Kim, et al. (2010). "Biological applications of microfluidic gradient devices." <u>Integrative Biology</u> **2**(11-12): 584-603.
- Kohidai, L. and G. Csaba (1998). "Chemotaxis and chemotactic selection induced with cytokines (IL-8, RANTES and TNF-alpha) in the unicellular Tetrahymena pyriformis." Cytokine 10(7): 481-486.
- Kumar, A. and G. M. Whitesides (1993). "Features of Gold Having Micrometer to Centimeter Dimensions Can Be Formed through a Combination of Stamping with an Elastomeric Stamp and an Alkanethiol Ink Followed by Chemical Etching."

 <u>Applied Physics Letters</u> **63**(14): 2002-2004.
- Lander, A. D., Q. Nie, et al. (2002). "Do morphogen gradients arise by diffusion?" <u>Developmental Biology</u> **247**(2): 471-471.
- Lane, T. and E. Sage (1994). "The biology of SPARC, a protein that modulates cell-matrix interactions." The FASEB Journal 8(2): 163.
- Lange, S., V. Benes, et al. (2004). "Microcontact printing of DNA molecules." <u>Anal.</u> Chem **76**(6): 1641-1647.
- LeDue, J. M., M. Lopez-Ayon, et al. (2009). "High Q optical fiber tips for NC-AFM in liquid." Nanotechnology **20**(26): -.
- Lee, C. J., P. Huie, et al. (2002). "Microcontact printing on human tissue for retinal cell transplantation." <u>Archives of Ophthalmology</u> **120**(12): 1714-1718.
- Lee, K., J. Lim, et al. (2003). "Protein nanostructures formed via direct-write dip-pen nanolithography." J. Am. Chem. Soc **125**(19): 5588-5589.
- Lin, F., W. Saadi, et al. (2004). "Generation of dynamic temporal and spatial concentration gradients using microfluidic devices." Lab on a Chip 4(3): 164-167.
- Lis, D., A. Peremans, et al. (2009). "Self-Assembled Film Organization in Fast Microcontact Printing Investigated by Sum Frequency Generation Spectroscopy." <u>Journal of Physical Chemistry C</u> 113(22): 9857-9864.
- Liu, A. P., D. Loerke, et al. (2009). "Global and Local Regulation of Clathrin-Coated Pit Dynamics Detected on Patterned Substrates." <u>Biophysical Journal</u> **97**(4): 1038-1047.
- Liu, Y., J. Sai, et al. (2008). "Microfluidic switching system for analyzing chemotaxis responses of wortmannin-inhibited HL-60 cells." <u>Biomedical Microdevices</u> **10**(4): 499-507.
- Lohof, A., M. Quillan, et al. (1992). "Asymmetric modulation of cytosolic cAMP activity induces growth cone turning." Journal of Neuroscience **12**(4): 1253.
- Lumsden, A. G. S. and A. M. Davies (1983). "Earliest Sensory Nerve-Fibers Are Guided to Peripheral Targets by Attractants Other Than Nerve Growth-Factor." <u>Nature</u> **306**(5945): 786-788.
- Luster, A. D. (2002). "The role of chemokines in linking innate and adaptive immunity." <u>Current Opinion in Immunology</u> **14**(1): 129-135.
- Lyuksyutova, A., C. Lu, et al. (2003). "Anterior-posterior guidance of commissural axons by Wnt-frizzled signaling." <u>Science</u> **302**(5652): 1984.
- M.M. Segal, R. W. B., K.A. Jones and J.E. Huettner (1998). Mass cultures and microislands of neurons from postnatal rat brain. <u>Culturing nerve cells</u>. G. B. a. K. Goslin. Cambridge MIT Press: 309–338.

- Mai, J., L. Fok, et al. (2009). "Axon initiation and growth cone turning on bound protein gradients." <u>Journal of Neuroscience</u> **29**(23): 7450.
- Martuza, R., A. Malick, et al. (1991). "Experimental therapy of human glioma by means of a genetically engineered virus mutant." <u>Science</u> **252**(5007): 854.
- Masuko, S., S. Nakajima, et al. (1992). "Dissociated High-Purity Dopaminergic Neuron Cultures from the Substantia-Nigra and the Ventral Tegmental Area of the Postnatal Rat." <u>Neuroscience</u> **49**(2): 347-364.
- McLaughlin, T. and D. D. M. O'Leary (2005). "Molecular gradients and development of retinotopic maps." <u>Annual Review of Neuroscience</u> **28**: 327-355.
- Meira, M., R. Masson, et al. (2009). "Memo is a cofilin-interacting protein that influences PLC gamma 1 and cofilin activities, and is essential for maintaining directionality during ErbB2-induced tumor-cell migration." <u>Journal of Cell Science</u> **122**(6): 787-797.
- Ming, G., H. Song, et al. (1997). "cAMP-dependent growth cone guidance by netrin-1." Neuron **19**(6): 1225-1235.
- Moghe, P. V., R. D. Nelson, et al. (1995). "Cytokine-Stimulated Chemotaxis of Human Neutrophils in a 3-D Conjoined Fibrin Gel Assay." <u>Journal of Immunological Methods</u> **180**(2): 193-211.
- Moore, S. W. and T. E. Kennedy (2008). <u>Dissection and Culture of Embryonic Spinal Commissural Neurons</u>, John Wiley & Sons, Inc.
- Moore, S. W., M. Tessier-Lavigne, et al. (2007). "Netrins and their receptors." <u>Axon Growth and Guidance</u> **621**: 17-31.
- Moroi, M., M. Okuma, et al. (1992). "Platelet adhesion to collagen-coated wells: analysis of this complex process and a comparison with the adhesion to matrigel-coated wells." <u>Biochimica et Biophysica Acta (BBA)-Molecular Cell Research</u> **1137**(1): 1-9.
- Mortimer, D., T. Fothergill, et al. (2008). "Growth cone chemotaxis." <u>Trends in Neurosciences</u> **31**(2): 90-98.
- Mortimer, D., Z. Pujic, et al. (2010). "Axon guidance by growth-rate modulation."

 <u>Proceedings of the National Academy of Sciences of the United States of America</u> **107**(11): 5202-5207.
- Mrksich, M. and G. M. Whitesides (1996). "Using self-assembled monolayers to understand the interactions of man-made surfaces with proteins and cells." <u>Annual Review of Biophysics and Biomolecular Structure</u> **25**: 55-78.
- Muller, A., B. Homey, et al. (2001). "Involvement of chemokine receptors in breast cancer metastasis." Nature **410**(6824): 50-56.
- Nelson, D. and M. Cox (2004). <u>Lecture notebook for Lehninger principles of biochemistry</u>, WH Freeman & Co.
- Nelson, R., P. Quie, et al. (1975). "Chemotaxis under agarose: a new and simple method for measuring chemotaxis and spontaneous migration of human polymorphonuclear leukocytes and monocytes." <u>The Journal of Immunology</u> **115**(6): 1650.
- Parkhurst, M. R. and W. M. Saltzman (1992). "Quantification of human neutrophil motility in three-dimensional collagen gels. Effect of collagen concentration." Biophysical Journal **61**(2): 306-315.

- Perl, A., D. N. Reinhoudt, et al. (2009). "Microcontact Printing: Limitations and Achievements." <u>Advanced Materials</u> **21**(22): 2257-2268.
- Petty, H. R. (2007). "Fluorescence microscopy: Established and emerging methods, experimental strategies, and applications in immunology." <u>Microscopy Research and Technique</u> **70**(8): 687-709.
- Pla-Roca, M., J. G. Fernandez, et al. (2007). "Micro/nanopatterning of proteins via contact printing using high aspect ratio PMMA stamps and NanoImprint apparatus." Langmuir **23**(16): 8614-8618.
- Queval, A., N. R. Ghattamaneni, et al. (2010). "Chamber and microfluidic probe for microperfusion of organotypic brain slices." <u>Lab on a Chip</u> **10**(3): 326-334.
- Renault, J., A. Bernard, et al. (2003). "Fabricating arrays of single protein molecules on glass using microcontact printing." J. Phys. Chem. B **107**(3): 703-711.
- Renault, J., A. Bernard, et al. (2002). "Fabricating microarrays of functional proteins using affinity contact printing." <u>Angewandte Chemie</u> **114**(13): 2426-2429.
- Renault, J. P., A. Bernard, et al. (2002). "Fabricating microarrays of functional proteins using affinity contact printing." <u>Angewandte Chemie-International Edition</u> **41**(13): 2320-2323.
- Rodnight, R., C. A. Goncalves, et al. (1997). "Control of the phosphorylation of the astrocyte marker glial fibrillary acidic protein (GFAP) in the immature rat hippocampus by glutamate and calcium ions: Possible key factor in astrocytic plasticity." <u>Brazilian Journal of Medical and Biological Research</u> **30**(3): 325-338.
- Rosentreter, S. M., R. W. Davenport, et al. (1998). "Response of retinal ganglion cell axons to striped linear gradients of repellent guidance molecules." <u>Journal of Neurobiology</u> **37**(4): 541-562.
- Rosoff, W. J., R. McAllister, et al. (2005). "Generating controlled molecular gradients in 3D gels." <u>Biotechnology and Bioengineering</u> **91**(6): 754-759.
- Rosoff, W. J., J. S. Urbach, et al. (2004). "A new chemotaxis assay shows the extreme sensitivity of axons to molecular gradients." <u>Nature Neuroscience</u> 7(6): 678-682.
- Rosoff, W. J., J. S. Urbach, et al. (2004). "A new chemotaxis assay shows the extreme sensitivity of axons to molecular gradients (vol 7, pg 678, 2004)." <u>Nature Neuroscience</u> **7**(7): 785-785.
- Ruiz, S. and C. Chen (2008). "Emergence of patterned stem cell differentiation within multicellular structures." Stem Cells **26**(11): 2921-2927.
- Saadi, W., S. Rhee, et al. (2007). "Generation of stable concentration gradients in 2D and 3D environments using a microfluidic ladder chamber." <u>Biomedical Microdevices</u> **9**(5): 627-635.
- Sage, E. and P. Bornstein (1991). "Extracellular proteins that modulate cell-matrix interactions. SPARC, tenascin, and thrombospondin." <u>Journal of Biological Chemistry</u> **266**(23): 14831-14834.
- Sage, H., R. Vernon, et al. (1989). "SPARC, a secreted protein associated with cellular proliferation, inhibits cell spreading in vitro and exhibits Ca+ 2-dependent binding to the extracellular matrix." The Journal of Cell Biology 109(1): 341.
- Schirmeisen, A., H. Holscher, et al. (2005). "Dynamic force spectroscopy using the constant-excitation and constant-amplitude modes." <u>Nanotechnology</u> **16**(3): S13-S17.

- Seo, N., B. Russell, et al. (2010). "An Engineered 1 Integrin-binding Collagenous Sequence." <u>Journal of Biological Chemistry</u> **285**(40): 31046.
- Serafini, T., T. E. Kennedy, et al. (1994). "The Netrins Define a Family of Axon Outgrowth-Promoting Proteins Homologous to C-Elegans Unc-6." Cell **78**(3): 409-424.
- Shamloo, A., N. Ma, et al. (2008). "Endothelial cell polarization and chemotaxis in a microfluidic device." <u>Lab on a Chip</u> **8**(8): 1292-1299.
- Shen, K., J. Qi, et al. (2008). "Microcontact printing of proteins for cell biology." <u>Journal of Visualized Experiments</u>(22).
- Shen, K., J. Qi, et al. (2008). "Microcontact Printing of Proteins for Cell Biology." <u>J Vis</u> Exp(22): e1065.
- Shima, S. and H. Sakai (1981). "Poly-L-lysine produced by Streptomyces. Part II. Taxonomy and fermentation studies." <u>Agricultural and Biological Chemistry</u> **45**(11): 2497-2502.
- Shima, S. a. S. H. (1977). "Polylysine produced by Streptomyces." <u>Agricultural and</u> Biological Chemistry **41**: 1807–1809.
- Shimizu, M., K. Minakuchi, et al. (1997). "Chondrocyte migration to fibronectin, type I collagen, and type II collagen." Cell Structure and Function **22**(3): 309-315.
- Shirasaki, R., C. Mirzayan, et al. (1996). "Guidance of circumferentially growing axons by netrin-dependent and -independent floor plate chemotropism in the vertebrate brain." Neuron **17**(6): 1079-1088.
- Sigal, G. B., M. Mrksich, et al. (1998). "Effect of surface wettability on the adsorption of proteins and detergents." <u>Journal of the American Chemical Society</u> **120**(14): 3464-3473.
- Simon, K., E. Nutt, et al. (1997). "The v 3 integrin regulates 5 1-mediated cell migration toward fibronectin." <u>Journal of Biological Chemistry</u> **272**(46): 29380.
- Smith, J. T., J. K. Tomfohr, et al. (2004). "Measurement of cell migration on surface-bound fibronectin gradients." <u>Langmuir</u> **20**(19): 8279-8286.
- Solis, D. J., S. R. Coyer, et al. (2010). "Single Virus Arrays: Large-Scale Arrays of Aligned Single Viruses (Adv. Mater. 1/2010)." <u>Advanced Materials</u> **22**(1): n/a-n/a.
- Soon, L., G. Mouneimne, et al. (2005). "Description and characterization of a chamber for viewing and quantifying cancer cell chemotaxis." <u>Cell Motility and the Cytoskeleton</u> **62**(1): 27-34.
- Sperry, R. W. (1963). "Chemoaffinity in Orderly Growth of Nerve Fiber Patterns and Connections." <u>Proceedings of the National Academy of Sciences of the United States of America</u> **50**(4): 703-&.
- Srinivasan, K., P. Strickland, et al. (2003). "Netrin-1/neogenin interaction stabilizes multipotent progenitor cap cells during mammary gland morphogenesis." Developmental Cell 4(3): 371-382.
- Taha, H., R. Marks, et al. (2003). "Protein printing with an atomic force sensing nanofountainpen." <u>Applied Physics Letters</u> **83**: 1041.
- Tan, C. P., B. R. Cipriany, et al. (2010). "Nanoscale Resolution, Multicomponent Biomolecular Arrays Generated By Aligned Printing With Parylene Peel-Off." Nano Letters 10(2): 719-725.

- Tanabe, Y. and T. Jessell (1996). "Diversity and pattern in the developing spinal cord." Science **274**(5290): 1115.
- Tessier-Lavigne, M. and C. Goodman (1996). "The molecular biology of axon guidance." <u>Science</u> **274**(5290): 1123.
- Tian, W. and E. Finehout (2009). "Introduction to Microfluidics." <u>Microfluidics for Biological Applications</u>: 1-34.
- Tjia, J., B. Aneskievich, et al. (1999). "Substrate-adsorbed collagen and cell secreted fibronectin concertedly induce cell migration on poly (lactide-glycolide) substrates." <u>Biomaterials</u> **20**(23-24): 2223-2233.
- Toetsch, S., P. Olwell, et al. (2009). "The evolution of chemotaxis assays from static models to physiologically relevant platforms." <u>Integrative Biology</u> **1**(2): 170-181.
- Tovar, K. and G. Westbrook (1999). "The incorporation of NMDA receptors with a distinct subunit composition at nascent hippocampal synapses in vitro." <u>Journal of Neuroscience</u> **19**(10): 4180.
- Trinkle, C. A. and L. P. Lee (2011). "High-precision microcontact printing of interchangeable stamps using an integrated kinematic coupling." <u>Lab on a Chip.</u>
- Trousse, F., E. Martí, et al. (2001). "Control of retinal ganglion cell axon growth: a new role for Sonic hedgehog." Development **128**(20): 3927.
- Tsuyuki, E., H. Tsuyuki, et al. (1956). "The synthesis and enzymatic hydrolysis of poly-D-lysine." <u>Journal of Biological Chemistry</u> **222**(1): 479.
- Tu, Y., Y. Huang, et al. (2001). "A new focal adhesion protein that interacts with integrin-linked kinase and regulates cell adhesion and spreading." The Journal of Cell Biology **153**(3): 585.
- von Philipsborn, A., S. Lang, et al. (2006). "Microcontact printing of axon guidance molecules for generation of graded patterns." <u>Nature Protocols</u> **1**(3): 1322-1328.
- von Philipsborn, A. C., S. Lang, et al. (2006). "Microcontact printing of axon guidance molecules for generation of graded patterns." <u>Nat. Protocols</u> **1**(3): 1322-1328.
- von Philipsborn, A. C., S. Lang, et al. (2006). "Growth cone navigation in substrate-bound ephrin gradients." <u>Development</u> **133**(13): 2487-2495.
- Wadu-Mesthrige, K., S. Xu, et al. (1999). "Fabrication and Imaging of Nanometer-Sized Protein Patterns." Langmuir **15**(25): 8580-8583.
- Walter, J., B. Kernveits, et al. (1987). "Recognition of Position-Specific Properties of Tectal Cell-Membranes by Retinal Axons Invitro." <u>Development</u> **101**(4): 685-696.
- Wang, C. J., X. Li, et al. (2008). "A microfluidics-based turning assay reveals complex growth cone responses to integrated gradients of substrate-bound ECM molecules and diffusible guidance cues." <u>Lab on a Chip</u> 8(2): 227-237.
- Webb, S. E., J. W. Pollard, et al. (1996). "Direct observation and quantification of macrophage chemoattraction to the growth factor CSF-1." <u>Journal of Cell Science</u> **109**: 793-803.
- Whitesides, G. M. (2006). "The origins and the future of microfluidics." <u>Nature</u> **442**(7101): 368-373.
- Wilson, D. L., R. Martin, et al. (2001). "Surface organization and nanopatterning of collagen by dip-pen nanolithography." <u>Proceedings of the National Academy of Sciences of the United States of America</u> **98**(24): 13660-13664.

- Winblade, N., I. Nikolic, et al. (2000). "Blocking Adhesion to Cell and Tissue Surfaces by the Chemisorption of a Poly-l-lysine-graft-(poly (ethylene glycol); phenylboronic acid) Copolymer." Biomacromolecules **1**(4): 523-533.
- Xia, Y. N., J. J. McClelland, et al. (1997). "Replica molding using polymeric materials: A practical step toward nanomanufacturing." <u>Advanced Materials</u> **9**(2): 147-149.
- Xu, C., P. Taylor, et al. (2003). "Microcontact printing of DNA-surfactant arrays on solid substrates." <u>Journal of Materials Chemistry</u> **13**(12): 3044-3048.
- Xu, X. H., A. K. Y. Fu, et al. (2005). "Agrin regulates growth cone turning of Xenopus spinal motoneurons." <u>Development</u> **132**(19): 4309-4316.
- Yam, P. T., S. D. Langlois, et al. (2009). "Sonic Hedgehog Guides Axons through a Noncanonical, Src-Family-Kinase-Dependent Signaling Pathway." <u>Neuron</u> **62**(3): 349-362.
- Yavin, E. and Z. Yavin (1974). "Attachment and culture of dissociated cells from rat embryo cerebral hemispheres on polylysine-coated surface." <u>The Journal of Cell Biology</u> **62**(2): 540.
- Yee, K. T., H. H. Simon, et al. (1999). "Extension of long leading processes and neuronal migration in the mammalian brain directed by the chemoattractant netrin-1."

 Neuron 24(3): 607-622.
- Yu, S. R., M. Burkhardt, et al. (2009). "Fgf8 morphogen gradient forms by a source-sink mechanism with freely diffusing molecules." <u>Nature</u> **461**(7263): 533-U100.
- Zicha, D., G. A. Dunn, et al. (1991). "A New Direct-Viewing Chemotaxis Chamber." Journal of Cell Science 99: 769-775.
- Zigmond, S. (1977). "Ability of polymorphonuclear leukocytes to orient in gradients of chemotactic factors." <u>The Journal of Cell Biology</u> **75**(2): 606.
- Zlotnik, A. (2006). "Chemokines and cancer." <u>International Journal of Cancer</u> **119**(9): 2026-2029.
- Zou, Y., E. Stoeckli, et al. (2000). "Squeezing Axons Out of the Gray Matter:: A Role for Slit and Semaphorin Proteins from Midline and Ventral Spinal Cord." <u>Cell</u> **102**(3): 363-375.